

CLEAN RESOURCES FINAL PUBLIC REPORT TEMPLATE

PROJECT INFORMATION:

Project Title:	TECHNOLOGY PATHWAY TO CO-PROCESS BIOCRUDES FROM WASTE BIOMASS IN PETROLEUM REFINERIES
Alberta Innovates Project Number:	2609 (#G2019000695)
Submission Date:	June, 2022
Total Project Cost:	\$1,950,000
Alberta Innovates Funding:	\$300,000
AI Project Advisor:	Mehr Nikoo

APPLICANT INFORMATION:

Applicant (Organization):	CanmetENERGY in Devon
Address:	One Oil Patch Drive Devon, Alberta T9G 1A8
Applicant Representative Name:	Dr. Jinwen Chen
Title:	Director, Hydrocarbon Conversion Program
Phone Number:	(780) 987-8763
Email:	jinwen.chen@canada.ca

Alberta Innovates and Her Majesty the Queen in right of Alberta make no warranty, express or implied, nor assume any legal liability or responsibility for the accuracy, completeness, or usefulness of any information contained in this publication, nor for any use thereof that infringes on privately owned rights. The views and opinions of the author expressed herein do not reflect those of Alberta Innovates or Her Majesty the Queen in right of Alberta. The directors, officers, employees, agents and consultants of Alberta Innovates and The Government of Alberta are exempted, excluded and absolved from all liability for damage or injury, howsoever caused, to any person in connection with or arising out of the use by that person for any purpose of this publication or its contents.

PROJECT REPORTS:

Co-processing of biomass-derived crude oil (“biocrudes”) with petroleum streams is a promising approach to transition to lower carbon liquid transportation fuels without major capital investment. In 2019, CanmetENERGY Devon and University of Alberta joined efforts with Alberta Innovates and with the support from a network of major stakeholders, to develop the knowledge base for commercial implementation of co-processing biocrudes in existing oil refineries. The project consists of four major research components involving lab- and pilot-scale studies, combined with modelling activities, to: (1) deliver approaches to treat biocrude before co-processing, (2) set quality specifications for refinery intake, (3) establish guidelines for co-processing biocrude in refinery units, and (4) assess economics and carbon intensity. This report including two parts: CanmetENERGY report presents the final results of first components 1, 2, along with partial results of the component 3, and University of Alberta U of A report presents the results of component 4. The project tasks were carried out using two biocrudes produced by proprietary hydrothermal liquefaction (HTL) technologies developed by two companies separately.



PROTECTED BUSINESS INFORMATION

PROJECT REPORT

TECHNOLOGY PATHWAY TO CO-PROCESS BIOCRUDES FROM WASTE BIOMASS IN PETROLEUM REFINERIES

S. Badoga, A. Alvarez-Majmutov, and Jinwen Chen
NATURAL RESOURCES CANADA, CanmetENERGY Devon

Work performed for:
ALBERTA INNOVATES

APRIL 2022

NATURAL RESOURCES CANADA
DIVISION REPORT CDEV-2022-0019-RE

Canada

DISCLAIMER

This report and its contents, the project in respect of which it is submitted, and the conclusions and recommendations arising from it do not necessarily reflect the views of the Government of Canada, its officers, employees, or agents.

COPYRIGHT

This report was created during the authors' course of employment with CanmetENERGY at the Devon Research Centre, Natural Resources Canada, and as such, Her Majesty the Queen in Right of Canada, as represented by the Minister of Natural Resources Canada (Her Majesty), is the sole copyright owner of the report. Natural Resources Canada is a federal government department and any copyrighted material created by a federal employee is Crown copyright. Under Canadian law, Crown copyright cannot be assigned without an Order-in-council.

EXECUTIVE SUMMARY

Co-processing of biomass-derived crude oil (“biocrudes”) with petroleum streams is a promising approach to transition to lower carbon liquid transportation fuels without major capital investment. In 2019, CanmetENERGY Devon and University of Alberta joined efforts with Alberta Innovates and with the support from a network of major stakeholders, to develop the knowledge base for commercial implementation of co-processing biocrudes in existing oil refineries. The project consists of four major research components involving lab- and pilot-scale studies, combined with modelling activities, to: (1) deliver approaches to treat biocrude before co-processing, (2) set quality specifications for refinery intake, (3) establish guidelines for co-processing biocrude in refinery units, and (4) assess economics and carbon intensity. This report presents the final results of first two components, along with partial results of the third one.

The project tasks were carried out using two biocrudes produced by proprietary hydrothermal liquefaction (HTL) technologies developed by two companies separately. One biocrude was derived from agricultural waste, whereas the other one was from forest residue biomass. The first task sought to develop approaches for pre-treating biocrudes based on existing oil refining technologies, namely solvent deasphalting and hydrotreating. The second task was focused on establishing quality specifications to optimize biocrudes for refinery intake, emphasizing their compatibility with petroleum. The third and last task covered in this report, aimed at understanding impacts of co-processing biocrudes on refinery performance.

Analytical characterization of the two biocrudes showed that the one from agricultural waste was rich in oxygen and nitrogen (13.2 and 2.3 wt%, respectively) and was largely made up of carboxylic acids, whereas the one from forest residue biomass was also high in oxygen content (11.3 wt%), but had very little nitrogen (0.3 wt%), and was phenolic in nature. Both biocrudes were determined to have high corrosiveness potential and nearly 50 wt% of them boiling above 524 °C. In addition, they were completely immiscible in vacuum gas oil (VGO), the reference petroleum feedstock used in this work.

The development of the solvent-based pre-treatment approach was aimed at identifying solvents that could selectively reject contaminants and petroleum-insoluble components in the biocrude. Screening of ten different solvents ranging in polarity using a lab-scale setup allowed

selecting four potential solvents for further testing: toluene, dichloromethane, ethyl acetate, and *n*-pentane. Evaluation of these solvents at a larger scale showed that this form of biocrude pre-treatment did not bring a meaningful improvement in overall quality. There was rejection of high boiling components in the biocrudes, but the concentrations of contaminants like oxygen and nitrogen remained practically unchanged. Moreover, the solvent-treated biocrudes were in most cases still immiscible with VGO. The biocrudes treated with *n*-pentane did show improvement in miscibility, but this was at the expense of 54.4–61.1% mass rejection. Altogether these observations strongly suggested that the solvent-based treatment approach is not a viable option for enhancing biocrude quality for refinery intake.

The biocrude pre-treatment approach based on hydrotreating was investigated using CanmetENERGY Devon's PP-11 batch reactor unit. Experiments were designed to scout a range of conditions under which the biocrudes would be deoxygenated to a point where they became miscible in VGO, thereby facilitating co-processing. This method effectively reduced oxygen content in the biocrudes by 72.3–73.9% and converted the high boiling fractions into distillates. Biocrude hydrotreating was best achieved at relatively high catalyst-to-feed ratios and using gradual temperature steps without exceeding 300–320 °C to prevent the biocrude from polymerizing. At oxygen levels between 2.9–3.5 wt%, the hydrotreated biocrudes became fully miscible in VGO. This could potentially indicate that biocrudes might need to be deoxygenated to under 3.5 wt% oxygen to be acceptable for refinery intake.

Finally, a preliminary co-processing study was done in the same batch reactor unit using blends of raw and hydrotreated biocrude (3.5 wt% oxygen) with VGO. Co-processing the hydrotreated biocrude was found to significantly reduce the impacts on catalytic performance with respect to directly co-processing raw biocrude. It was also observed that co-processing severity would need to be increased depending on how much deoxygenation the biocrude had been subjected to.

CONTENTS

DISCLAIMER	i
COPYRIGHT	i
EXECUTIVE SUMMARY	ii
1.0 INTRODUCTION	8
2.0 OBJECTIVE	9
3.0 TASK OVERVIEW	10
4.0 EXPERIMENTAL	11
4.1. MATERIALS	11
4.2. BIOCRUDE PRE-TREATMENT USING SOLVENTS	12
4.3. BIOCRUDE PRE-TREATMENT USING HYDROTREATING	12
4.4. BIOCRUDE CO-PROCESSING TESTS	15
4.5. FEED AND PRODUCT ANALYSIS	16
4.6. BLENDING COMPATIBILITY TESTING	16
5.0 RESULTS AND DISCUSSION	17
5.1. TASK 1 – BIOCRUDE PRE-TREATMENT	17
5.1.1. FEEDSTOCK CHARACTERIZATION	17
5.1.2. PRE-TREATMENT USING SOLVENTS	19
5.1.3. BIOCRUDE A PRE-TREATMENT USING HYDROTREATING	24
5.1.4. BIOCRUDE B PRE-TREATMENT USING HYDROTREATING	29
5.2. TASK 2 – BIOCRUDE QUALITY METRIC	31
5.2.1. BLENDING COMPATIBILITY STUDY OF SOLVENT-TREATED BIOCRUDES	31

5.2.2. BLENDING COMPATIBILITY STUDY OF HYDROTREATED BIOCRUDES	35
5.2.3. NMR SPECTROSCOPY CHARACTERIZATION OF HYDROTREATED BIOCRUDES	39
5.3. TASK 3 – BIOCRUDE CO-PROCESSING	42
6.0 CONCLUSIONS.....	44
7.0 ACKNOWLEDGMENT.....	45
APPENDIX A: SIMULATED DISTILLATION DATA SETS.....	47

TABLES

Table 1 – Experimental conditions of the Biocrude A hydrotreating experiments	13
Table 2 – Experimental conditions of the Biocrude B hydrotreating experiments.....	14
Table 3 – Experimental conditions of the co-processing experiments with Biocrude A.....	16
Table 4 – Properties of Biocrude A, Biocrude B, and VGO.....	18
Table 5 – Solvent screening tests using Biocrude A.....	20
Table 6 – Solvent treatment tests with Biocrudes A and B	21
Table 7 – Properties of Biocrude A extracts.....	22
Table 8 – Properties of Biocrude B extracts	23
Table 9 – Elemental composition of Biocrude A hydrotreating products	25
Table 10 – Product yields and catalytic performance of Biocrude A hydrotreating experiments	26
Table 11 – GC analysis of Biocrude A gas products	28
Table 12 – Elemental composition of Biocrude B hydrotreating products	29
Table 13 – Product yields and catalytic performance of Biocrude B hydrotreating experiments.....	30

Table 14 – GC analysis of Biocrude B gas products	31
Table 15 – ¹ H NMR spectra of Biocrude A and its hydrotreated products	39
Table 16 – ¹³ C NMR spectra of Biocrude A and its hydrotreated products	41
Table 17 – ³¹ P NMR spectra of Biocrude A and its hydrotreated products.....	41
Table 18 – ³¹ P NMR spectra of Biocrude B and its hydrotreated products	42
Table 19 – Elemental composition of the feedstocks and products of the co- processing tests	43
Table 20 – Catalytic performance of the co-processing tests	43
Table A 1 – SimDis data for Biocrude A.....	48
Table A 2 – SimDis data for Biocrude B.....	49
Table A 3 – SimDis data for VGO.....	50
Table A 4 – SimDis data for Biocrude A extract using <i>n</i> -pentane	51
Table A 5 – SimDis data for Biocrude A extract using toluene	52
Table A 6 – SimDis data for Biocrude A extract using dichloromethane	53
Table A 7 – SimDis data for Biocrude A extract using ethyl acetate	54
Table A 8 – SimDis data for Biocrude B extract using <i>n</i> -pentane.....	55
Table A 9 – SimDis data for Biocrude B extract using toluene.....	56
Table A 10 – SimDis data for Biocrude B extract using dichloromethane	57
Table A 11 – SimDis data for Biocrude B extract using ethyl acetate	58
Table A 12 – SimDis data for Run UR#3 product.....	59
Table A 13 – SimDis data for Run UR#4 product.....	60
Table A 14 – SimDis data for Run UR#6 product.....	61
Table A 15 – SimDis data for Run UR#7 product.....	62
Table A 16 – SimDis data for Run UR#8 product.....	63

Table A 17 – SimDis data for Run UR#9 product.....	64
--	----

FIGURES

Figure 1 – Proposed co-processing scheme	9
Figure 2 – PP-11 schematic	14
Figure 3 – Simulated distillation profiles of Biocrude A extracts	22
Figure 4 – Simulated distillation profiles of Biocrude B extracts	24
Figure 5 – Reactor unloading after a biocrude hydrotreating test	27
Figure 6 – Boiling point distribution of Biocrude A and selected hydrotreated products.....	28
Figure 7 – Boiling point distribution of Biocrude B and its hydrotreated products	30
Figure 8 – Blending compatibility test with raw Biocrude A.....	32
Figure 9 – Blending compatibility tests with Biocrude A after solvent treatment	33
Figure 10 – Blending compatibility tests with Biocrude B after solvent treatment.....	34
Figure 11 – Blending compatibility test for Biocrude A Run UR#1 product.....	35
Figure 12 – Blending compatibility test for Biocrude A Run UR#3, 4 and 6 products.....	37
Figure 13 – Blending compatibility test for Biocrude B Run UR#7, 8 and 9 products.....	38
Figure 14 – Effect of feed oxygen content on catalytic performance during co- processing	44

1.0 INTRODUCTION

Co-processing of biomass-derived crude oil (“biocrudes”) with petroleum streams is a promising approach to transition to lower carbon liquid transportation fuels without major capital investment. With its sizeable petroleum refining and bitumen upgrading infrastructure, as well as its abundant low-value biomass resources, Alberta has a unique opportunity to produce a range of bio-products via co-processing. This approach possesses the ability to add bio-based content to all refined products (gasoline, jet fuel, diesel, heating/fuel oil, and petrochemicals), making it an attractive option for refineries to meet GHG emissions reduction targets and comply with government regulations for renewable content in fuels.

The strategy to co-process a biocrude in a petroleum refining scheme remains an open question. Each biocrude is unique on its own depending on the specific thermochemical conversion technology (fast pyrolysis, hydrothermal liquefaction (HTL), thermo-catalytic reforming, etc.) and the source of waste biomass (forest residue, agriculture waste, sewage sludge, and algae) used for producing it. For this reason, quality specifications to optimize biocrudes for refinery intake have not yet been developed. It is also known that biocrudes pose major challenges for co-processing in a refinery owing to their chemical instability, high corrosiveness, and immiscibility in petroleum. There is some consensus in the technical literature that pre-treatment is required to upgrade biocrudes into a more amenable intermediate for co-processing, but the level and form of this pre-treatment are not well-established. In addition, while it is intuitive that feeding biocrude into a refinery will result in the production of fuels with renewable content, the exact refinery units that should be targeted and the conditions at which they should be operated are poorly defined.

In 2019, CanmetENERGY Devon and University of Alberta joined efforts with Alberta Innovates and with the support from a network of Canadian refiners, biocrude technology developers, and government policy agencies to develop the knowledge base for commercial implementation of co-processing biocrudes with petroleum streams in existing refineries. The project pursues a specific technology pathway, as illustrated in Figure 1. It is proposed that a raw biocrude would be first pre-treated via solvent extraction or mild hydrotreating technologies to remove or convert petroleum insoluble material and other contaminants to a level that is acceptable for refinery intake. The treated biocrude would then be dropped in adequate

proportions into a heavy gas oil stream entering a hydrotreating unit at the front of either a fluid catalytic cracking (FCC) unit or a hydrocracking unit. This would enable near complete removal of biocrude contaminants in parallel to those from heavy gas oil. The co-processed product from this hydrotreating unit would then be processed further in the FCC or hydrocracking unit to produce the final fuel products with renewable content.

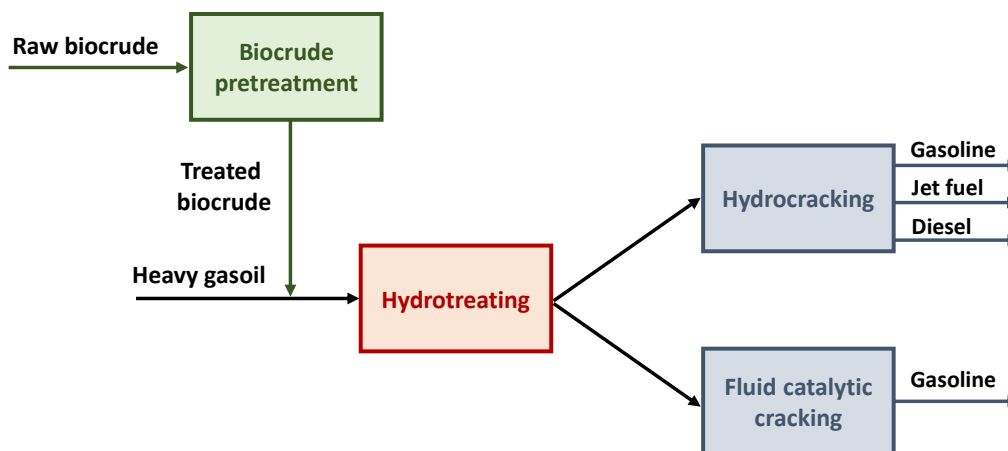


Figure 1 – Proposed co-processing scheme

The project consists of four major research components or tasks involving lab- and pilot-scale studies, combined with modelling activities, to: (1) deliver approaches to treat biocrude before co-processing, (2) set quality specifications for refinery intake, (3) establish guidelines for co-processing biocrude in various refinery units, and (4) assess economics and carbon intensity. This report presents the final results of the first two components, along with partial results of the third one.

2.0 OBJECTIVE

The overall objective of this project is to advance the concept of biocrude co-processing to demonstration-ready status (TRL-6). The specific goals that were pursued through this project were the following:

- Demonstrate that solvent extraction and mild hydrotreating technologies can be effectively applied to contaminant treatment in biocrude feedstocks prior to co-processing.

- Establish a quality metric to characterize the compatibility of biocrude feeds with petroleum streams at refinery conditions.
- Develop operational guidelines for co-processing adequate proportions of biocrude feedstock in fluid catalytic cracking and hydrocracking units to produce fuel products that meet current renewable fuel regulations.
- Quantify the economic and GHG reduction benefits from co-processing.

3.0 TASK OVERVIEW

Below is an overview of the project tasks covered in this report:

Task 1 – Biocrude pre-treatment

Biocrudes contain various contaminants and unconverted biomass requiring treatment before they can be dropped into a refinery. In addition, because of their elevated oxygen content, most biocrudes are immiscible or partially miscible in petroleum. The first task of this project sought to adapt two existing technologies in oil refining for use in biocrude pre-treatment. Analogously to solvent deasphalting in oil refining, the first approach uses solvents to selectively reject contaminants and petroleum-insoluble components in biocrude. The second one is catalytic hydrotreating under mild conditions to remove oxygen contaminants, but only to the extent that the biocrude becomes miscible in petroleum. The two approaches were explored at the bench- or lab-scale using biocrude samples from different origins and conversion technologies.

Task 2 – Biocrude quality metric

Biocrudes currently do not have a “quality certificate” equivalent to a petroleum assay, which can be used by refiners to assess new feedstocks. This “certificate” would provide vital information about the prospective feedstock’s blending compatibility with the existing feed pool, product yields and quality during its co-refining, and potential issues such as equipment corrosion and fouling. This task was an analytical characterization component aimed at understanding how the chemistry and quality of biocrudes relate to their compatibility with petroleum and refinery conditions. The intention was to establish quality specifications based on readily available methods used for hydrocarbon analysis to define biocrude compatibility for co-refining.

Task 3 – Biocrude co-processing (only partially covered in this report)

For this technology pathway to be attractive for refiners, it is imperative to achieve meaningful co-processing volumes (or blending ratio) to satisfy government regulations for renewable fuel products while maintaining operational integrity in the refinery. Through systematic pilot-scale studies, the third task of this project aimed at optimizing co-processing performance in fluid catalytic cracking and hydrocracking units. These two units were identified as the most feasible drop in points for biocrude co-processing in a refinery. The proposed pilot testing campaigns would help understanding how biocrude quality and feed blending ratio impact refinery unit performance and provide guidance into adjusting operating conditions for optimum unit operation. In addition, product testing would determine the distribution of biogenic carbon across co-processed fuel products.

4.0 EXPERIMENTAL

4.1. MATERIALS

Two biocrudes produced by proprietary hydrothermal liquefaction (HTL) technologies were used in Tasks 1 through 3. The first one (hereafter referred to as Biocrude A) was derived from agricultural waste, specifically a combination of waste canola meal and wheat flour. This biocrude sample was kindly provided by NULIFE GreenTech Inc., based in Saskatoon, Saskatchewan. The second one (hereafter referred to as Biocrude B) originated from forest residue biomass and was kindly supplied by Steeper Energy based in Calgary, Alberta.

A series of chemicals were used in the solvent treatment study (Task 1): *n*-pentane, *n*-heptane, toluene, dichloromethane, tetrahydrofuran, chloroform, ethyl acetate, methyl ethyl ketone, acetone, and methanol. All these chemicals were purchased from Fischer Scientific Canada.

A commercial NiMo hydrotreating catalyst available in-house was used in the biocrude hydrotreating and co-processing experiments under Tasks 1 and 3, respectively. Light gas oil (LGO, boiling range ~204–343 °C) and dimethyl disulfide (DMDS) were used for the activation of the hydrotreating catalysts. Vacuum gas oil (VGO, boiling range ~343–524 °C) from Alberta oil sands bitumen available in-house was used as the reference petroleum feedstock for the

blending compatibility tests and the preliminary co-processing study under Tasks 2 and 3, respectively.

4.2. BIOCRUDE PRE-TREATMENT USING SOLVENTS

A solvent assessment study was conducted to identify potential solvents that can selectively reject contaminants and petroleum-insoluble components in Biocrudes A and B. The solvent treatment experiments were executed based on a modified version of ASTM D4055M method. This standard test method is commonly used in hydrocarbon analysis for the determination of *n*-pentane insolubles in crude oils and refinery products.

In the initial phase of the study, ten solvents with varying degrees of polarity (see Section 4.1) were screened based on their ability to reject contaminants in each biocrude. Among these solvents, *n*-pentane was considered as the benchmark as it is the most common solvent used in the aforementioned oil refining solvent treatment process called solvent deasphalting (see Section 3.0). In a typical test, ~2 g of biocrude were mixed with ~125 mL of solvent at room temperature. The solution was placed in an ultrasonic bath for 45 min and allowed to settle overnight. The precipitate was filtered through a 1.6 µm glass microfiber filter and washed with solvent until the solution ran clear. The precipitate was then dried in a fume hood at room temperature for 48 h and weighted afterwards to determine the amount of rejected material in the biocrude. Finally, the extract was subjected to rotary evaporation to remove the solvent and then weighted to determine the solvent-soluble portion of the biocrude. A solvent would be deemed promising for further study based on the resulting biocrude extraction yields.

The solvents identified during the screening phase were studied at a larger scale in the next phase. The solvent treatment methodology was almost the same, but using much larger batches of sample with a lower solvent/biocrude ratio (30 g of biocrude mixed with 800 mL of solvent) to obtain enough biocrude extract for property characterization. This included a blending compatibility study to determine whether pre-treatment with the selected solvent produced a biocrude extract that was miscible in VGO (reference petroleum feedstock).

4.3. BIOCRUDE PRE-TREATMENT USING HYDROTREATING

A biocrude hydrotreating test program was executed to scout a range of probable conditions under which Biocrudes A and B would be deoxygenated to a point where they

became miscible in VGO to facilitate co-processing. The detailed experimental plan for Biocrude A is presented in Table 1. In the first two Runs (UR#1 and 2), biocrude hydrotreating was performed at a single temperature (270 and 300 °C, respectively). In the four subsequent Runs (UR#3–6), hydrotreating was done in two or three temperature steps to first treat the most reactive oxygen species at a relatively low temperature, and then the more refractory ones at higher temperatures. For example, UR#4 temperature was first held at 240 °C for 3 h, then at 280 °C for another 3 h, and finally at 300 °C for 2.5 h. By including the extra time needed to increase temperature between steps, the total reaction for this run was 10 h. These reaction temperature ranges were based on typical values reported for biocrude hydrotreating. Catalyst-to-feed ratios and reaction times were selected to cover the typical range of weight hourly space velocities (WHSV) used in hydrotreating. Considering the concept of equivalent WHSV for a batch reactor which incorporates the amounts of feed and catalyst and residence time (equivalent WHSV = amount of feed / (amount of catalyst × residence time)), the equivalent WHSV used in this study was between 0.5–4.0 h⁻¹. All tests were performed at a pressure of 1400 psi. Each run was conducted only once.

Table 1 – Experimental conditions of the Biocrude A hydrotreating experiments

Run	Temperature, °C	Reaction time, h	Catalyst-to-feed ratio, g/g	Pressure, psi
Upgrading Run 1, UR#1	270	6.3	0.04	1400
Upgrading Run 2, UR#2	300	6.3	0.04	1400
Upgrading Run 3, UR#3	240, 290	11.5	0.05	1400
Upgrading Run 4, UR#4	240, 280, 300	10.0	0.06	1400
Upgrading Run 5, UR#5	240, 280, 310	9.0	0.06	1400
Upgrading Run 6, UR#6	240, 280, 300	11.5	0.19	1400

Hydrotreating experiments with Biocrude B were carried out some time after completing those with Biocrude A. Analysis of Biocrude A test results enabled narrowing down and optimizing the experimental plan for Biocrude B. As shown in Table 2, there were three tests at constant reaction time (9.0 h) and pressure (1400 psi), with fixed temperature steps (first at 250

°C for 3 h and then at 320 °C for 6 h). Catalyst-to-feed ratio was the variable parameter (0.06–0.11 g/g) in this set of tests used for increasing process severity.

Table 2 – Experimental conditions of the Biocrude B hydrotreating experiments

Run	Temperature, °C	Reaction time, h	Catalyst-to-feed ratio, g/g	Pressure, psi
Upgrading Run 7, UR#7	250, 320	9.0	0.06	1400
Upgrading Run 8, UR#8	250, 320	9.0	0.08	1400
Upgrading Run 9, UR#9	250, 320	9.0	0.11	1400

The experiments with both biocrudes were carried out using CanmetENERGY Devon's PP-11 batch reactor unit. The reactor is a 300 mL stainless steel vessel equipped with an overhead stirrer. It has a removable sleeve that can be used to hold the reactants and catalyst. Sample material is preloaded into this sleeve before heating and pressurizing with hydrogen. The reactor has a gas inlet port and an outlet port to collect non-condensable gas products during and after operation. The outlet gas is sent to a condenser, cooled in an ice bath to collect the light hydrocarbons and water. The unit is provided with a complete set of utilities: hydrogen, hydrogen sulfide, nitrogen, cooling water and air. Temperature control is achieved by electric heating zones. The unit has a data acquisition software package that allows capture and trending of the operating variables, such as temperatures and pressures. The schematic of this unit is shown in Figure 2.

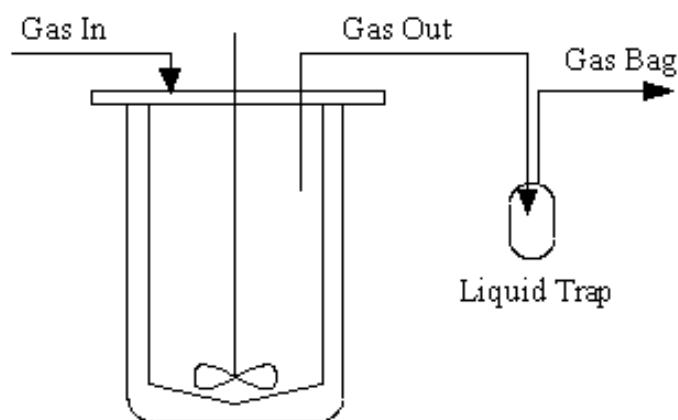


Figure 2 – PP-11 schematic

In a typical hydrotreating experiment, about 100 g of feed and 4–19 g of sulfided catalyst (depending on the catalyst-to-feed ratio) were loaded into the reactor sleeve. Each test was done using a new sulfided catalyst sample. Because biocrudes are very low in sulfur, approximately 1 wt% DMDS was added to the biocrude to maintain the catalyst in sulfided state during the experiments. After pressure testing, the reactor was pressurized with hydrogen and heated up to attain the desired reaction conditions. Temperature was ramped at 1.0 °C/min. During operation, hydrogen was added periodically to maintain reactor pressure constant. Stirring speed was set at 700 rpm. After a test, the reactor was cooled down and the off-gases were collected in a gas bag for volume measurement and gas chromatography (GC) analysis before depressurizing the unit. Liquid and solid samples were collected in the sleeve when the reactor was cooled down to room temperature and depressurized. In addition, at the bottom of the sleeve there was a sludge-like residue containing the spent catalyst, which had to be scraped out. The light product accumulated in the condenser was also collected. The products were weighed for mass balance calculations.

Prior to the hydrotreating experiments, the catalyst was activated in the same batch reactor unit using liquid phase sulfiding. The sulfiding process was done in two stages using a LGO spiked with DMDS. The first stage was carried out at the following conditions: temperature 240–250 °C, hydrogen pressure 800 psi, and reaction time 4 h. The conditions of the second stage were: temperature 320 °C, hydrogen pressure 1400 psi, and reaction time 2 h.

4.4. BIOCRUDE CO-PROCESSING TESTS

A preliminary co-processing study was conducted using blends of raw and hydrotreated Biocrude A with VGO. The experiments were done in the same batch reactor unit (CanmetENERGY Devon PP-11), by following the same experimental procedures described in Section 4.3. The details of the experimental plan are presented in Table 3. The Baseline Run was done using pure VGO to create a baseline for the study. Run Co-Pro-R#1 was performed using a blend of 10 wt% raw Biocrude A in 90 wt% VGO and Run Co-Pro-R#2 using a blend of 10 wt% hydrotreated Biocrude A in 90 wt% VGO. The testing conditions were the same for the three experiments: temperature 375 °C, reaction time 9.0 h, catalyst-to-feed ratio 0.07 g/g, and pressure 1400 psi.

Table 3 – Experimental conditions of the co-processing experiments with Biocrude A

Run	Temperature, °C	Reaction time, h	Catalyst-to-feed ratio, g/g	Pressure, psi
Baseline Run	375	9.0	0.07	1400
Co-processing Run 1, Co-Pro-R#1	375	9.0	0.07	1400
Co-processing Run 2, Co-Pro-R#2	375	9.0	0.07	1400

4.5. FEED AND PRODUCT ANALYSIS

The analytical methods that were used for analyzing the physical and chemical properties of the various feed materials and product samples were the following:

- Liquid density (ASTM D4052)
- Simulated distillation (ASTM D7169)
- Carbon, hydrogen, nitrogen (ASTM D5291)
- Oxygen (In-house method)
- Sulfur (ASTM D1552)
- Total acid number (TAN) (ASTM D8045)
- SARA (saturates, aromatics, resins, and asphaltenes) analysis (ASTM D2700M)
- Water content by Karl-Fischer method (ASTM D4377)
- Hydroxyl speciation by ³¹P Phosphorus NMR (NREL/TP-5100-65887)
- Proton spectrum by ¹H NMR (In-house method)
- Carbon typing by ¹³C NMR (In-house method)
- Refinery gas analysis by GC (In-house method)

4.6. BLENDING COMPATIBILITY TESTING

The biocrude samples treated by either solvents or hydrotreating were subjected to blending compatibility testing to determine how miscible they were in VGO. These blending compatibility tests were performed using a qualitative in-house procedure. Accordingly, a blend having 10 wt% biocrude in 90 wt% VGO was prepared in a 2 oz (60 mL) graduated vial at room temperature using a shaker. The blend was mixed for 2 h and then the sample vial was turned

upside down to observe any material precipitation. A sub-sample of the blend was taken to study its homogeneity using microscopy (Zeiss optical microscope). Some of the samples were re-inspected after 7 days of settling.

5.0 RESULTS AND DISCUSSION

5.1. TASK 1 – BIOCRUDE PRE-TREATMENT

5.1.1. FEEDSTOCK CHARACTERIZATION

The analytical properties of the two biocrude samples are reported in Table 4. It also contains the properties of the VGO used as the reference petroleum feedstock in the blending compatibility study and co-processing tests. Biocrudes A and B are characterized by having elevated oxygen content (13.2 and 11.3 wt%, respectively) and minimum amounts of sulfur (0.1–0.2 wt%). Their high densities (1.0519 and 1.0880 g/cm³, respectively) can be attributed to their relatively low hydrogen content (9.3 and 8.5 wt%, respectively). Biocrude A is particularly high in nitrogen (2.3 wt%) because of the proteins present in agriculture wastes. In contrast, VGO is rich in sulfur (3.3 wt%) and comparatively low in oxygen (0.5 wt%) and nitrogen (0.2 wt%). Given its higher hydrogen content (11.5 wt%), VGO is substantially less dense (0.9752 g/cm³) than the two biocrudes. Both biocrudes have traces of moisture (0.4 wt%) and elevated TAN (102.4 and 67.7 mg KOH/g, respectively), which is indicative of high corrosion potential.

SARA analysis reveals major differences in hydrocarbon types between the two biocrudes and VGO. It should be noted that the SARA method is not entirely applicable to biocrudes, but is performed for comparative purposes. The biocrudes are largely polar (48.1 and 34.3 wt%, respectively), with minimum saturates (1.7 and 2.3 wt%, respectively). Biocrude B has some aromatics (13.6 wt%), whereas Biocrude A does not have much (1.8 wt%). Conversely, VGO is rich in saturates (38.7 wt%) and aromatics (53.9 wt%) and does not have that much polars (7.4 wt%). Nearly half of each biocrude (48.5 and 49.8 wt%, respectively) is material insoluble in *n*-pentane, which is likely composed of highly polar oligomeric structures residing in their high boiling fractions. This marked difference in hydrocarbon type composition, particularly the large shares of polars and *n*-pentane insolubles in each biocrude, is an early indication of their blending incompatibility with VGO.

Table 4 – Properties of Biocrude A, Biocrude B, and VGO

Property	Biocrude A	Biocrude B	VGO
Density at 15.6 °C, g/cm ³	1.0519	1.0880	0.9752
Carbon, wt%	75.1	79.6	84.5
Hydrogen, wt%	9.3	8.5	11.5
Nitrogen, wt%	2.3	0.3	0.2
Sulfur, wt%	0.2	0.1	3.3
Oxygen, wt%	13.2	11.3	0.5
TAN, mg KOH/g	102.4	67.7	-
Water, wt%	0.4	0.4	-
SARA analysis			
Saturates, wt%	1.7	2.3	38.7
Aromatics, wt%	1.6	13.6	53.9
Polars, wt%	48.1	34.3	7.4
Pentane insolubles, wt%	48.5	49.8	-
Fractional composition ¹⁾			
Naphtha (35–204 °C), wt%	1.6	2.6	0.0
Light gas oil (204–343 °C), wt%	8.1	14.5	5.1
Heavy gas oil (343–524 °C), wt%	42.7	31.9	86.6
Vacuum residue (>524 °C), wt%	47.6	51.0	8.3
Hydroxyl content			
Aliphatic OH, mmol OH/g	0.27	0.26	-
Phenolic OH, mmol OH/g	1.05	2.10	-
Carboxylic OH, mmol OH/g	1.69	0.87	-

¹⁾ Based on simulated distillation.

Table 4 also reports the fractional composition obtained by the simulated distillation analysis of the two biocrudes and VGO. The simulated distillation data sets can be found in Appendix A (Tables A 1–A 3). The two biocrudes are found to be similar in fractional composition. Both are very low in naphtha (1.6 and 2.6 wt%, respectively) and have about 50 wt% vacuum residue, which means that only about half of them is distillable material. Biocrude

A has more heavy gas oil (42.7 wt%) than Biocrude B (31.9 wt%), but at the same time, less light gas oil (8.1 wt% in Biocrude A vs. 14.5 wt% in Biocrude B). VGO is largely within the boiling range of heavy gas oil (86.6 wt%), with relatively small amounts of light gas oil (5.1 wt%) and residue (8.3 wt%). It is noted that the simulated distillation method has limitations for the analysis of biocrudes as it is not well-suited for oxygen-rich samples. This is because most biocrudes do not fully dissolve in the solvent used by this test method (carbon disulfide (CS₂)), therefore the analysis is only performed on the CS₂-soluble part of the biocrude. This means that the biocrude distillation fractions reported in Table 4 exclude the part that did not dissolve in CS₂.

The hydroxyl content analysis of Biocrude A indicates abundance of carboxylic acid components (1.69 mmol OH/g) and to some extent of phenolic species (1.05 mmol OH/g). This shows that carboxylic acids structures are prevalent in the agriculture waste from which this biocrude was produced. In contrast, Biocrude B is predominantly phenolic (2.10 mmol OH/g), which is consistent with the chemical structure of lignocellulosic biomass. These oxygen components likely constitute the polars and *n*-pentane insolubles fractions of the SARA analysis.

5.1.2. PRE-TREATMENT USING SOLVENTS

The selection of solvents in this work was done based on polarity index and boiling point. The set of selected solvents ranged from non-polar, as is the case of *n*-pentane (polarity index = 0), to polar solvents such as acetone and methanol (polarity index = 5.1). Solvent boiling points were required to be relatively low (<120 °C) to facilitate separation from the extract. Table 5 presents the properties of the assessed solvents and the results of the screening tests with Biocrude A. The term “insolubles” in Table 5 refers to the mass percentage of biocrude rejected by the solvent. Three of the most polar solvents (tetrahydrofuran, chloroform, and methyl ethyl ketone) gave practically no insolubles (0.1–1.7 wt%), meaning that there was virtually no material rejection from Biocrude A and for this reason they were discarded from further consideration. In contrast, with *n*-heptane, one of the non-polar solvents, mass rejection was as much as 72.9 wt%. This means that only 27.1 wt% of the biocrude would be usable for co-processing, making this solvent impractical for this application. A similar observation can be made regarding the benchmark solvent, *n*-pentane (61.1 wt% insolubles).

Table 5 – Solvent screening tests using Biocrude A

Solvent	Boiling point, °C	Polarity index	Insolubles, wt%
<i>n</i> -pentane	36.1	0.0	61.1
<i>n</i> -heptane	98.4	0.1	72.9
toluene	110.6	2.4	19.4
dichloromethane	39.6	3.1	3.8
tetrahydrofuran	66.0	4.0	0.1
chloroform	61.2	4.1	1.4
ethyl acetate	77.1	4.4	10.9
methyl ethyl ketone	79.6	4.7	1.7
acetone	56.0	5.1	3.7
methanol	64.7	5.1	10.0

The results produced by the other five solvents (toluene, dichloromethane, ethyl acetate, acetone, and methanol) were more in line with the expectations for this technology. With insolubles yields between 3.7–19.4 wt%, the amount of treated biocrude available for co-processing would be in the order of 80.6–96.3 wt%. Among these five solvents, there were pairs of solvents that gave very similar results (3.7–3.8 wt% insolubles for dichloromethane and acetone; 10.0–10.9 wt% insolubles for ethyl acetate and methanol), so only the ones that gave the highest insolubles yield from each pair were selected for the next phase of study. Thus, the final selection included: toluene, dichloromethane, ethyl acetate, and once again *n*-pentane as the benchmark solvent.

In the next phase of the study, the final selection of solvents was tested with both Biocrudes A and B, and the resulting biocrude extracts (the soluble fractions) were characterized after removing the solvent. Table 6 reports the insolubles yields for each biocrude. It is noted that there is a good correspondence in insolubles yields between Biocrudes A and B, with the exception of dichloromethane. This solvent rejects much more mass from Biocrude B (27.9 wt%) than from Biocrude A (3.0 wt%). This shows that the class of compounds that is insoluble in dichloromethane is more widespread in Biocrude B, which ultimately could be related to the fact that the two biocrudes are from completely different waste biomass sources.

Table 6 – Solvent treatment tests with Biocrudes A and B

Solvent	Biocrude A insolubles, wt%	Biocrude B insolubles, wt%
<i>n</i> -pentane	61.1	54.4
toluene	23.8	35.6
dichloromethane	3.0	27.9
ethyl acetate	14.6	16.2

Table 7 presents the properties of Biocrude A extracts after solvent removal. As can be seen, toluene, dichloromethane, and ethyl acetate did not achieve a meaningful reduction in oxygen (11.8–12.5 wt%) and nitrogen (2.2–2.6 wt%) levels with respect to the raw Biocrude A (13.2 wt% oxygen, 2.3 wt% nitrogen). *n*-Pentane performs a little better in this sense (10.2 wt% oxygen, 1.0 wt% nitrogen), but at the expense of 61.1 wt% mass rejection (see Table 6). TAN of the extracts is the range of 89.0–134.6 mg KOH/g, which means that their corrosivity is still too high. For the toluene, dichloromethane, ethyl acetate extracts there is no major change in hydrocarbon type distributions (SARA analysis) in comparison to the raw Biocrude A (Table 4). Treatment with *n*-pentane does seem to change such hydrocarbon distribution quite visibly by reducing pentane insolubles content to a minimum while raising the share of polars to 97.2 wt%. There is a slight reduction in carboxylic acids (1.42–1.64 mmol OH/g), which are dominant in Biocrude A (1.69 mmol OH/g). From these results it is evident that the proposed solvent treatment approach did not bring a meaningful improvement in biocrude quality. The blending compatibility aspect of the biocrude extracts is presented further in Section 5.2.1.

Figure 3 shows the boiling point distributions of Biocrude A extracts. The simulated distillation data sets can be found in Appendix A (Tables A 4–A 7). The boiling point profile of the raw Biocrude A is also included for reference (black solid line). Unlike the other properties discussed in Table 7, in most cases, boiling point distribution does change significantly after treating the biocrude with solvents. The distillation curve of the extracts tends to shift to the right, which is indicative of less high boiling components. This means that the insolubles rejected by the solvents are mostly heavy components residing in the high boiling fractions of the biocrude. Therefore, solvent treatment appears to work in an analogous way to distillation.

Table 7 – Properties of Biocrude A extracts

Property	<i>n</i> -pentane	toluene	dichloro methane	ethyl acetate
Carbon, wt%	77.3	76.6	75.2	75.8
Hydrogen, wt%	10.7	9.5	8.9	9.3
Nitrogen, wt%	1.0	2.2	2.6	2.4
Sulfur, wt%	<0.1	0.2	0.3	0.2
Oxygen, wt%	10.2	11.8	12.2	12.5
TAN, mg KOH/g	89.0	133.1	94.5	134.6
SARA analysis				
Saturates, wt%	1.1	0.8	0.7	0.8
Aromatics, wt%	0.7	7.2	4.4	4.1
Polars, wt%	97.2	42.7	43.5	44.9
Pentane insolubles, wt%	1.1	49.4	51.4	50.2
Hydroxyl content				
Aliphatic OH, mmol OH/g	<0.20	<0.20	<0.20	<0.20
Phenolic OH, mmol OH/g	<0.20	0.71	0.97	0.89
Carboxylic OH, mmol OH/g	1.64	1.42	1.48	1.51

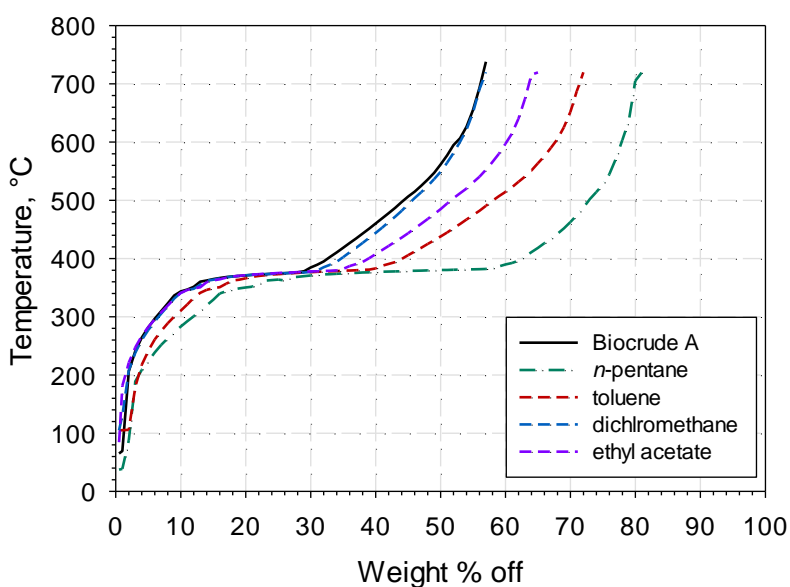


Figure 3 – Simulated distillation profiles of Biocrude A extracts

Biocrude B showed a similar pattern in terms of the quality of the extracts, as indicated in Table 8. Oxygen removal was fairly low (8.6–10.8 wt%) in relation to the raw Biocrude B (11.3 wt%). In one case (ethyl acetate), oxygen actually got concentrated in the extract (12.1 wt% oxygen). Similar to Biocrude A, there was no improvement in TAN (55.4–84.9 mg KOH/g). Hydrocarbon type distributions did change for this biocrude as a function of the solvent. In all cases, pentane insoluble content was reduced to some extent, which in turn increased the share of polars and aromatics. There was reduction in phenol content (1.03–1.54 mmol OH/g) except in the case of ethyl acetate (2.14 mmol OH/g). Carboxylic acids appear to have increased in most cases (0.97–1.31 mmol OH/g), most likely due to a concentration effect. In summary, solvent treatment did not improve much the quality of Biocrude B either.

Table 8 – Properties of Biocrude B extracts

Property	<i>n</i> -pentane	toluene	dichloro methane	ethyl acetate
Carbon, wt%	80.6	80.6	79.7	78.6
Hydrogen, wt%	10.5	9.4	9.2	9.0
Nitrogen, wt%	<0.02	<0.02	0.1	0.2
Sulfur, wt%	<0.1	<0.1	<0.1	0.1
Oxygen, wt%	8.6	8.9	10.8	12.1
TAN, mg KOH/g	68.6	55.4	83.0	84.9
SARA analysis				
Saturates, wt%	5.0	2.8	2.8	2.5
Aromatics, wt%	22.1	13.3	14.4	12.8
Polars, wt%	72.6	55.6	48.1	40.4
Pentane insolubles, wt%	0.3	28.3	34.6	44.3
Hydroxyl content				
Aliphatic OH, mmol OH/g	<0.20	<0.20	<0.20	0.21
Phenolic OH, mmol OH/g	1.03	1.54	1.52	2.14
Carboxylic OH, mmol OH/g	1.32	0.97	0.81	0.97

Figure 4 shows the boiling point distributions of Biocrude B extracts. The simulated distillation data sets can be found in Appendix A (Tables A 8–A 11). The boiling point profile of the raw Biocrude B is also included for reference (black solid line). Similar to Biocrude A, the distillation curve of Biocrude B extracts shifts to the right due to the removal of high boiling components. The flat horizontal segment of the toluene profile indicates that the biocrude extract still had toluene with a concentration of about 13 wt%.

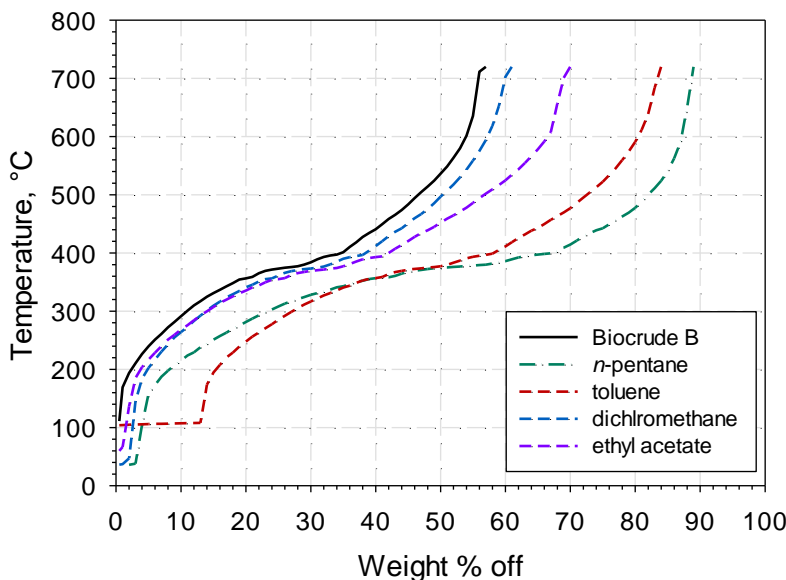


Figure 4 – Simulated distillation profiles of Biocrude B extracts

5.1.3. BIOCRUDE A PRE-TREATMENT USING HYDROTREATING

Tables 9 through 11 report the results of Biocrude A hydrotreating experiments. Table 9 shows the elemental composition of Biocrude A hydrotreated products. Except for Run UR#2, all products showed an increase in hydrogen content in relation to the raw biocrude (9.3 wt% hydrogen), which is evidence of hydrogen uptake. Oxygen content is brought down to 3.5–8.0 wt% as a result of deoxygenation, whereas nitrogen appears to have concentrated (2.4–3.1 wt%) when compared to the raw biocrude (2.3 wt% nitrogen). This shows that the nitrogen in Biocrude A could not be removed under the tested conditions.

Table 9 – Elemental composition of Biocrude A hydrotreating products

Property	UR#1	UR#2	UR#3	UR#4	UR#5	UR#6
Carbon, wt%	78.9	82.1	79.6	80.5	79.2	82.7
Hydrogen, wt%	9.6	9.0	10.0	10.1	10.5	10.8
Nitrogen, wt%	2.8	3.1	2.8	2.6	2.6	2.5
Oxygen, wt%	8.0	4.6	6.9	6.0	6.5	3.5

Table 10 shows the product yields and catalytic performance of Biocrude A hydrotreating experiments. The experimental liquid recovery, here defined as the percentage of physically recovered liquid product relative to the biocrude feed, varied between 67.7–94.6 wt%. Based on these liquid recoveries and the carbon contents in the biocrude and its products, the carbon balance in the liquid can be estimated at 72.6–96.2%. The products were very viscous, with some portions of product left stuck to the reactor internals upon collection (see Figure 5). This problem was quite evident during Runs UR#1 and 2 where only one temperature step was used. Run UR#2 at 300 °C resulted in an oxygen removal of 64.2%, but the product was particularly viscous at this temperature, leading to the lowest liquid recovery among all tests (67.7 wt%). Considering the drop in hydrogen content in the product of this Run (see Table 9) and low liquid recovery, it is possible that the most reactive species in the biocrude underwent polymerization when directly exposed to such an elevated temperature for a long time.

The stepwise increase in temperature used in Runs UR#3 and 4 brought a significant improvement in liquid recovery (87.7–88.2 wt%), which is likely related to the stabilization of said reactive oxygen compounds at the lowest temperature (240 °C). Run UR#4 gave higher oxygen removal (52.1%) than Run UR#3 (46.0%), owing to higher temperatures. Run UR#5 gave slightly higher oxygen removal (53.0%) as a result of raising temperature in last step to 310 °C. However, liquid recovery was poor (75.8 wt%) because some a froth was formed in the reactor, causing liquid product spillage upon collection (see Figure 5). Based on the product collection issues experienced during Runs UR#2 and 5, it became apparent that the thermal instability of the biocrude was a limiting factor impacting the achievable oxygen removal in the test reactor.

Table 10 – Product yields and catalytic performance of Biocrude A hydrotreating experiments

Parameter	UR#1	UR#2	UR#3	UR#4	UR#5	UR#6
Reaction temperature, °C	270	300	240–290	240–300	240–310	240–300
Mass recovery						
Liquid recovery, wt%	80.6	67.7	87.7	88.2	75.8	86.5
Catalytic performance						
Hydrodeoxygenation, %	37.2	64.2	46.0	52.1	53.0	72.3
Liquid product distribution						
Naphtha (35–204 °C), wt%	-	-	3.4	4.0	-	6.5
Light gas oil (204–343 °C) (wt%)	-	-	15.0	17.2	-	28.1
Atmospheric residue (>343 °C), wt%	-	-	81.6	78.8	-	65.4

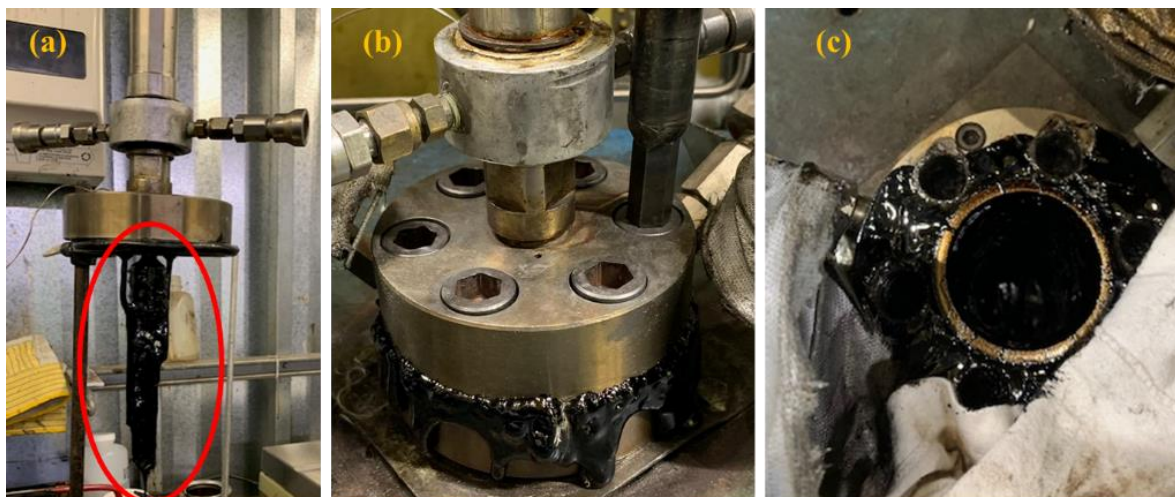


Figure 5 – Reactor unloading after a biocrude hydrotreating test

(Images of (a) the liquid product stuck to the reactor internals in Run UR#2, (b) liquid product spillage due to frothing in Run UR#5 (product oozing out of the reactor during unloading), and (c) top view of the open reactor during Run UR#5)

On account of the thermal instability of Biocrude A, Run UR#6 was carried out using a much higher catalyst-to-feed ratio (0.19 g/g) than in the previous runs (0.04–0.06 g/g), while keeping the temperature of the last step at 300 °C (see Table 1). With this change the equivalent WHSV was substantially reduced from 1.7–4.0 h⁻¹ in Runs UR#1–5 to 0.5 h⁻¹ in Run UR#6, representing an increase in reaction severity. This adjustment led to the highest oxygen removal among all tests (72.3%), with a liquid recovery of 86.5 wt%. This highlights the importance of having sufficiently high catalyst volume per unit of incoming feed to augment oxygen removal while managing the thermal stability aspect of biocrude. However, the commercial implication would be a large catalyst bed volume to achieve a relatively low WHSV for a given throughput.

Table 10 also includes the distribution of distillation fractions for selected Runs with high liquid recoveries (UR#3, 4, and 6). The yields of these fractions were obtained from the simulated distillation analysis of the products, as shown in Figure 6. The boiling point distribution of Biocrude A is also included in Figure 6 for reference. The distillation profile of the Biocrude A shows that 66.0 wt% eluted out of the GC column and the balance is regarded as heavy material boiling above 720 °C. Hydrotreating converted some of these high boiling components, increasing the amount of material eluted out of the GC column to 75–88 wt%. The distribution of fractions presented in Table 10 indicates that the hydrotreated biocrude products

are predominantly (65.4–81.6 wt%) in the boiling range of an atmospheric distillation residue (>343 °C), with some (15.0–28.1 wt%) light gas oil (203–343 °C), and a little (3.4–6.5 wt%) naphtha (35–204 °C). The simulated distillation data sets for these products are provided in Appendix A (Tables A 12–A 14).

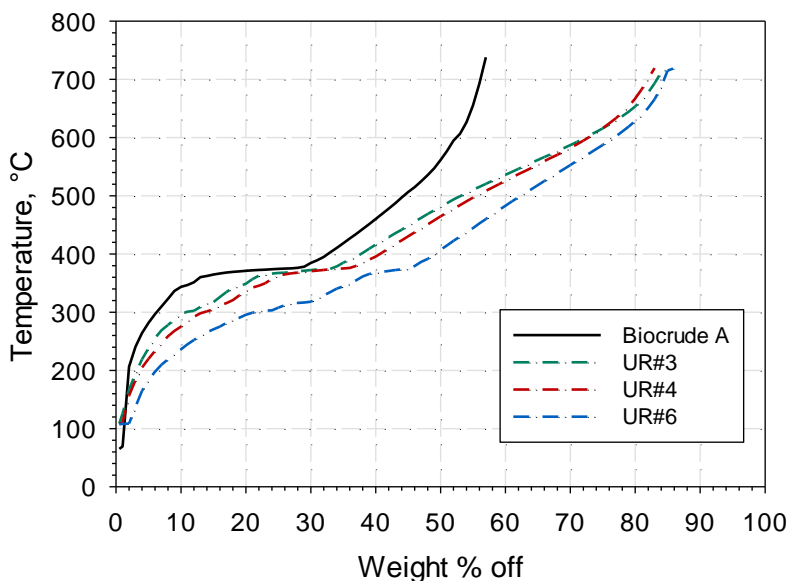


Figure 6 – Boiling point distribution of Biocrude A and selected hydrotreated products

Table 11 reports the concentrations of key gas products generated during the hydrotreating experiments with Biocrude A. The presence of carbon dioxide (CO₂) in the gas products at levels of 9.5–18.4 mol% confirms that some of the oxygen was removed via decarboxylation. Decarbonylation reactions leading to carbon monoxide (CO) generation were minor in this case (<0.2 mol%).

Table 11 – GC analysis of Biocrude A gas products

Component	UR#1	UR#2	UR#3	UR#4	UR#5	UR#6
CH ₄ , mol%	14.6	23.6	14.0	18.4	24.8	19.0
CO, mol%	0.2	0.0	0.0	0.0	0.0	0.1
CO ₂ , mol%	12.2	18.4	14.1	16.7	10.4	16.5

The considerable levels (14.0–24.8 mol%) of methane (CH₄) could be an indication of methanation reactions involving CO and hydrogen. However, in this study, it is also likely that a

substantial amount of methane originated from the sulfiding agent (DMDS) that was added to the biocrude to keep the catalyst active. The rest of the gas was largely unreacted hydrogen, with small amounts of light hydrocarbons.

5.1.4. BIOCRUDE B PRE-TREATMENT USING HYDROTREATING

The elemental composition of Biocrude B hydrotreated products is reported in Table 12. From the table it is clear that oxygen content is greatly reduced from 11.3 wt% in raw Biocrude B to 2.9–4.6 wt% in the products. Oxygen removal comes along with visible hydrogen addition, as evidenced by the change in hydrogen content of the products (9.9–10.4 wt%) with respect to the raw biocrude (8.5 wt% hydrogen). Biocrude B was very low in nitrogen (0.3 wt%), which explains why there is no measurable change in nitrogen in the products. This is alignment with Biocrude A results showing virtually no nitrogen removal under the tested conditions.

Table 12 – Elemental composition of Biocrude B hydrotreating products

Property	UR#7	UR#8	UR#9
Carbon, wt%	84.9	85.6	86.1
Hydrogen, wt%	10.0	9.9	10.4
Nitrogen, wt%	0.3	0.3	0.3
Oxygen, wt%	4.6	4.0	2.9

Table 13 provides the product yields and catalytic performance of Biocrude B hydrotreating experiments. The liquid recoveries achieved for this set of experiments (89.4–91.3 wt%) were overall much better than in the set with Biocrude A (67.7–88.2 wt%). This is mainly the result of optimizing the testing conditions and, possibly, the better thermal stability of Biocrude B. As discussed in Section 5.1.3, thermal instability was the primary cause of the low liquid recoveries in most of the experiments with Biocrude A. The maximum oxygen removal obtained for Biocrude B (73.9%) was fairly similar to Biocrude A (72.3%). Increasing oxygen removal beyond this point would require higher catalyst-to-feed ratios and/or pressures, because the ability to raise reaction temperature is greatly restricted by the stability of the biocrude.

In terms of distillation fractions, Biocrude B hydrotreated products were to a great extent in the atmospheric residue range (59.9–67.6 wt%), with the rest being mostly light gas oil

(26.9–30.9 wt%) and some naphtha (5.5–9.2 wt%). Such a distribution is actually quite similar to that of Biocrude A products (see Table 10). The full distillation profiles of Biocrude B and its hydrotreated products are shown in Figure 7. Once again it is observed that the distillation curves of the products are displaced to the right indicating conversion of high boiling material. The corresponding simulated distillation data sets are given in Appendix A (Tables A 15–A 17).

Table 13 – Product yields and catalytic performance of Biocrude B hydrotreating experiments

Parameter	UR#7	UR#8	UR#9
Reaction temperature, °C	250–320	250–320	250–320
Mass recovery			
Liquid recovery, wt%	89.4	90.0	91.2
Catalytic performance			
Hydrodeoxygenation, %	59.3	63.3	73.9
Liquid product distribution			
Naphtha (35–204 °C), wt%	5.5	5.8	9.2
Light gas oil (204–343 °C) (wt%)	26.9	28.8	30.9
Atmospheric residue (>343 °C), wt%	67.6	65.4	59.9

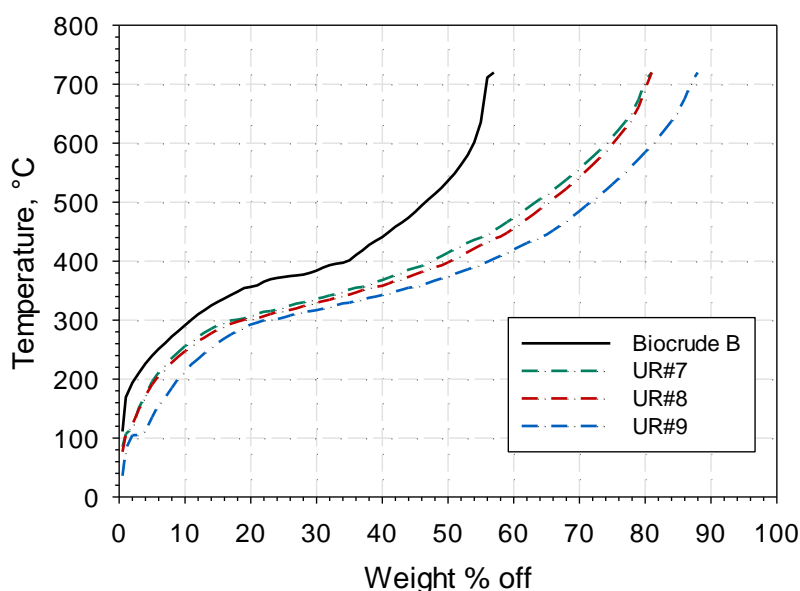


Figure 7 – Boiling point distribution of Biocrude B and its hydrotreated products

The concentrations of key gas components produced during Biocrude B hydrotreating experiments are listed in Table 14. Similar to Biocrude A, the appearance of CO₂ (9.9–15.9 mol%) indicates that some of the oxygen in Biocrude B was removed via decarboxylation reactions. The fact that CO generation was minor (<0.3 mol%) shows that there was practically no oxygen removal via decarbonylation. Once again there was a substantial amount of CH₄ (16.7–20.9 mol%), which could have been due to methanation reactions between CO and hydrogen or the decomposition of the sulfiding agent (DMDS).

Table 14 – GC analysis of Biocrude B gas products

Component	UR#7	UR#8	UR#9
CH ₄ , mol%	18.9	20.9	16.7
CO, mol%	0.3	0.0	0.1
CO ₂ , mol%	10.0	15.9	9.9

5.2. TASK 2 – BIOCRUDE QUALITY METRIC

Aside from the analytical characterization of the treated biocrudes presented in Section 5.1, a blending compatibility study was conducted to help defining the optimum level of treatment required to make a biocrude miscible in the reference petroleum feedstock (VGO) and ultimately more amenable for co-processing. This was complemented with a detailed nuclear magnetic resonance (NMR) spectroscopy study to better understand the nature of the chemical compounds that need to be converted in biocrude in order to make it an acceptable feedstock for refinery intake.

5.2.1. BLENDING COMPATIBILITY STUDY OF SOLVENT-TREATED BIOCRUDES

As described in Section 4.6, the blending compatibility tests consisted of mixing 10 wt% raw or treated biocrude in 90 wt% VGO and the resulting mixtures were inspected visually and using microscopy. Figure 8 shows the blending compatibility test for the raw Biocrude A. The figure shows photographs of the inverted sample vial and its microscopic image. Immediately upon mixing, a portion separated out of the mixture and settled at the bottom of the vial. The microscopic image of the soluble phase shows aggregates varying in size in the VGO matrix.

This clearly demonstrates that Biocrude A in its original form is incompatible with VGO at this blending ratio. A very similar behavior was observed with Biocrude B.

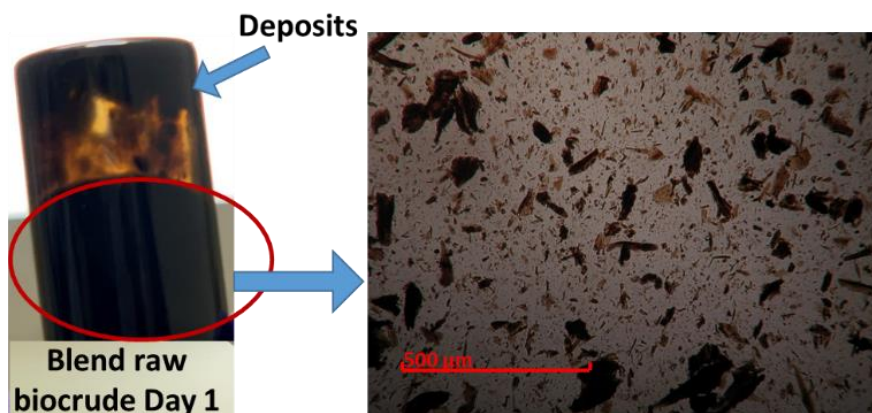


Figure 8 – Blending compatibility test with raw Biocrude A

The results of the blending compatibility tests with Biocrude A after solvent treatment are provided in Figure 9. The figure includes the Biocrude A extracts obtained using ethyl acetate (top left panel), dichloromethane (top right panel), *n*-pentane (bottom left panel), and toluene (bottom right panel). It can be observed that the ethyl acetate and dichloromethane extracts did not mix well with VGO from Day 1, clearly indicating incompatibility. The microscopic images show large agglomerates of Biocrude A particles in the VGO matrix. On Day 2, there was increased settling of particles in the test bottles.

The toluene extract blend showed some improvement in miscibility with VGO. On Day 1 the blend was fairly homogenous; however, after 7 days there was particle settling in the test bottle, indicating phase separation over time. The microscopic images show a more or less uniform texture, without any large agglomerates as the ones observed for the ethyl acetate and dichloromethane extracts. The *n*-pentane extract was found to be completely compatible with VGO, even after 7 days of settling. Nevertheless, the issue with using *n*-pentane to treat Biocrude A is that about 60 wt% of its mass is lost as an insoluble residue. These results, together with those from Section 5.1.2., suggest that solvent treatment with the solvents investigated in this work is not a viable option for improving Biocrude A quality and miscibility with petroleum.



Figure 9 – Blending compatibility tests with Biocrude A after solvent treatment

The blending compatibility tests with Biocrude B extracts gave somewhat different results, as illustrated in Figure 10. The dichloromethane extract (top left panel) was quite miscible in VGO on Day 1, which is in contrast with what was observed for Biocrude A. Its microscopic image shows a fairly uniform texture except for one large agglomerate seen close to the middle of the image. By Day 7, there was some material deposition in the test bottle, which came with a change in texture in the microscopic image. This is an indication that the blend was not stable over time. The ethyl acetate extract (top right panel) did not blend very well with VGO, but it was still better than the corresponding Biocrude A extract. The toluene and *n*-pentane extracts (bottom right and left panels, respectively) were observed to be compatible with

VGO and the resulting blends were relatively stable during the 7 days of settling. However, once again the downside of these two solvents is the level of mass rejection with Biocrude B (35.6 wt% for toluene, 54.4 wt% for *n*-pentane). This further indicates that solvent treatment with the solvents investigated in this work may not be a technically sound option for upgrading biocrudes prior to co-processing.

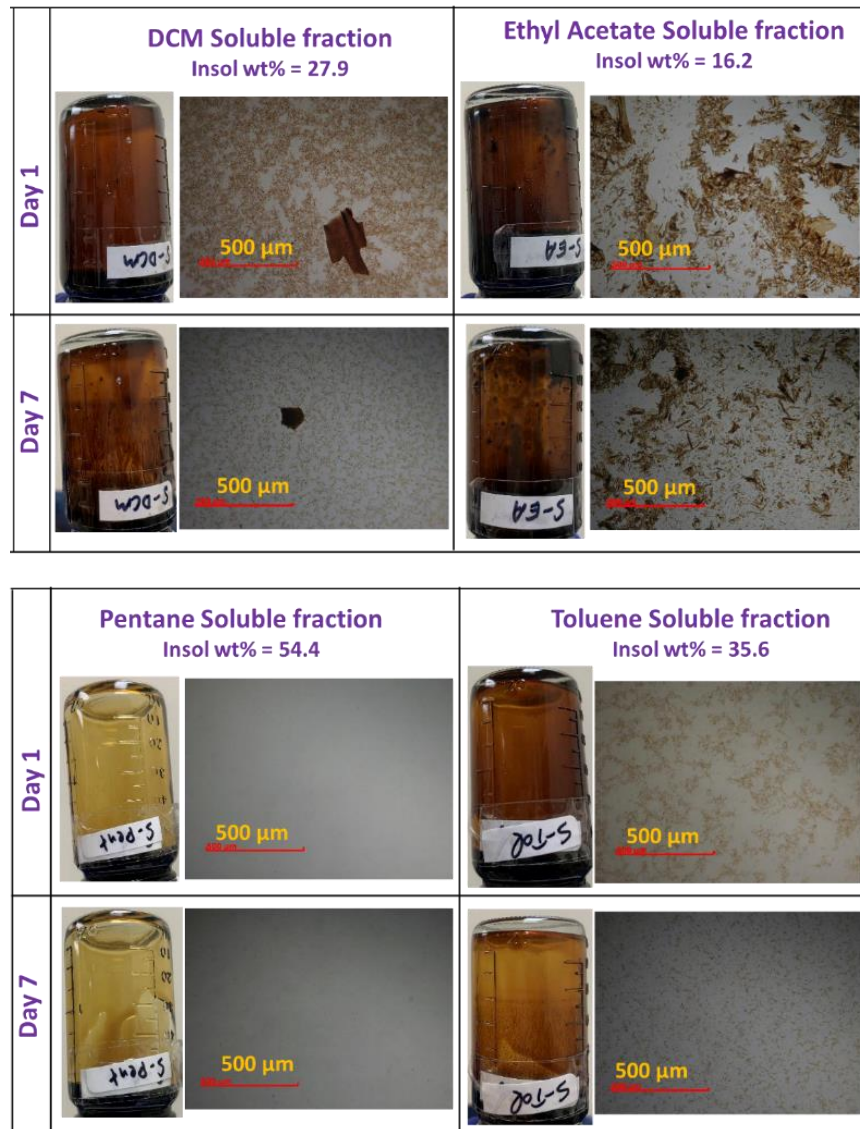


Figure 10 – Blending compatibility tests with Biocrude B after solvent treatment

5.2.2. BLENDING COMPATIBILITY STUDY OF HYDROTREATED BIOCRUDES

Figure 11 shows images of the blending compatibility test for the hydrotreated product from Biocrude A Run UR#1 (8.0 wt% oxygen content). Upon mixing, a portion separated out of the mixture and settled at the bottom of the vial. The microscopic image shows particle aggregation in the soluble phase, but the particles appear to be more homogenous in size than in the raw Biocrude A (Figure 8). Consequently, this is an early indication that reducing oxygen content to 8.0 wt% is insufficient to achieve miscibility in VGO.

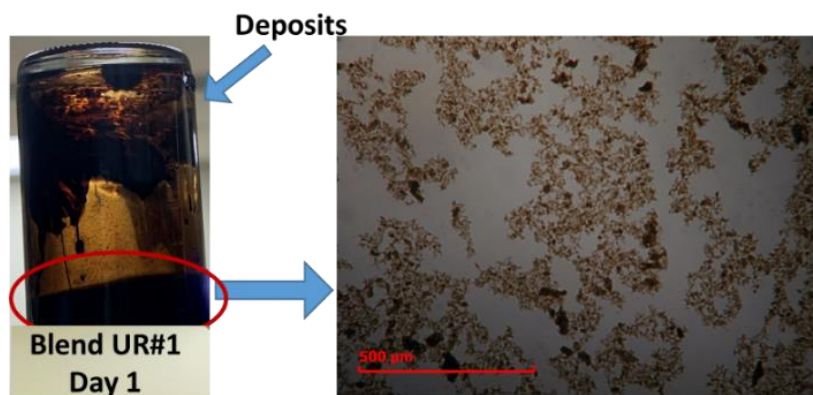


Figure 11 – Blending compatibility test for Biocrude A Run UR#1 product

Figure 12 shows the images of blending compatibility tests for the products from Biocrude A Runs UR#3, 4 and 6, containing 6.9 wt%, 6.0 wt%, and 3.5 wt% oxygen, respectively (see Table 9). The blends of all three products were found to be fairly homogeneous on Day 1. Microscopic images show less aggregation in the VGO matrix, particularly for the product having 3.5 wt% oxygen (Run UR#6). This clearly shows that oxygen content reduction improves biocrude miscibility in VGO. After 7 days, the blends were re-inspected and the Run UR#3 product blend started to show some fine deposits on the walls of the container, while the smallest aggregates on the microscopic image seen on Day 1 disappeared. This means that the aggregation process in this blend continued throughout the 7 days of observation until it reached the onset of precipitation. Similar behavior, but to a lesser degree, was noted for the Run UR#4 product. Run UR#6 product blend, on the other hand, was stable after 7 days.

Figure 13 shows a very similar pattern for Biocrude B products with 2.9–4.6 wt% oxygen (Table 12). All of their blends with VGO were homogeneous on Day 1, but after 7 days the blends involving the products having 4.6 and 4.0 wt% oxygen (Runs UR#7 and 8, respectively)

started showing some deposits on the walls of the test bottle. At the same time, the product with 2.9 wt% oxygen (Run UR#9) resulted in a blend that was stable over 7 days. This optimum oxygen level for blend stability somewhat coincides with the one observed for Biocrude A (3.5 wt%). From these observations it can be concluded that deoxygenation is key for improving not only the miscibility of the biocrude in VGO, but also the stability of the resulting blend. Judging by the results obtained with Runs UR#6 and 9 products, it appears that oxygen content in biocrude needs to be reduced to levels within 2.9–3.5 wt% to achieve good miscibility and stability in VGO.



Figure 12 – Blending compatibility test for Biocrude A Run UR#3, 4, and 6 products

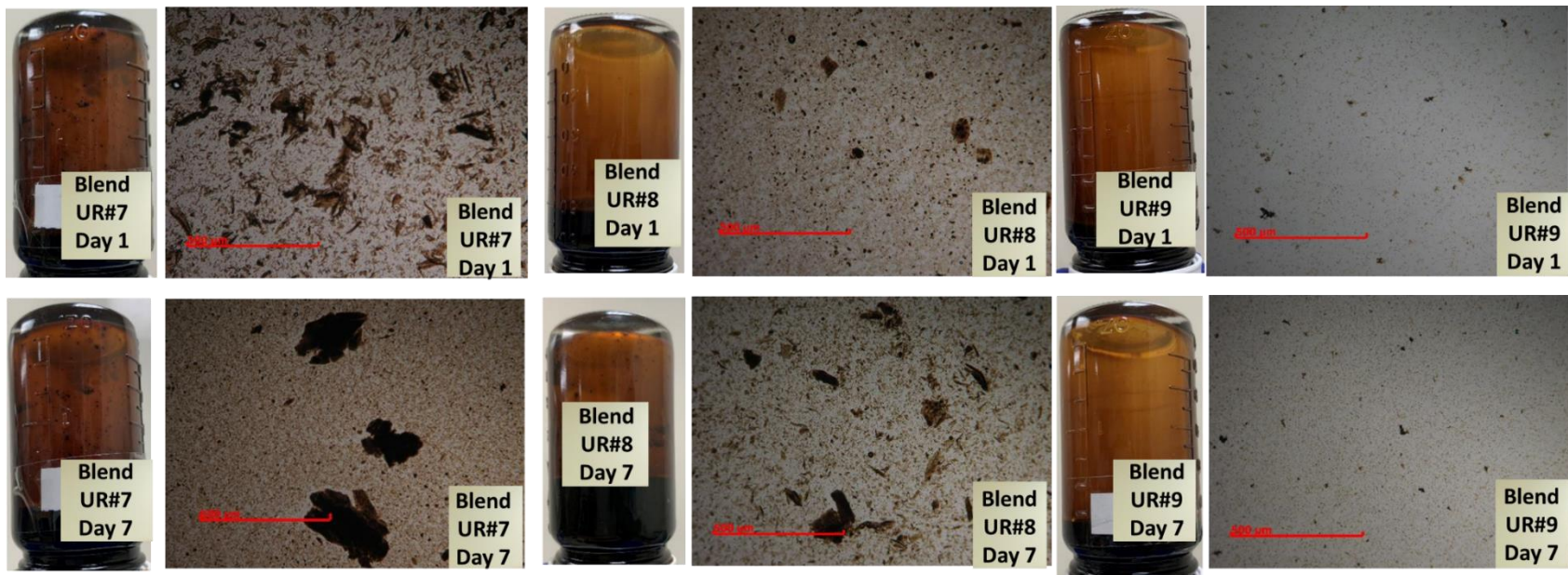


Figure 13 – Blending compatibility test for Biocrude B Run UR#7, 8, and 9 products

5.2.3. NMR SPECTROSCOPY CHARACTERIZATION OF HYDROTREATED BIOCRUDES

Biocrude A and its hydrotreated products were characterized using ^1H NMR, ^{13}C NMR, and ^{31}P NMR. Table 15 presents the results of the ^1H NMR characterization. Nearly 57% of protons in the Biocrude A are in the 0.0–1.5 ppm region, indicating abundance of alkane chains. At the same time, 13.2% of the protons in the 1.5–2.0 ppm region and 16.6% of the protons in the 2.0–3.0 ppm region correspond to alkyl groups adjacent to double bonds, aromatic rings, and carbonyl groups. The low percentage (5.3%) of protons in the 6.0–8.0 ppm region, which is characteristic of aromatic and conjugated olefin protons, is consistent with the minimum amount of aromatics in Biocrude A (Table 4).

Table 15 – ^1H NMR spectra of Biocrude A and its hydrotreated products

Hydrogen type assignment	Chemical shift region, ppm	Biocrude A, %	UR#1, %	UR#3, %	UR#4, %	UR#6, %
–CH ₃ and –CH ₂ – mostly in alkanes, far away from aromatics	0.0–1.5	56.7	59.9	59.0	62.1	67.8
aliphatic protons adjacent to double bonds or aliphatic OH	1.5–2.0	13.2	11.1	11.0	11.0	9.3
protons (CH ₃ , CH ₂ , CH) attached to aromatic rings, unsaturation located alpha to carbonyl group	2.0–3.0	16.6	16.9	17.6	17.0	14.7
protons attached to carbon in an ether group, aliphatic alcohols, and methylene groups between two aromatic rings	3.0–4.2	3.0	2.9	2.9	2.5	1.3
non-conjugated olefins, phenols and anomeric protons from carbohydrates, methoxy groups, alcohol	4.3–6.0	3.4	2.2	2.1	1.7	1.0
hetro-aromatic proton and conjugated olefinic proton	6.0–8.0	5.3	5.2	5.6	4.8	5.3
aldehydes, carboxylic acids, downfield aromatics	8.0–10.0	1.8	1.8	1.8	1.1	0.7

For Biocrude A Runs UR#1, 3, 4, 6, Table 15 shows a decrease in protons in the 3.0–4.2 and 4.3–6.0 ppm regions, resulting from the oxygen removal from ethers, aliphatic alcohols,

methoxy groups, and phenols. Further, a decrease in aldehydes and carboxylic acids was also present, as indicated by the changes in the 8.0–10.0 ppm region. All together, these changes are illustrative of the broad reactivity range of oxygen compounds in this biocrude.

Also in Table 15, the increase in alkyl groups in the 0.0–1.5 ppm region is indicative of the formation of alkanes during hydrotreating. The reduction in protons in the 1.5–2.0 ppm region points towards the saturation of olefins. The most notable changes in the 0.0–1.5 and 1.5–2.0 ppm regions are observed for the experiment with the highest oxygen removal, that is Run UR#6. The nearly constant percentage of protons in the 2.0–3.0, 6.0–8.0, and 8.0–10.0 ppm regions in Runs UR#1 and 3, shows that the process conditions of those experiments were not severe enough to convert aromatics, phenolics, and carboxylic acids.

The results of the ^{13}C NMR characterization are reported in Table 16. Biocrude A contains 67.0% alkyl carbon, with the majority (40.6%) being secondary and tertiary alkyl carbon. This shows that this biocrude is mostly composed of aliphatic chains, which is related to the feedstock used to produce Biocrude A. Proportionally to oxygen removal, the products show an increase in short chain aliphatic carbon (0–24 ppm) and less secondary and tertiary carbon (24–34 ppm), which implies a reduction in molecular weight. The total increase in alkyl chains (0–54 ppm) aligns with the ^1H NMR findings showing an increase in aliphatic protons (0.0–3.0 ppm).

The peaks in the 120–142 ppm region correspond to alkenes and aromatic carbons. Peaks in this region are seen to be less intense in the hydrotreated products as compared to the raw Biocrude A. Nevertheless, the percentage of carbon in the 120–142 ppm region is similar in all hydrotreated products, as reported in Table 16. Given that ^1H NMR analysis indicated that aromatics were the least reactive at the tested conditions, the trend for the carbon in the 120–142 ppm region in hydrotreated products can be largely attributed to stable aromatic carbon. The changes in the 142–166 ppm region correspond to the removal of aromatic oxygenates, such as phenols. This happens co-currently with the removal of alcohols, ethers, carbohydrates, and methoxy groups, as observed from Table 16. The reduction of carbon in the 166–200 ppm region also confirms the removal of carboxylic acids and carbonyls, in consistency with what is seen for the 8.0–10.0 ppm region in ^1H NMR (Table 15).

Table 16 – ^{13}C NMR spectra of Biocrude A and its hydrotreated products

Carbon type assignment	Chemical shift region, ppm	Biocrude A, %	UR#1, %	UR#3, %	UR#4, %	UR#6, %
aliphatics, mostly primary and some secondary carbon	0–24	19.5	22.0	24.3	27.0	28.3
mostly secondary and tertiary carbons	24–34	40.6	39.9	37.3	36.7	37.0
short, long, and branched aliphatics	0–54	67.0	70.1	70.9	72.3	75.1
alcohols, ethers, carbohydrates, methoxy groups	55–95	1.1	1.0	0.9	0.8	0.1
carbons in aromatics further from an O atom, olefins	120–142	25.0	22.9	23.0	22.4	22.3
aromatic C-O, phenols	142–166	4.2	3.9	3.5	3.1	1.7
carboxylic acids, carbonyls	166–200	2.7	2.1	1.7	1.4	0.8

Table 17 reports the hydroxyl content analysis obtained by ^{31}P NMR analysis. Carboxylic acids are predominant in the raw Biocrude A, with a moderate amount of phenolics and a small quantity of aliphatics. Hydroxyl content tends to decline as a function of oxygen removal, with the lowest hydroxyl levels being obtained for Run UR#6. Compared to carboxylic acids, phenolics generally appear to be more difficult to remove. This is because phenols, being an aromatic oxygen compound, require higher reaction severity to react.

Table 17 – ^{31}P NMR spectra of Biocrude A and its hydrotreated products

Hydroxyl type	Biocrude A	UR#1	UR#3	UR#4	UR#6
aliphatic OH, mmol OH/g	0.27	0.11	0.18	0.15	0.09
phenolic OH, mmol OH/g	1.05	0.41	0.75	0.65	0.52
carboxylic acid OH, mmol OH/g	1.69	0.74	1.02	1.08	0.54

Biocrude B was to be analyzed using the three aforementioned NMR spectroscopy methods, but at the time of the finalization of this report only the ^{31}P NMR analysis results were available due to unexpected technical issues with the NMR instrument. Table 18 presents the

hydroxyl content analysis results. It can be seen that the concentration of phenolics, which were the dominant hydroxyl species in Biocrude B, was substantially brought down from 2.10 to 1.20–1.50 mmol OH/g. Considering the blending compatibility test results, it is possible to hypothesize that phenolics reduction is likely a major contributor to improving the miscibility of this biocrude in petroleum. Aliphatic OH species and carboxylic acids are also important contributors, but they were found in smaller quantities in this particular biocrude.

Table 18 – ^{31}P NMR spectra of Biocrude B and its hydrotreated products

Hydroxyl type	Biocrude B	UR#7	UR#8	UR#9
aliphatic OH, mmol OH/g	0.26	<0.20	<0.20	<0.20
phenolic OH, mmol OH/g	2.10	1.50	1.50	1.20
carboxylic acid OH, mmol OH/g	0.87	0.22	0.24	<0.20

5.3. TASK 3 – BIOCRUDE CO-PROCESSING

The results of the preliminary co-processing tests with Biocrude A/VGO are presented in Tables 19 and 20. Table 19 provides the elemental analysis of the two Biocrude A/VGO feed blends and their corresponding co-processing products, together with the product from the baseline test with pure VGO. The main difference between the two feed blends is their oxygen content: the feed blend having 10 wt% raw Biocrude A (Run Co-Pro-R#1) has 1.9 wt% oxygen, whereas the one made with 10 wt% hydrotreated Biocrude A from Run UR#6 (Co-Pro-R#2) has 0.9 wt% oxygen. Sulfur (3.0 wt%) and nitrogen (0.4–0.5 wt%) contents are virtually identical in the two blends. The sulfur in these blends comes almost entirely from VGO, whereas the nitrogen is from both VGO and Biocrude A (see Table 4). After hydrotreating, the baseline product had the lowest levels of heteroatom (sulfur, nitrogen, and oxygen), followed by the product from the blend made with hydrotreated biocrude (Run Co-Pro-R#2). The product from the blend made with raw Biocrude A (Run Co-Pro-R#1) is the highest in sulfur and nitrogen among the three, highlighting the impact of oxygen species on co-processing.

Table 19 – Elemental composition of the feedstocks and products of the co-processing tests

Property	Feed Co-Pro-R#1 ¹⁾	Feed Co-Pro-R#2 ²⁾	Product Co-Pro-R#1	Product Co-Pro-R#2	Product Baseline Run
Carbon, wt%	83.5	84.3	86.5	87.1	87.3
Hydrogen, wt%	11.2	11.4	12.1	11.7	12.2
Nitrogen, wt%	0.4	0.5	0.3	0.1	0.03 ³⁾
Sulfur, wt%	3.0	3.0	0.9	0.6	0.3
Oxygen, wt%	1.9	0.9	0.3	0.3	0.2

¹⁾10 wt% raw Biocrude A in 90 wt% VGO.

²⁾10 wt% hydrotreated Biocrude A from Run UR#6 in 90 wt% VGO.

³⁾Measured by trace nitrogen method.

On comparing the co-processing experiments in terms of catalytic performance for hydrodesulfurization (HDS), hydrodenitrogenation (HDN), and hydrodeoxygenation (HDO) in Table 20, the benefit of biocrude pre-treatment through hydrotreating is emphasized further. Figure 14 illustrates this effect in a graphic manner. Co-processing the raw Biocrude A blend having 1.9 wt% oxygen (Run Co-Pro-R#1) leads to HDS (69.7%) and HDN (41.2%) levels well under the baseline test (90.0% HDS and 84.4% HDN) with pure VGO (0.5 wt% oxygen). This is most likely because more of the catalyst's capacity is used for removing oxygen from the raw Biocrude A (84.8% HDO). With its reduced oxygen content (0.9 wt%), the hydrotreated Biocrude A (Run Co-Pro-R#2) clearly diminishes this negative impact, giving HDS (81.6%) and HDN (75.3%) levels not far away from the baseline.

Table 20 – Catalytic performance of the co-processing tests

Catalytic performance	Co-Pro-R#1	Co-Pro-R#2	Baseline Run
Hydrodesulfurization, %	69.7	81.6	90.0
Hydrodenitrogenation, %	41.2	75.3	84.4
Hydrodeoxygenation, %	84.8	69.1	67.2

All together these results indicate that to be able to match the baseline product quality in a hydrotreating unit, co-processing severity would need to be increased depending on how much deoxygenation the biocrude had been subjected to. This, however, would likely increase hydrogen consumption in the refinery hydrotreating unit.

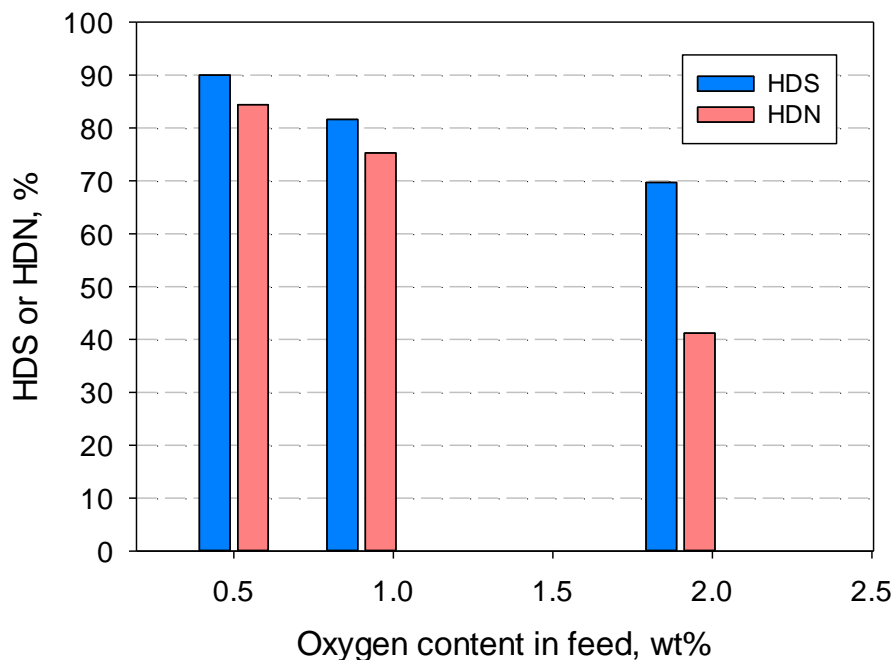


Figure 14 – Effect of feed oxygen content on catalytic performance during co-processing

6.0 CONCLUSIONS

A comprehensive study was conducted to establish a technology pathway to integrate biocrudes derived from different biomass origins into petroleum refining units. The major conclusions of each project task are the following:

Task 1

- The biocrude from agricultural waste was rich in oxygen and nitrogen (13.2 and 2.3 wt%, respectively) and was largely made up of carboxylic acids. The biocrude from forest residue biomass was high in oxygen (11.3 wt%), but did not have much nitrogen (0.3 wt%), and was phenolic in nature. Furthermore, both of them were completely immiscible in the reference petroleum feedstock (VGO).
- Pre-treating the two biocrudes with a range of solvents (toluene, dichloromethane, ethyl acetate, and *n*-pentane) did not produce a meaningful improvement in overall quality.

While there was rejection of high boiling components, the concentration of contaminants (such as oxygen and nitrogen) in the biocrudes remained practically unchanged.

- Biocrude pre-treatment based on hydrotreating was effective at reducing oxygen content down to 2.9–3.5 wt% (72.3–73.9% oxygen removal) and converting high boiling fractions into distillates. Owing to the thermal stability and reactivity of the biocrudes, hydrotreating was best achieved in gradual temperature steps without exceeding 300–320 °C and at relatively high catalyst-to-feed ratios.

Task 2

- The solvent-treated biocrudes were to a large extent immiscible with VGO, except for the ones treated with *n*-pentane. The major downside of using *n*-pentane is that it rejects a large portion of the biocrude (54.4–61.1%), further indicating that the solvent treatment approach with the solvents used in this work is not a viable option for enhancing biocrude quality for refinery intake.
- Hydrotreating the biocrudes to oxygen levels between 2.9–3.5 wt% was found to make them fully miscible in VGO and the resulting blend was stable over 7 days. Directionally, this could indicate that biocrudes need to be deoxygenated to under 3.5 wt% oxygen to be acceptable for refinery intake for VGO hydrotreating.
- Through the use of NMR spectroscopy techniques it was possible to identify carboxylic acids and phenolics as the major contributors to the miscibility issues of the two biocrudes.

Task 3

- Co-processing the hydrotreated biocrude with VGO was found to significantly reduce the impacts on catalytic performance for HDS and HDN with respect to directly co-processing raw biocrude. However, co-processing severity would still need to be increased depending on how much deoxygenation the biocrude had been subjected to.

7.0 ACKNOWLEDGMENTS

The authors would like to acknowledge Alberta Innovates' Clean Resources Program and Government of Canada's Office of Energy Research and Development (OERD) for co-funding this project. The authors are grateful to NULIFE GreenTech Inc. and Steeper Energy for kindly supplying the HTL biocrude samples used in this study. The authors also would like to thank the pilot plant and analytical lab staff at CanmetENERGY Devon. Technical comments and

suggestions from Dr. Rafal Gieleciak and assistance in internal review process from Ms. K. J. Meharg are appreciated.

The authors would like to specially thank Mehr Nikoo and Susan Carlisle of Alberta Innovates for their kind support throughout the project. Technical advice from the following is also greatly appreciated: Devin O’Grady and David Schick of Canadian Fuels Association, Prashant Reddy of Alberta Climate Change Office, Mario Ochoa of Suncor Energy, and Gary Lee of Parkland Fuel Corporation.

APPENDIX A: SIMULATED DISTILLATION DATA SETS

Table A 1 – SimDis data for Biocrude A

wt%	BP, °C	wt%	BP, °C	wt%	BP, °C	wt%	BP, °C
0.5	124.4	26	374.8	52	521.2	78	
1	175.0	27	375.4	53	528.0	79	
2	221.6	28	375.8	54	534.8	80	
3	252.2	29	376.2	55	539.6	81	
4	272.6	30	376.8	56	546.2	82	
5	288.6	31	378.0	57	554.0	83	
6	302.2	32	382.0	58	562.8	84	
7	314.4	33	387.6	59	571.6	85	
8	326.6	34	391.4	60	581.4	86	
9	339.0	35	397.6	61	593.0	87	
10	344.6	36	405.4	62	605.0	88	
11	347.2	37	413.0	63	616.8	89	
12	350.8	38	420.0	64	639.6	90	
13	360.8	39	427.2	65	676.0	91	
14	363.2	40	434.2	66	719.6	92	
15	364.8	41	441.8	67		93	
16	367	42	449.4	68		94	
17	368.6	43	457.2	69		95	
18	369.6	44	465.0	70		96	
19	370.6	45	472.2	71		97	
20	371.4	46	479.6	72		98	
21	372.2	47	487.2	73		99	
22	372.8	48	494.8	74		99.5	
23	373.4	49	502.0	75			
24	373.8	50	508.6	76			
25	374.6	51	515.0	77			

Table A 2 – SimDis data for Biocrude B

wt%	BP, °C	wt%	BP, °C	wt%	BP, °C	wt%	BP, °C
0.5	111.2	26	374.6	52	563.4	78	
1	169.2	27	375.8	53	580.0	79	
2	193.8	28	377.2	54	601.6	80	
3	210.6	29	380.2	55	635.4	81	
4	226.4	30	384.0	56	711.6	82	
5	239.6	31	389.2	57	720.0	83	
6	251.2	32	393.2	58		84	
7	261.2	33	395.6	59		85	
8	272.2	34	397.2	60		86	
9	281.4	35	401.4	61		87	
10	291.4	36	410.4	62		88	
11	300.8	37	418.2	63		89	
12	309.8	38	427.6	64		90	
13	317.2	39	434.6	65		91	
14	324.8	40	440.8	66		92	
15	331.2	41	449.4	67		93	
16	336.8	42	458.4	68		94	
17	342.6	43	465.6	69		95	
18	348.2	44	473.8	70		96	
19	354.4	45	483.6	71		97	
20	356.4	46	494.4	72		98	
21	358.8	47	504.6	73		99	
22	365.2	48	514.2	74		99.5	
23	369.2	49	524.4	75			
24	371.6	50	536.4	76			
25	373.2	51	548.6	77			

Table A 3 – SimDis data for VGO

wt%	BP, °C	wt%	BP, °C	wt%	BP, °C	wt%	BP, °C
0.5	290.0	26	397.8	52	437.4	78	481.6
1	307.4	27	399.6	53	438.8	79	483.8
2	321.4	28	401.2	54	440.2	80	486.0
3	330.4	29	403.0	55	441.8	81	488.2
4	337.0	30	404.6	56	443.2	82	490.6
5	342.8	31	406.4	57	444.8	83	493.2
6	347.4	32	408.0	58	446.4	84	495.8
7	351.4	33	409.6	59	447.8	85	498.6
8	355.2	34	411.2	60	449.2	86	501.4
9	358.4	35	412.6	61	450.8	87	504.4
10	361.6	36	414.2	62	452.6	88	507.8
11	364.6	37	415.8	63	454.2	89	511.4
12	367.6	38	417.2	64	455.8	90	515.4
13	370.0	39	418.8	65	457.4	91	520.0
14	372.6	40	420.2	66	459.0	92	524.0
15	375.0	41	421.6	67	460.8	93	532.0
16	377.4	42	423.0	68	462.6	94	541.0
17	379.6	43	424.4	69	464.4	95	555.8
18	382.0	44	426.0	70	466.2	96	634.6
19	384.2	45	427.4	71	468.0	97	481.6
20	386.2	46	428.8	72	469.8	98	483.8
21	388.2	47	430.0	73	471.6	99	486.0
22	390.2	48	431.6	74	473.4	99.5	488.2
23	392.2	49	433.0	75	475.4		
24	394.0	50	434.4	76	477.4		
25	396.0	51	436.0	77	479.4		

Table A 4 – SimDis data for Biocrude A extract using *n*-pentane

wt%	BP, °C	wt%	BP, °C	wt%	BP, °C	wt%	BP, °C
0.5	37.4	26	362.2	52	381.2	78	603.4
1	39.0	27	367.2	53	381.4	79	637.6
2	88.2	28	368.8	54	381.8	80	705.0
3	188.8	29	370.0	55	382.0	81	720.0
4	208.8	30	371.2	56	382.4	82	
5	224.2	31	372.0	57	383.4	83	
6	238.8	32	372.8	58	386.6	84	
7	251.8	33	373.4	59	390.0	85	
8	263.2	34	374.0	60	392.6	86	
9	273.4	35	374.6	61	396.4	87	
10	283.6	36	375.2	62	403.4	88	
11	292.6	37	375.6	63	411.2	89	
12	301.2	38	376.2	64	418.6	90	
13	310.4	39	376.6	65	426.6	91	
14	319.6	40	377.0	66	434.2	92	
15	329.6	41	377.4	67	442.6	93	
16	340.2	42	377.8	68	452.2	94	
17	343.8	43	378.2	69	463.0	95	
18	347.0	44	378.4	70	474.4	96	
19	349.0	45	378.8	71	487.8	97	
20	350.6	46	379.2	72	502.2	98	
21	352.0	47	379.4	73	514.2	99	
22	356.2	48	379.8	74	527.2	99.5	
23	362.0	49	380.0	75	544.6		
24	363.2	50	380.4	76	571.6		
25	364.2	51	380.6	77	381.2		

Table A 5 – SimDis data for Biocrude A extract using toluene

wt%	BP, °C	wt%	BP, °C	wt%	BP, °C	wt%	BP, °C
0.5	105.0	26	374.2	52	452.2	78	
1	105.4	27	375.0	53	459.6	79	
2	106.0	28	375.6	54	467.2	80	
3	180.2	29	376.2	55	474.6	81	
4	217.4	30	376.8	56	482.2	82	
5	242.0	31	377.4	57	490.8	83	
6	261.2	32	378.0	58	499.4	84	
7	275.8	33	378.4	59	507.4	85	
8	289.0	34	378.8	60	514.8	86	
9	300.4	35	379.2	61	522.6	87	
10	310.8	36	379.6	62	532.2	88	
11	321.4	37	380.2	63	540.8	89	
12	332.4	38	380.6	64	551.4	90	
13	341.4	39	381.2	65	563.4	91	
14	346.4	40	383.4	66	576.0	92	
15	349.2	41	387.8	67	590.4	93	
16	351.0	42	391.0	68	605.2	94	
17	357.2	43	394.2	69	625.4	95	
18	362.2	44	399.4	70	651.6	96	
19	363.8	45	406.0	71	687.4	97	
20	366.4	46	412.2	72	720.0	98	
21	368.8	47	418.6	73		99	
22	370.4	48	425.2	74		99.5	
23	371.6	49	431.4	75			
24	372.6	50	438.2	76			
25	373.4	51	445.0	77			

Table A 6 – SimDis data for Biocrude A extract using dichloromethane

wt%	BP, °C	wt%	BP, °C	wt%	BP, °C	wt%	BP, °C
0.5	104.8	26	375.0	52	581.0	78	
1	130.6	27	375.6	53	600.0	79	
2	208.4	28	376.0	54	621.0	80	
3	238.0	29	376.4	55	650.4	81	
4	260.4	30	377.2	56	690.2	82	
5	277.4	31	379.4	57	720.0	83	
6	292.4	32	385.4	58		84	
7	305.6	33	389.6	59		85	
8	318.2	34	394.6	60		86	
9	331.4	35	402.6	61		87	
10	341.6	36	410.8	62		88	
11	345.8	37	418.8	63		89	
12	348.2	38	427.2	64		90	
13	355.2	39	435.6	65		91	
14	362.0	40	444.2	66		92	
15	363.8	41	453.4	67		93	
16	366.2	42	462.8	68		94	
17	368.0	43	472.2	69		95	
18	369.4	44	482.2	70		96	
19	370.4	45	493.2	71		97	
20	371.4	46	504.0	72		98	
21	372.2	47	514.0	73		99	
22	372.8	48	524.6	74		99.5	
23	373.4	49	536.6	75			
24	374.0	50	549.2	76			
25	374.6	51	564.6	77			

Table A 7 – SimDis data for Biocrude A extract using ethyl acetate

wt%	BP, °C	wt%	BP, °C	wt%	BP, °C	wt%	BP, °C
0.5	84.6	26	376.0	52	503.6	78	
1	181.4	27	376.4	53	512.4	79	
2	221.4	28	377.0	54	520.6	80	
3	247.4	29	377.4	55	530.8	81	
4	267.2	30	378.0	56	540.6	82	
5	282.6	31	378.4	57	552.4	83	
6	296.0	32	378.8	58	565.8	84	
7	307.8	33	379.2	59	580.0	85	
8	319.2	34	380.0	60	596.8	86	
9	331.2	35	382.4	61	614.4	87	
10	341.4	36	387.4	62	640.0	88	
11	346.2	37	390.8	63	674.0	89	
12	348.8	38	394.4	64	716.0	90	
13	350.8	39	400.8	65	720.0	91	
14	359.8	40	408.0	66		92	
15	362.8	41	415.0	67		93	
16	364.6	42	422.0	68		94	
17	367.4	43	429.0	69		95	
18	369.2	44	436.2	70		96	
19	370.6	45	443.8	71		97	
20	371.6	46	451.6	72		98	
21	372.6	47	459.8	73		99	
22	373.4	48	468.2	74		99.5	
23	374.2	49	476.4	75			
24	374.8	50	485.2	76			
25	375.4	51	494.8	77			

Table A 8 – SimDis data for Biocrude B extract using *n*-pentane

wt%	BP, °C	wt%	BP, °C	wt%	BP, °C	wt%	BP, °C
0.5		26	313.4	52	376.4	78	463.0
1		27	317.0	53	377.0	79	469.6
2	36.0	28	321.0	54	377.8	80	477.8
3	38.2	29	324.6	55	378.6	81	488.6
4	105.0	30	328.4	56	379.4	82	500.4
5	159.4	31	331.2	57	380.2	83	511.6
6	173.2	32	333.6	58	382.0	84	524.2
7	187.6	33	337.2	59	383.8	85	540.2
8	197.8	34	341.2	60	386.2	86	562.6
9	207.2	35	343.2	61	389.4	87	591.2
10	215.0	36	346.6	62	392.6	88	650.6
11	224.0	37	350.0	63	394.6	89	720.0
12	229.6	38	352.6	64	396.2	90	
13	238.0	39	355.6	65	397.6	91	
14	243.8	40	356.8	66	398.6	92	
15	251.2	41	357.6	67	399.6	93	
16	257.6	42	358.4	68	402.4	94	
17	263.4	43	361.0	69	409.4	95	
18	269.8	44	364.8	70	414.6	96	
19	275.2	45	367.8	71	421.4	97	
20	281.6	46	369.6	72	429.0	98	
21	287.6	47	371.2	73	433.8	99	
22	293.0	48	372.6	74	439.4	99.5	
23	298.4	49	373.8	75	442.6		
24	303.2	50	374.6	76	449.4		
25	308.4	51	375.4	77	456.8		

Table A 9 – SimDis data for Biocrude B extract using toluene

wt%	BP, °C	wt%	BP, °C	wt%	BP, °C	wt%	BP, °C
0.5	104.0	26	292.2	52	383.2	78	559.6
1	104.4	27	299.0	53	387.2	79	574.2
2	105.0	28	305.4	54	391.0	80	590.6
3	105.4	29	311.8	55	393.6	81	611.6
4	105.8	30	316.8	56	395.4	82	639.0
5	106.2	31	322.2	57	396.8	83	683.8
6	106.4	32	327.4	58	399.0	84	720.0
7	106.8	33	331.4	59	405.4	85	
8	107.0	34	335.8	60	411.6	86	
9	107.2	35	340.8	61	418.8	87	
10	107.6	36	344.0	62	426.0	88	
11	107.8	37	348.8	63	432.0	89	
12	108.0	38	353.0	64	438.6	90	
13	108.2	39	355.8	65	442.8	91	
14	173.8	40	357.0	66	450.0	92	
15	194.8	41	359.0	67	457.4	93	
16	207.8	42	363.8	68	463.4	94	
17	220.4	43	367.4	69	470.0	95	
18	229.0	44	369.6	70	477.2	96	
19	239.4	45	371.4	71	486.0	97	
20	248.0	46	372.8	72	495.4	98	
21	256.6	47	373.8	73	504.4	99	
22	263.4	48	375.0	74	513.2	99.5	
23	270.8	49	376.0	75	522.6		
24	277.8	50	377.4	76	534.0		
25	285.2	51	380.0	77	545.6		

Table A 10 – SimDis data for Biocrude B extract using dichloromethane

wt%	BP, °C	wt%	BP, °C	wt%	BP, °C	wt%	BP, °C
0.5	36.2	26	366.2	52	517.6	78	
1	37.4	27	369.0	53	529.8	79	
2	47.4	28	370.8	54	543.0	80	
3	146.2	29	372.4	55	558.4	81	
4	184.0	30	373.6	56	575.0	82	
5	202.6	31	374.8	57	593.8	83	
6	217.2	32	377.0	58	618.4	84	
7	230.6	33	380.6	59	652.4	85	
8	242.8	34	385.2	60	702.4	86	
9	255.0	35	390.2	61	720.0	87	
10	264.2	36	393.0	62		88	
11	273.2	37	394.8	63		89	
12	283.4	38	396.8	64		90	
13	292.6	39	404.4	65		91	
14	301.0	40	412.2	66		92	
15	309.6	41	420.6	67		93	
16	316.6	42	429.2	68		94	
17	323.6	43	436.8	69		95	
18	329.4	44	442.6	70		96	
19	335.0	45	451.2	71		97	
20	341.4	46	460.0	72		98	
21	345.6	47	467.0	73		99	
22	351.2	48	475.6	74		99.5	
23	355.2	49	485.8	75			
24	356.6	50	496.8	76			
25	361.4	51	507.4	77			

Table A 11 – SimDis data for Biocrude B extract using ethyl acetate

wt%	BP, °C	wt%	BP, °C	wt%	BP, °C	wt%	BP, °C
0.5	60.0	26	357.2	52	464.6	78	
1	66.8	27	362.2	53	471.2	79	
2	136.4	28	365.6	54	478.2	80	
3	185.4	29	367.8	55	486.2	81	
4	203.8	30	369.4	56	494.4	82	
5	216.8	31	370.6	57	502.2	83	
6	228.6	32	371.8	58	509.8	84	
7	240.2	33	372.8	59	517.0	85	
8	251.2	34	374.4	60	525.2	86	
9	259.6	35	377.4	61	534.6	87	
10	268.6	36	381.0	62	544.0	88	
11	276.0	37	385.6	63	554.8	89	
12	284.6	38	389.4	64	566.2	90	
13	292.6	39	391.6	65	578.0	91	
14	300.0	40	393.2	66	591.4	92	
15	307.4	41	394.4	67	607.8	93	
16	314.4	42	400.2	68	656.2	94	
17	320.0	43	407.6	69	701.0	95	
18	325.8	44	413.8	70	720.0	96	
19	330.6	45	420.8	71		97	
20	335.6	46	428.0	72		98	
21	341.0	47	434.0	73		99	
22	344.4	48	439.2	74		99.5	
23	349.8	49	445.2	75			
24	354.0	50	452.4	76			
25	355.4	51	459.2	77			

Table A 12 – SimDis data for Run UR#3 product

wt%	BP, °C	wt%	BP, °C	wt%	BP, °C	wt%	BP, °C
0.5	108.8	26	368.2	52	493.8	78	637.0
1	126.2	27	369.2	53	499.4	79	644.8
2	167.0	28	370.6	54	504.8	80	653.8
3	195.6	29	371.6	55	510.2	81	664.0
4	218.8	30	372.6	56	515.6	82	677.2
5	238.8	31	373.6	57	520.8	83	693.2
6	255.8	32	374.2	58	526.0	84	712.4
7	269.0	33	374.8	59	531.2	85	719.4
8	278.2	34	379.0	60	536.4	86	
9	287.8	35	385.4	61	541.4	87	
10	297.2	36	390.2	62	546.6	88	
11	301.2	37	395.4	63	551.6	89	
12	302.6	38	402.0	64	556.6	90	
13	309.2	39	409.4	65	561.8	91	
14	315.2	40	416.2	66	566.8	92	
15	317.6	41	422.8	67	571.6	93	
16	326.4	42	429.2	68	576.8	94	
17	335.0	43	435.8	69	582.2	95	
18	341.8	44	442.0	70	587.4	96	
19	344.8	45	448.8	71	592.6	97	
20	349.2	46	455.6	72	598.2	98	
21	357.2	47	462.4	73	604.2	99	
22	363.0	48	469.0	74	610.2	99.5	
23	364.6	49	475.2	75	616.2		
24	366.6	50	481.4	76	622.8		
25	367.6	51	487.6	77	630.0		

Table A 13 – SimDis data for Run UR#4 product

wt%	BP, °C	wt%	BP, °C	wt%	BP, °C	wt%	BP, °C
0.5	107.8	26	365.2	52	477.8	78	642.8
1	111.0	27	367.0	53	484.2	79	653.8
2	156.8	28	368.2	54	490.8	80	666.8
3	183.6	29	369.4	55	497.0	81	683.0
4	204.8	30	370.6	56	502.8	82	701.6
5	220.0	31	371.8	57	508.6	83	719.4
6	233.8	32	372.8	58	514.4	84	
7	247.0	33	373.8	59	520.2	85	
8	258.6	34	374.6	60	526.0	86	
9	268.2	35	375.4	61	531.6	87	
10	275.6	36	376.2	62	537.2	88	
11	284.8	37	379.8	63	542.6	89	
12	292.2	38	386.0	64	548.2	90	
13	298.4	39	390.6	65	554.0	91	
14	301.8	40	396.0	66	559.6	92	
15	305.2	41	402.8	67	565.4	93	
16	312.0	42	410.0	68	570.8	94	
17	315.8	43	417.2	69	576.6	95	
18	321.0	44	423.8	70	582.6	96	
19	329.0	45	430.6	71	588.6	97	
20	336.8	46	437.4	72	595.0	98	
21	342.4	47	444.0	73	601.8	99	
22	345.8	48	451.0	74	609.0	99.5	
23	350.0	49	458.0	75	616.4		
24	357.6	50	465.0	76	624.6		
25	363.2	51	471.6	77	633.4		

Table A 14 – SimDis data for Run UR#6 product

wt%	BP, °C	wt%	BP, °C	wt%	BP, °C	wt%	BP, °C
0.5	107.6	26	312.2	52	422.6	78	610.6
1	108.2	27	314.8	53	430.2	79	619.2
2	109.0	28	316.2	54	437.6	80	628.8
3	137.8	29	317.0	55	444.8	81	638.8
4	164.8	30	318.2	56	452.8	82	651.0
5	184.2	31	323.4	57	460.4	83	666.0
6	198.0	32	329.0	58	468.2	84	687.4
7	209.8	33	334.8	59	475.6	85	715.0
8	219.2	34	340.8	60	483.0	86	719.4
9	228.0	35	344.4	61	490.6	87	
10	236.6	36	348.8	62	497.8	88	
11	245.0	37	355.0	63	504.8	89	
12	252.6	38	361.6	64	511.6	90	
13	259.4	39	366.0	65	518.6	91	
14	265.6	40	367.8	66	525.6	92	
15	270.8	41	369.8	67	532.6	93	
16	275.6	42	371.2	68	539.4	94	
17	281.8	43	372.6	69	546.2	95	
18	286.6	44	373.6	70	553.2	96	
19	290.8	45	374.2	71	560.2	97	
20	296.0	46	379.6	72	566.8	98	
21	299.2	47	386.6	73	573.6	99	
22	301.8	48	391.8	74	580.6	99.5	
23	302.6	49	399.2	75	587.6		
24	303.4	50	407.4	76	594.8		
25	308.0	51	415.2	77	602.4		

Table A 15 – SimDis data for Run UR#7 product

wt%	BP, °C	wt%	BP, °C	wt%	BP, °C	wt%	BP, °C
0.5	85.4	26	325.0	52	426.4	78	652.8
1	107.2	27	328.4	53	431.6	79	674.0
2	117.4	28	330.2	54	436.4	80	706.2
3	151.8	29	333.2	55	440.2	81	720.0
4	173.0	30	336.6	56	445.4	82	
5	195.8	31	338.8	57	452.0	83	
6	211.6	32	342.2	58	459.2	84	
7	225.0	33	344.2	59	466.6	85	
8	235.8	34	348.6	60	474.0	86	
9	246.0	35	352.2	61	481.4	87	
10	256.2	36	355.4	62	489.6	88	
11	264.6	37	356.4	63	497.8	89	
12	271.8	38	360.4	64	505.4	90	
13	279.4	39	365.0	65	513.0	91	
14	285.6	40	368.2	66	520.8	92	
15	291.6	41	372.4	67	529.6	93	
16	295.8	42	376.6	68	538.4	94	
17	299.8	43	381.0	69	547.6	95	
18	301.0	44	385.8	70	557.4	96	
19	303.2	45	389.0	71	567.2	97	
20	307.4	46	392.2	72	577.2	98	
21	311.0	47	397.6	73	587.6	99	
22	314.4	48	403.2	74	598.6	99.5	
23	315.6	49	408.8	75	610.6		
24	318.2	50	414.6	76	623.0		
25	321.8	51	420.6	77	636.8		

Table A 16 – SimDis data for Run UR#8 product

wt%	BP, °C	wt%	BP, °C	wt%	BP, °C	wt%	BP, °C
0.5	76.6	26	317.6	52	409.6	78	641.6
1	107.0	27	320.4	53	415.6	79	661.2
2	123.2	28	323.8	54	421.6	80	691.2
3	149.2	29	327.4	55	427.6	81	720.0
4	172.0	30	329.6	56	432.8	82	
5	191.2	31	332.4	57	438.0	83	
6	206.2	32	334.8	58	442.0	84	
7	217.2	33	338.4	59	448.4	85	
8	228.2	34	341.6	60	455.8	86	
9	238.4	35	343.6	61	463.8	87	
10	247.6	36	347.2	62	471.8	88	
11	256.6	37	351.0	63	479.8	89	
12	264.6	38	355.0	64	488.6	90	
13	270.8	39	356.4	65	497.6	91	
14	278.0	40	358.4	66	506.0	92	
15	284.4	41	362.6	67	514.4	93	
16	289.8	42	367.0	68	523.0	94	
17	294.2	43	369.6	69	533.0	95	
18	297.8	44	373.6	70	542.4	96	
19	300.8	45	377.8	71	553.0	97	
20	301.8	46	382.0	72	563.8	98	
21	303.2	47	386.6	73	574.6	99	
22	307.0	48	389.8	74	586.2	99.5	
23	310.6	49	393.0	75	598.2		
24	314.2	50	398.2	76	611.6		
25	315.6	51	403.8	77	626.0		

Table A 17 – SimDis data for Run UR#9 product

wt%	BP, °C	wt%	BP, °C	wt%	BP, °C	wt%	BP, °C
0.5	36.0	26	308.2	52	382.4	78	562.2
1	82.0	27	311.6	53	386.4	79	573.2
2	104.8	28	314.4	54	390.0	80	584.8
3	105.4	29	315.4	55	394.4	81	596.6
4	112.8	30	317.2	56	399.2	82	609.6
5	135.4	31	319.6	57	404.2	83	623.0
6	157.4	32	322.6	58	409.2	84	637.6
7	169.0	33	325.4	59	414.6	85	654.0
8	185.0	34	328.6	60	420.0	86	675.2
9	201.6	35	329.8	61	425.6	87	703.0
10	213.4	36	332.8	62	431.0	88	720.0
11	225.2	37	335.2	63	436.2	89	
12	234.4	38	338.2	64	440.0	90	
13	244.4	39	340.2	65	445.2	91	
14	253.4	40	342.8	66	452.4	92	
15	261.8	41	345.2	67	460.0	93	
16	269.2	42	348.8	68	468.2	94	
17	276.0	43	352.0	69	476.4	95	
18	282.2	44	355.2	70	485.2	96	
19	287.8	45	356.2	71	494.4	97	
20	292.8	46	359.4	72	503.2	98	
21	296.2	47	363.4	73	511.8	99	
22	300.0	48	367.4	74	520.6	99.5	
23	301.0	49	370.8	75	530.6		
24	301.8	50	374.6	76	540.6		
25	304.8	51	378.6	77	551.0		

A TECHNO-ECONOMICAL ASSESSMENT OF COPROCESSING HYDROTHERMAL LIQUEFACTION BIO-CRUDE AND VGO THROUGH THE HYDROPROCESSING AND FLUID CATALYTIC CRACKING UNITS

Final Report

Prepared for:

**CanmetEnergy Devon
Natural Resources Canada (NRCan)
1 Oil Patch Drive
Devon, Alberta T9G 1A8**

Submitted by:

**Abayomi O. Oni, Debarati Biswas, Vinoj Kurian, Arun
Srikumar, Amit Kumar**

**Department of Mechanical Engineering
University of Alberta, Edmonton, Canada**

March 31, 2022

Contact Information

For further information and clarification, please contact Dr. Amit Kumar. Contact details are given below.

Amit Kumar, Ph.D., P.Eng., FCSBE

Professor

NSERC/Cenovus/Alberta Innovates Associate Industrial Research Chair in Energy and Environmental Systems Engineering

Cenovus Energy Endowed Chair in Environmental Engineering

Deputy Director - Future Energy Systems (FES)

Faculty of Engineering

Department of Mechanical Engineering

10-263 Donadeo Innovation Centre for Engineering

9211 116 Street NW

University of Alberta

Edmonton, Alberta, Canada T6G 1H9

Tel: +1-780-492-7797

E-mail to: amit.kumar@ualberta.ca

<http://www.ualbertaenergysystems.ca>

Disclaimers

“The University of Alberta (UofA) is furnishing this report ‘as is’. UofA does not provide any warranty of the contents of the report whatsoever, whether express, implied, or statutory, including, but not limited to, any warranty of merchantability or fitness for a particular purpose or any warranty that the contents of the report will be error-free.”

All conclusions, recommendations, and opinions are solely the authors’ and are endorsed neither by the financial sponsor of this work nor by the many people who offered comments and suggestions. All developed results are based on the publicly available data and information.

This document is the final report.

Acknowledgments

The authors are grateful to CanmetEnergy Devon, Natural Resources Canada (NRCan) and Alberta Innovates for the support to carry out this project.

The authors would like to thank the steering committee for their frequent input and feedback during the term of this project. The steering committee was made up of Anton. Alvarez-Majmutov and Jinwen Chen from CanmentEnergy Devon.

The authors would like to thank Astrid Blodgett for editing this report.

All conclusions, recommendations, and opinions are solely the authors' and are endorsed neither by the financial sponsor of this work nor by the many people who offered comments and suggestions. All developed results are based on publicly available data and information.

Executive Summary

Greenhouse gas (GHG) emissions from the use of fossil fuels are the main contributors to human-caused climate change impacts. There are international and national commitments to reduce the impacts of GHG emissions by promoting low-carbon fuels. In Canada, the federal government developed the Clean Fuel Standard (CFS), which requires that the GHG emission intensities of fuels used in the country be lowered. It is a performance-based approach that encourages the use of low-carbon fuels, energy, and technologies. The CFS sets requirements to reduce the life cycle GHG emission intensities of fuels supplied each year. These require refineries in Canada to find ways to lower transportation fuels' GHG footprints. To meet the goal of a low-carbon fuel, coprocessing bio-crude from renewable sources with a refinery intermediate has been proposed and is one of the pathways. Coprocessing bio-crude with petroleum residue oil in an existing refinery has the potential to address these challenges and is currently being investigated.

Hydrothermally liquefied (HTL) bio-crude is a promising feed for coprocessing. It has a relatively low oxygen content and is expected to require mild hydrotreating compared to bio-based pyrolysis oil. While several experimental studies have shown that coprocessing HTL bio-crude with vacuum gas oil (VGO) in the hydroprocessing and fluid catalytic cracking (FCC) units is feasible to produce transportation fuels, few studies have reported its economic impact. In this study, we explore the cost of producing fuels from coprocessing HTL bio-crude and VGO in the hydroprocessing and FCC units. The specific objectives of this study are to:

- Develop a process model for coprocessing HTL bio-crude with VGO in hydroprocessing and FCC units.
- Evaluate the incremental change in production cost of transportation fuels produced from coprocessing HTL bio-crude with VGO in the hydroprocessing and FCC unit.

To achieve these objectives, process models were developed for a 75,000 barrel per day feedstock to extract the data needed to perform techno-economic analyses. We considered two scenarios for both the hydroprocessing and FCC units. Each processing unit handled pure VGO and a VGO blend with HTL distillate. In the first scenario, we developed a simulation model to process pure VGO in the hydroprocessing and FCC units. For the second scenario, we blended HTL bio-crude distillate with VGO at a ratio of 1:9 by weight for the same capacity as in the first scenario. The hydroprocessed product serves as feedstock to the FCC unit for further processing into transportation fuels. We extracted equipment size, utility, and material data from these models to conduct a techno-economic analysis. In this report, the first and second scenarios are referred to as pure VGO and HTL blend, respectively. The input data to the process models were the experimental results of coprocessed VGO with a 10% HTL blend from the CanmetEnergy Devon. These results were also used to validate the output of the process models.

The hydroprocessing plant comprises the preprocessing unit. In the preprocessing unit, 55.1% (13.6 kg/s) of the raw HTL bio-crude meets the distillate requirement for a 10% blend with VGO. 24.7 kg/s of HTL bio-crude is required to produce the distillate. The boiling range of the distillate fraction is from IBP-521°C with its D1160 95% at 476°C. 44.9% of the raw feed is discharged as residue (D1160 5% at 465°C).

Table E1 presents the utility consumed in the hydroprocessing units. The hydrotreated (HT) blend consumes more utilities than pure VGO, primarily because of the additional energy needed to separate distillate from bio-crude. Table E2 presents the utilities consumed in the FCC units. The

main utilities consumed in the FCC units are make-up water (for cooling), electricity, and make-up catalyst. The amine regenerator in both cases does not require fuel energy to generate steam as there is sufficient process heat within the plant. For the unused process heat, we assume it is supplied to other units in the refinery, a common practice to improve energy use and lower operating costs.

Table E1: Utility consumed in the hydroprocessing units

Utility	HT-VGO	HT blend
Natural gas (kg/s)	0.86	1.08
Make-up water (kg/s)	31.34	33.73
Electricity (MWh)	653.73	687.35
Hydrogen consumed (scf/bbl.)	940.50	944.30

Table E2: Utility consumed in the FCC unit

Utility	Pure VGO	HTL blend
Make-up water kg/s	93.9	94.7
Steam credit(kg/s)	12.7	13.0
Column stripping steam (kg/s)	7.63	7.63
Dispersion steam (kg/s)	2.62	2.65
Riser stripping steam (kg/s)	4.90	5.19
Electricity (MWh)	67.95	71.91
Electricity credit (MWh)	447.27	478.54
Fresh catalyst make-up rate (kg/h)	238.2	408.8

The production costs of HT-VGO and a HT blend are summarized in Table E3. The cost of producing an HT blend in the hydroprocessing unit is \$95.30/bbl, which is 18.7% more than an HT-VGO. The higher production cost is due to the increase in the cost of feedstock and the cost of integrating the preprocessing unit. The feedstock cost increases because of the high cost of bio-crude. Bio-crude price raises the feedstock cost by 20.8%, an estimated \$36,773 per day. The economic impact of the preprocessing unit is not significant; it is less than 1.0% of the HT blend production cost. The cost of preprocessing a tonne of HTL bio-crude is \$16.40.

Table E3: Cost breakdown of HT blend and HT-VGO products for a hydroprocessing plant capacity of 75,000 barrels per day at a \$56.50/bbl crude oil price and \$586.50/tonne HTL bio-oil price

Components	HT blend	HT-VGO
Capital cost, \$M	336.2	327.3
Manufacturing cost (COM), \$M/y	2,288.1	1,922
Raw material, \$M/y	1,775.0	1,481.0

Components	HT blend	HT-VGO
Utilities, \$M/y	17.9	15.8
Operating labor, \$M/y	8.3	8.3
Production cost, \$/bbl.	95.30	81.30

A summary of the economic evaluation of the overall system (hydroprocessing and FCC units) is given in Table E4. The cost of products under the pure VGO scenario is lower than the HTL-blend scenario. The cost of producing a liter of liquefied petroleum gas, gasoline, light cycle oil (LCO), and heavy cycle oil (HCO) in the HTL blend scenario is increased by $\phi 8.4 \pm 4.1/L$, $\phi 9.0 \pm 4.4/L$, $\phi 10.5 \pm 5.2/L$, and $\phi 10.4 \pm 5.1/L$, respectively, at a 90% confidence interval. The variation in the cost increase is primarily due to crude oil and bio-crude prices, which contribute 91.4% to the variability. For competitive HTL blend fuels, the price differential between a barrel of crude oil and a barrel of HTL bio-crude must be less than \$36. These results indicate that coprocessing HTL bio-crude and VGO in hydroprocessing and FCC units will be competitive when the crude oil price increases and the bio-crude price decreases favorably.

Table E4: Cost breakdown of HTL-blend and pure-VGO products for the overall system*

Components	HTL-blend	Pure-VGO
Total capital cost, \$M	658.30	649.40
Total cost of manufacturing (COM), \$M/y	2508.97	2067.04
Utilities, \$M/y	131.98	68.14
Raw material, \$M/y	1,774.73	1,480.59
Operating labor \$M/y	16.56	16.56
Liquefied petroleum gas (LPG) (\$/liter)	0.54	0.45
Gasoline (\$/liter)	0.58	0.48
Light cycle oil (LCO) (\$/liter)	0.68	0.56
Heavy cycle oil (HCO) (\$/liter)	0.67	0.56

*The overall system includes the hydroprocessing and FCC units

Key observations and recommendations

Based on the results of this project, following are the key observations and recommendations.

- For 75,000 bbl/day plant, the cost of producing a liter of liquefied petroleum gas, gasoline, light cycle oil (LCO), and heavy cycle oil (HCO) in the HTL blend (10% HTL biocrude and 90% VGO) scenario increases by $\phi 8.4 \pm 4.1/L$, $\phi 9.0 \pm 4.4/L$, $\phi 10.5 \pm 5.2/L$, and $\phi 10.4 \pm 5.1/L$, respectively, at a 90% confidence interval compared to a VGO only processing.
- A comprehensive economic analysis of hydrotreating HTL bio-crude before blending in the hydroprocessing unit is recommended. This information will indicate whether it is economically viable to hydrotreat HTL in a standalone hydroprocessing unit in the petroleum refinery before blending.
- Investigating the GHG emissions impact of coprocessing HTL oil using the hydroprocessing and FCC units is recommended. A life cycle GHG emissions assessment is necessary to compare the emissions from processing an HTL blend and pure VGO into transportation fuels.
- Investigating how carbon pricing will impact the attractiveness of coprocessing HTL bio-crude in a petroleum refinery is recommended. This investigation will provide information on how carbon pricing can be used to formulate policies on coprocessing the HTL bio-crude to produce transportation fuels.

Table of Contents

Contact Information	2
Disclaimers	3
Executive Summary	5
1.0 Introduction	13
2.0 Process descriptions and methods	16
2.1 Process description.....	16
2.1.1 HTL bio-crude preprocessing	16
2.1.2 Hydroprocessing unit	16
2.1.3 Fluid catalytic cracking unit	16
2.2 Process modeling	19
2.2.1 Model development.....	19
2.2.2 Feed selection and properties.....	19
2.3 Development of techno-economic models	20
2.4 Sensitivity and uncertainty analyses	24
3.0 Results	26
3.1 Material and product quality.....	26
3.1.1 Hydroprocessing unit	26
3.1.2 Fluid catalytic cracking unit	27
3.2 Techno-economic assessment.....	31
3.2.1 Hydroprocessing unit	31
3.2.2 Fluid catalytic cracking unit and the overall system.....	36
4.0 Discussion.....	41
5.0 Key Observations	43
6.0 Key Recommendations	44

List of Tables

Table 1: Properties of VGO and Bio-crude Blend [24]	20
Table 2: Assumptions for estimating plant capital cost and manufacturing cost.....	22
Table 3: Assumptions for the economic model.....	22
Table 4: Ratio of product prices to gasoline price.....	23
Table 5: Range of parameters used in the sensitivity and uncertainty analyses	25
Table 6: Utility consumed in the hydroprocessing units	27
Table 7: Comparing the fractions of yields (wt%) from the experimental and process simulation results	28
Table 8: Utility consumed in the FCC unit	31
Table 9: Cost breakdown of HT blend and HT-VGO products for a hydroprocessing plant capacity of 75,000 barrels per day at \$56.5/bbl. crude oil price and \$586.5/tonne HTL oil price.....	33
Table 10: Cost breakdown of HTL blend and pure-VGO products for the overall system	38

List of Figures

Fig. 1: Simplified process flow diagram of hydroprocessing and fluid catalytic cracking units.....	18
Fig. 2: Mass balance of the hydroprocessing and FCC units for the pure-VGO scenario	29
Fig. 3: Mass balance of the hydroprocessing and FCC units for HT-blend scenario.....	30
Fig. 4: Morris sensitivity plot for (a) HT blend and (b) HT-VGO production cost; and (c) Uncertainty results for the HT blend and HT-VGO production cost	34
Fig. 5: (a) Morris sensitivity plot for Δ_{prod} , (b) uncertainty results for Δ_{prod} , and (c) Sobol results for Δ_{prod}	35
Fig. 6: (a) Morris plot for the percentage difference in the production cost (b) Sobol result for $\% \Delta_{\text{prod}}$	39
Fig. 7: The uncertainty in the HTL blend and pureVGO products	40
Fig. 8 (a) The uncertainty in the differences in the cost of similar product (b) The uncertainty in percentage difference in the overall production cost of liquid products from the HTL blend and the pure-VGO	40

Abbreviations

APEA	Aspen Process Economic Analyzer
COM	Cost of manufacturing
DEA	Diethanolamine
FCC	Fluid catalytic cracking units
HBED	Hydroprocessing bed
HC	Hydroprocessing separation column
HCO	Heavy cycle oil
HT blend	Hydrotreated blend
HT-VGO	Hydrotreated VGO
HPS	high-pressure separator
HTL	Hydrothermal liquefaction
IRR	Internal rate of return
LCO	Light cycle oil
LPG	Liquefied petroleum gases
LPS	Low-pressure separator
RUST	Regression, Uncertainty, and Sensitivity Tool
TIC	Total installation cost
TPEC	Total Purchase Equipment Cost
VGO	Vacuum gas oil

1.0 Introduction

The depletion of fossil fuels coupled with increasing environmental concerns over climate change has led to the search for clean energy sources like biomass. Biomass is an energy resource with the potential to mitigate the environmental challenges of fossil fuel use. Biomass can be converted into solid, gaseous, and liquid fuels [1]. However, converting biomass to meet the required fuel specifications of some applications, such as the use of petroleum fuels in vehicles, comes with many challenges [2]. The produced bio-crude from biomass is a complex mixture of water and organic oxygenated compounds, which lowers the quality of the oil for fuel use [3, 4]. For this reason, the bio-crude cannot be used directly and must be upgraded to meet acceptable fuel standards. Upgrading bio-crude comes with some level of investment and operating costs, which may make fuel production unattractive [5]. Research focusing on cost-effective biomass conversion pathways that meets the acceptable fuel specification is in high demand. Coprocessing bio-crude with petroleum residue oil in an existing refinery has the potential to address these challenges and is currently being investigated.

Bio-crude and petroleum residue can be processed in an existing refinery unit with little structural modification [6, 7]. This option can lower the processing cost of producing transportation fuels from biomass instead of upgrading directly in a standalone bio-refinery. Coprocessing is not suitable in some refinery units, such as atmospheric distillation, because bio-crude properties are highly reactive and not easily handled by these units [8]. These properties also affect the quality of fuels produced and reduce the lifespan of the processing units. According to a PNNL report, the main requirements of a coprocessing unit are the ability to treat the oxygenated compounds present in oil and to crack the larger compounds to derive useful products [9]. Thus, refinery units like the catalytic hydrotreater and fluid catalytic cracker (FCC) are suitable options for coprocessing [5]. These units handle heavy and light hydrocarbons with impurities. The purpose of hydroprocessing is to remove heteroatom impurities like nitrogen, sulfur, and oxygen compounds from the refinery feed streams and enhance the crudes with hydrogen [8]. To accomplish this, the feed stream is combined with hydrogen, vaporized, and passed over a catalyst under high temperature and pressure [8]. The FCC is designed to crack heavy feedstock like heavy gas oils and residual bottoms to produce high-value transportation fuels like gasoline, diesel, etc. [10]. Although its operations do not require external hydrogen supply, bitumen-derived feedstocks are hydrotreated because the heavy and polar oxygenate molecules in them can impede catalyst activity, leading to poor conversion into products [11]. Non-bitumen-derived feedstocks can also be hydrotreated, depending on the level of impurities. However, there are concerns about coprocessing bio-crudes and vacuum gas oil (VGO) in hydrotreaters and the FCC because oxygenates (organic oxygen content) present in bio-crude can reduce catalyst activity [12]. The oxygenates in bio-crude are highly reactive, leading to coke, CO, CO₂, and char formation, catalyst deactivation, and other operational issues [13]. Thus, they can swing yields among products like jet fuel, gasoline, and diesel and simultaneously lower product quality and yield during coprocessing. Also, operational issues like reactor nozzle plugging, coking, and immiscibility of feed have been reported [14, 15]. To reduce operational problems, it is advisable to set the bio-crude ratio to the coprocessing ratio of ≤ 10 wt% [16, 17].

Techno-economic analysis is an important aspect of the feasibility of coprocessing bio-crude and VGO in a refinery FCC unit. It helps to estimate the overall cost of the process and thus helps provide insights on how coprocessing operations will influence the FCC's economics. The operation of the FCC is complex and therefore needs detailed studies to predict the process conditions and product yield when feedstock changes. In the case of coprocessing, there are expectations that the product yield and utilities cost together with the additional capital investment will affect the overall economy of the process. Changes in feedstock properties, product yield,

and the impact on the process economy raise concerns for refiners. Refiners are eager to know the economic consequences of coprocessing bio-intermediates before committing to it. Hence techno-economic assessment of the pathway helps in understanding the economic viability of the pathway.

Hydrothermally liquefied (HTL) bio-crude has a relatively low oxygen content, and it is considered a promising feed for coprocessing [18]. While several experimental studies have shown that coprocessing HTL bio-crude with VGO in the FCC unit is feasible, few studies have reported its economic impact. Most studies focused on pyrolysis oil, so limited information is available on the economy of coprocessing HTL oil in the refinery. Although the insights gained from some of these studies help to understand the intricacies of the economics of coprocessing pyrolysis bio-oil, they raise more questions than providing critical economic information for using the HTL blend. For example, a legitimate question to address is how the cost of coprocessing HTL bio-crude will impact cost of transportation fuel compared to pyrolysis oil. Pyrolysis oil is a bio-crude produced by fast pyrolysis of biomass. Unlike HTL bio-crude, pyrolysis bio-crude is not stable and has a relatively high oxygenated content. Therefore, producing and processing it into transportation fuel requires a different conversion approach, which may differ economically from HTL bio-crude. The findings from these studies cannot be used to predict the fate of coprocessing HTL oil in the refinery. However, it will be interesting to understand their main findings and limitations, and how they can help inform HTL bio-crude's studies. Aasma et al. developed various correlation models to evaluate the cost of coprocessing pyrolysis bio-oil in an FCC unit [5]. They observed that coprocessing is highly sensitive to changes in prices of crude oil and petroleum products. At a crude oil price of 60\$/bbl and above 120\$/bbl, coprocessing is economically viable for raw and hydrodeoxygenated bio-oil, respectively. In a similar study, Wu et al. [19] performed a techno-economic analysis of coprocessing catalytic and fast pyrolysis-derived oil and hydrotreated fast pyrolysis bio-crude with VGO. They showed that gasoline prices are sensitive to changes in fuel yields, VGO and diesel prices, and FCC capability. A 2005 study by UOP Inc. showed that producing gasoline from hydroprocessing and hydrocracking bio-oil provides economic incentives when the price of pyrolysis oil decreases and crude oil price increases [20]. This incentive becomes attractive at pyrolysis oil and crude oil prices of \$18/bbl and \$50/bbl, respectively. Talmadge et al. conducted a high-level economic analysis of the coprocessing of fast pyrolysis bio-oil with VGO using data from Pinho et al.'s FCC demonstration-scale set-up [21]. Talmadge et al.'s results show that coprocessing 5wt.% and 10wt.% fast pyrolysis oil with VGO is economically feasible at 400 and 2000 dry t/day, respectively. These studies and many others have shown that coprocessing bio-crude with petroleum intermediates is economically feasible at a certain crude oil and bio-oil price, plant capacities, and with some restrictions in terms of technical feasibility. However, their results may not reflect the outcome of a coprocessed HTL oil because of compositional differences in the feedstock [13] and processing method [22]. These two factors account for energy, material, and utility use patterns, capital investment, and product quality, and thus the economic attractiveness of a technology. No previous work has examined the economic impact of coprocessing HTL bio-crude with VGO except for Wu et al.'s [23]. Wu et al. conducted a techno-economic analysis of coprocessing VGO and algae-derived HTL oil. According to their study, coprocessed bio-oil does not require hydroprocessing. While algae-derived oil may not require hydroprocessing, studies have shown that non-algae hydrothermal liquefaction oil requires treatment [22, 24]. Additional investments in pumps, distillation columns, hydrogen, etc., to achieve coprocessing in the FCC make hydroprocessing an important economic factor to consider. Furthermore, HTL bio-crude needs to be distilled to separate immiscible ends before hydroprocessing [17, 24]. Because non-algae biomass-feed for HTL oil production is readily available and abundant, it would be beneficial to understand how these pretreatments impact the economics of coprocessing in the refinery. Techno-economic analysis of coprocessing HTL oil with VGO in the refinery hydroprocessing and FCC units is therefore

important to provide decision-making information for refiners. In this study, we address these questions through a detailed techno-economic analysis of coprocessing HTL bio-crude with bitumen-derived VGO in the refinery hydroprocessing and FCC units through development of data-intensive techno-economic models.

The specific objectives of this study are to:

- Develop a process model for coprocessing HTL bio-crude with VGO in the hydroprocessing and FCC units;
- Evaluate the increase in production cost of transportation fuels produced from coprocessing HTL bio-crude with VGO in the hydroprocessing and FCC units.

2.0 Process descriptions and methods

In this study, we considered two scenarios each for both the hydroprocessing and FCC units. Each processing unit handled pure VGO and VGO blends with HTL distillate. In the first scenario, we developed a simulation model to process 75,000 barrels per day of VGO in the hydroprocessing unit. For the second scenario, we blended HTL bio-crude distillate with VGO at a ratio of 1:9 by weight at the same capacity as the previous case. The hydroprocessed product serves as feedstock to the FCC for further processing into transportation fuels. We extracted equipment size, utility, and material data from these models to conduct techno-economic analysis. In this study, the first and second scenarios are referred to as pure VGO and an HTL-blend, respectively.

2.1 Process description

2.1.1 HTL bio-crude preprocessing

Full-range HTL bio-crude (bio-crude) from woody biomass is produced in a bio-refinery and then transported to a petroleum refinery. Preprocessing is necessary because it enhances HTL bio-crude processability and miscibility with VGO. First, bio-crude is filtered and then distilled to separate heavy components and water [24]. We designed a distillation column to remove water and heavy components in the bio-crude. The distillate target cutoff temperature was set at 525°C. It is important to mention that the cutoff temperature must be consistent with VGO in terms of upper and lower boiling point limits [24].

2.1.2 Hydroprocessing unit

The hydroprocessing unit considered in this study is part of the FCC complex unit. It hydrotreats gas oils separated from bitumen through the vacuum and coker distillation towers by saturating olefins and aromatics and removing sulfur and nitrogen compounds. In this study, we considered straight-run VGO and distilled HTL as feedstocks to the hydroprocessing unit. Fig. 1 presents the schematic diagram of the hydroprocessing and FCC units. The hydroprocessing unit consists of a fired heater, hydroprocessing reactor, heat exchangers, high-pressure separator (HPS), low-pressure separator (LPS), and diethanolamine (DEA). Preheated feed is mixed with hydrogen-rich gases and brought up to reaction temperature through a fired heater. The mixture enters the reactor where hydroprocessing reactions take place. The heat released during reactions is used to preheat the feed streams in the heat exchanger train. The reactions occur under high pressure to increase purification by hydroprocessing and to encourage acid gas removal by DEA absorption. The hydroprocessing separation column (HC) separates unstabilized naphtha and fuel gases from the hydrotreated gas oil, the feedstock to the FCC unit.

2.1.3 Fluid catalytic cracking unit

FCC unit consists of a reactor, distillation towers, and a gas unit. The FCC reactor is a single-stage single-riser unit attached to a regenerator [25]. The feed is injected into the riser and mixed with the hot fluidized catalyst coming from the regenerator. The combined heat from the catalyst and the steam in the reactor pipe crack the feed on the catalyst surface. This cracking of the FCC feed forms carbocation, which undergoes further cracking, hydrogenation/dehydrogenation,

isomerization, and cyclization/recyclization to form the vapor product [26]. The catalyst in the vapor product is disengaged and sent to a regenerator for coke combustion. The flue gases are collected in the cyclone and sent for waste heat recovery. The regenerator plays a crucial role in maintaining catalyst activity by burning the coke off the catalyst and supplying the released heat from coke combustion to the reactor for cracking. Mostly the flue gases go through the cyclone separator stages to recover the catalyst. The coke combustion in the regenerator produces carbon dioxide, carbon monoxide, and sulfur dioxide aided by the air supply. The air supply ensures that carbon is emitted as carbon dioxide and that fewer coke deposits form on the regenerated catalyst. The vapor product is sent to the fractionator column where it is separated into dry gases (C1-C4), liquefied petroleum gases (LPG), naphtha, light cycle oil (LCO), heavy cycle oil (HCO), and decanted oil.

The fractionator downstream operation in our model consists of the main fractionator column from where we obtained overhead vapors, naphtha, and the cycle oil residue. There are side operations attached to the fractionator column like side strippers and several pump-arounds, which help draw out the products at different stages. Pump-arounds are attached to the main fractionator and help in heat distribution and recovery. The overhead vapors are recompressed in the overhead wet gas system to recover additional naphtha. The liquid product from the wet gas compression and naphtha from the main fractionator column enter the primary absorber. The primary absorber column feeds the stripping column with a gasoline stream. The stripping column separates the heavy components from the naphtha and returns them to the main fractionator. The rest of the liquid fraction is passed to a debutanizer where the top product is LPG and the bottom product is gasoline. FCC gasoline is the most important component supplied for gasoline formulations in a refinery. The heavier fractions like LCO can be used for blending fuel oil or for feed cutter stocks. The diesel obtained is blended in a diesel blending pool for transportation purposes. The flue gases generated by coke combustion are sent for steam and power recovery. The recovered steam is used for cracking in the FCC and the power is used for supplying air to the regenerator.

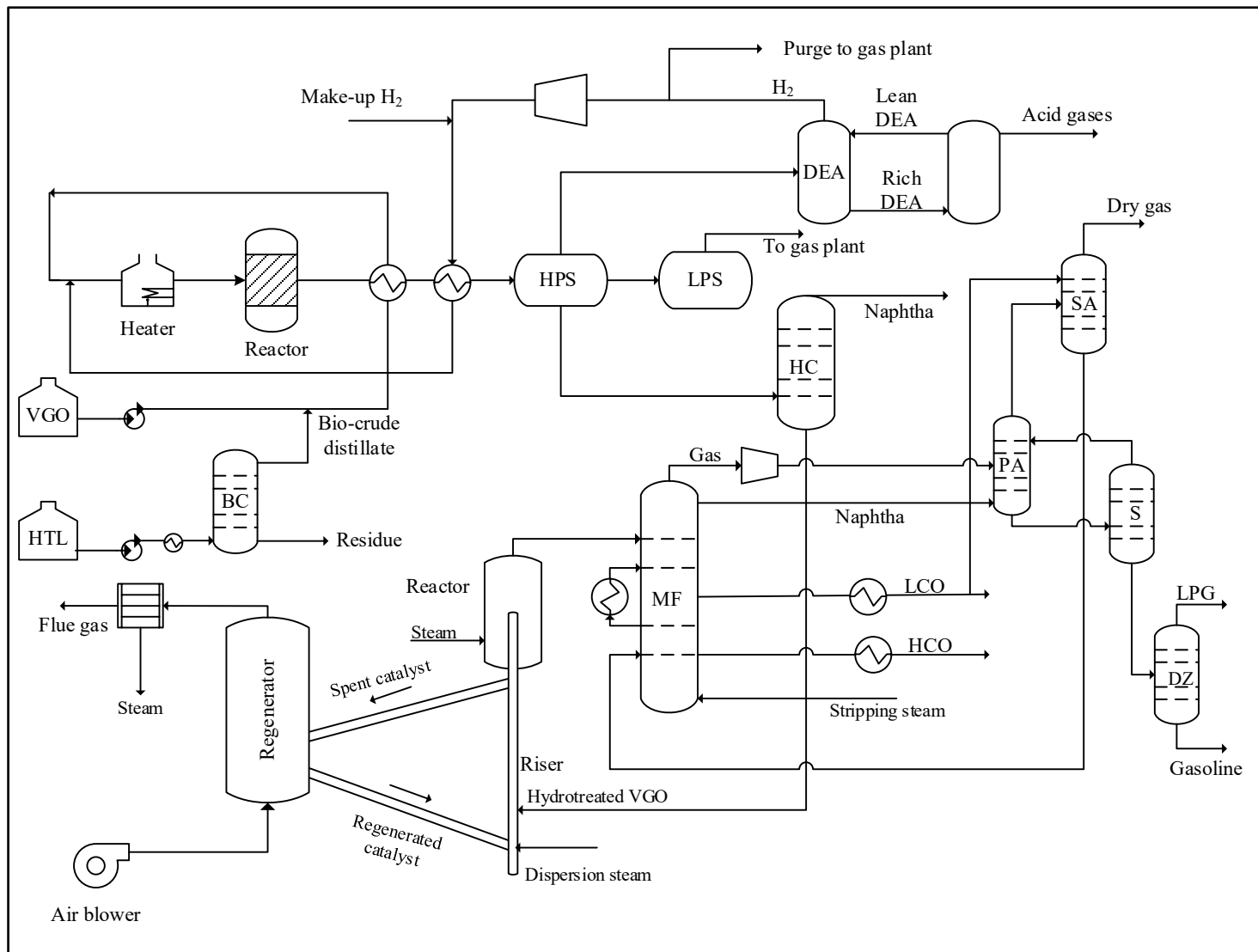


Fig. 1: Simplified process flow diagram of the hydroprocessing and fluid catalytic cracking units

2.2 Process modeling

2.2.1 Model development

We developed rigorous models of the hydroprocessing and FCC units using Aspen HYSYS version 12 [27]. The Peng-Robinson and acid gas-chemical solvent fluid packages were used to predict the fluid behavior under varying conditions of the hydrocarbons and acid gas process, respectively. Aspen HYSYS contains a hydroprocessing bed (HBED) and FCC reactor modules. These modules contain a detailed kinetics model of the reactions occurring in the hydroprocessing and FCC reactors. The HBED model contains rate equations for HDS, HDN, saturation, cracking, and ring-opening. These rate equations form a reaction network comprising 97 kinetic lumps and 177 reactions [28]. The rate equations for each reaction are encrypted to match industry process data. That is, in the HBED model, basic or advanced tuning can be adjusted to match plant performance. The FCC modeling also involves many reaction equations, which are complex to model. So, in the FCC model, a 21-kinetics reaction network is used to address this complexity. Each lump represents a different reaction pathway such as paraffinic cracking, naphthenic ring-opening, alkyl side chain cracking, kinetic coke, etc. The activity steps in the FCC are as follows: (1) In the FCC riser, feed is converted to product species using the 21-lump kinetics, (2) the reactor completes feed conversion and removes adsorbed hydrocarbons, (3) the coke on the catalyst undergoes combustion, and (4) 21 lump compositions are converted (de-lumping) into a set of true boiling points [28]. Like the HBED, the FCC has calibration factors, which can be adjusted to match plant performance. In this study, we used experimental data to validate both the HBED and FCC performances. In the HBED, only the basic tuning was adjusted to match the experimental data. Furthermore, we created a reaction model to account for the reactions between hydrogen and the oxygenated contents of the HTL bio-crude blend. This aspect is not available in the Aspen HYSYS HBED reactor modules, so we modeled the reaction separately. The HTL oxygenated compounds can be found in a Pacific Northwest National Laboratory (PNNL) report [29]. Aspen HYSYS manual version 9.0 contains the details and the interactions of the reactions in the HBED and FCC reactors [28].

2.2.2 Feed selection and properties

Vacuum gas oil and HTL bio-crude are the feedstocks to the process. The selected VGO and HTL bio-crude are produced from Canadian oil sands bitumen and woody biomass, respectively [17]. We used the NRCAN experimental results on coprocessing VGO and HTL bio-crude in the hydroprocessing and FCC reactors. The experimental results provide feedstock and product properties from the coprocessing outputs. Details of the experimental methods can be found in studies by Xing et al. [24] and Badoga et al. [17]. Table 1 presents the bulk properties and distillation curve of the feedstocks used in this study. For the feedstocks to the hydroprocessing unit, notable differences between the VGO and the 10% bio-crude blend are that the latter contains 1.4 wt% oxygen, more polar components, and a higher range of boiling point fractions. The increase in oxygenated contents is due to blending HTL bio-crude distillate with a 10.5 wt% oxygen with VGO. The properties of the hydrotreated product (HT-10% bio-crude) are of slightly lower grade than the VGO in terms of heteroatom content, primarily because of the effect of bio-crude on catalyst activity [24].

Table 1: Properties of VGO and bio-crude blend [24]

Property	VGO	Full range bio-crude	10% bio-crude blend
Density at 15.6 °C, g/cm ³	0.9759	1.0536	0.9780
Carbon, wt %	84.8	80.0	83.6
Hydrogen, wt %	11.1	9.4	11.5
Sulfur, wt %	3.6	0.0	3.2
Nitrogen, wt %	0.2	0.1	0.3
Oxygen, wt %	0.5	10.5	1.4
Simulated distillation			
IBP, °C	298.0	57.4	211.8
5 wt %, °C	344.0	190.4	323.4
10 wt %, °C	362.4	239.8	350.4
30 wt %, °C	405.2	353.6	396.6
50 wt %, °C	435.2	414.4	428.6
70 wt %, °C	467.0	604.8	459.6
90 wt %, °C	519.4		504.8
95 wt %, °C	568.0		526.6
FBP, °C			675.4

2.3 Development of techno-economic models

In this study, the hydroprocessing and FCC processes follow the configuration and capacity provided by an earlier study [25]. The refinery design handles heavy hydrocarbons like bitumen, making it a suitable configuration for the VGO (derived from bitumen) considered in this study.

We evaluated the capital cost, cost of manufacturing (COM), and production costs of the hydroprocessing and FCC units. First, the refinery hydroprocessing and FCC capital costs were evaluated using the costs provided by Netzer [25]. We then adjusted all the equipment costs for inflation from the base year (2015) to the reference year (2021). The capital cost estimate provided by the consultant includes equipment, materials, labor, indirect construction costs, engineering, and contingencies. The capital cost value of the additional equipment needed for pre-processing HTL bio-crude was evaluated using the process model. This cost was estimated using the total installation cost (TIC), total equipment costs (TPEC), indirect costs, and contingency. The installation factor is required for equipment costs and includes the piping, electrical, and other installation costs. Because the installation factor provided by the process model is relatively low, we used 3.02, a value suggested by Peters et al. for solid-liquid plants [30]. We estimated the indirect costs (IC) through engineering and supervision costs (32% of TPEC), legal and contractors' fees (23% of TPEC), and construction expenses (34% of TPEC) [30]. Project contingency is taken as 40% of the direct and indirect costs [25], which is the sum of the TIC and the IC. The value chosen for contingency is slightly higher than that found in most studies (the typical value is between 15% and 20%). However, earlier study [25] recommends using this value because of the reliability of refining cost data. The study mentions that the capital

cost of refinery plants is volatile because of the rapid change in crude oil price and subsequent increase in related capital projects. Lastly, we included a 10% location factor in the capital cost estimate. Table 2 summarizes the factors used to estimate the capital cost.

To estimate COM, we determined the direct manufacturing cost, fixed manufacturing cost, and general expenses. Details of each COM component are provided by Turton [31]. The cost of manufacturing (COM) was estimated using Equation (1) [31]:

$$COM = 0.18 FCI + 2.73(\text{operating labor}) + 1.23(\text{Utilities} + \text{Cost of raw material})$$

(1)

where FCI is fixed capital investment.

The operating labor is the cost of personnel required for plant operations. We assumed 10 plant operators/shift and two supervisors/shift for three shifts per day to operate the plant. The utilities consumed by the processes were obtained through the developed process simulation models. Plant utilities include fuel, electricity, cooling water, catalyst, and hydrogen. These costs are provided in Table 2. Feedstock (raw material) price is an important component of the production cost. The price of HTL bio-crude was estimated from an earlier study [29]. The estimated cost value was updated to the 2021 value using an inflation factor of 1.1. The price of VGO was calculated as a ratio of the crude oil price. We calculated the ratio from VGO and heavy crude oil prices from [32].

A discounted cash flow sheet was developed to estimate the production cost of products from the hydroprocessing and FCC units. Table 3 presents the economic assumptions used in the study. For the hydroprocessing unit, the main product is hydrotreated VGO. The products from the FCC are gasoline, liquefied petroleum gas (LPG), gasoline, light cycle oil (LCO), and heavy cycle oil (HCO), and dry gases. The dry gases essentially comprise lighter fractions and are used in the refinery for its fuel gas systems [10]. Therefore, we did not include them in the revenue calculation. We calculated the average wholesale prices for the last 12 months for gasoline, diesel, HCO, and LPG [38]. The ratio of the wholesale prices was established and expressed as a function of the gasoline price. The gasoline price is expressed as a function of crude oil price.

Table 4 shows the price ratios. For simplicity, the ratios were fixed in the discounted cash flow analysis to estimate the production cost of products.

Table 2: Assumptions for estimating plant capital cost and manufacturing cost

Parameter	Value	Reference
Capital cost		
Total purchase equipment cost (TPEC)	100% TPEC	[30]
Total installed cost (TIC)	302% TPEC	[30]
Indirect cost (IC)	89% TPEC	[30]
Total indirect cost (TDIC)	TIC + IC	[30]
Contingency	40% TDIC	[25]
Fixed capital investment (FCI)	TDIC + contingency	
Location factor (LF)	10% FCI	[30]
Total capital cost	FCI + LF	
Utility price		
Electricity	0.06 \$/kWh	[31]
Fuel (natural gas)	2.06 \$/GJ	[33]
Cooling water	0.983 \$/m ³	[34]
Hydrogen	1.22 \$/kg	
FCC catalyst	25.3 \$/kg	[35]
Hydroprocessing catalyst	27.1 \$/kg	
Dilbit (bitumen)	53.49 \$/bbl.	[33, 36]
Operating labor		
Operating labor	27.45 \$/hour	[37]
Operating supervisor	35.29 \$/hour	[37]

*All costs are in Canadian dollars except otherwise stated. Conversion factor (CAD to USD): 1.33 [33].

Table 3: Assumptions for the economic model

Parameter	Specification
Base year and currency	2021
Currency	Canadian dollars \$
Location	Alberta
Operating hours	8000 h/y
Capacity use	90%
Internal rate of return (IRR)	10%
Plant lifetime	25 years

Table 4: Ratio of product prices to gasoline price

Product	Ratio
Light cycle oil (LCO)	1.17
Heavy cycle oil (HCO)	1.16
Liquified petroleum gas (LPG)	0.93

2.4 Sensitivity and uncertainty analyses

Investigating the variabilities in the input assumptions in a model is essential to making meaningful inferences and decisions. Sensitivity and uncertainty analyses are widely used methods for investigating the robustness of the results of a model or system. They are used in this study to compare the variation in economic inputs and their influence on the outputs.

Sensitivity analysis helps to identify the influence of the inputs on the model outputs, providing insight into which variables should be estimated more accurately to determine the variability in the results. The accuracy of the sensitivity analysis depends on the type of model; for instance, global sensitivity analysis is suitable for non-linear models, while local one-at-a-time methods are appropriate for linear models [39]. Among the global sensitivity models, the Morris method is widely used because it can determine the influence of input variations on the model output [40]. Through a graphic analysis, the inputs on which the model output is more sensitive are readily identified.

In a Morris plot, parameters with a large mean and standard have a high influence on the output. Parameters with a relatively large standard deviation indicate either the model is non-linear or there is an interaction effect between parameters. Lastly, parameters with low/zero mean and standard deviations are fairly sensitive or not sensitive to the output and can be ignored. When it is not clear whether a parameter is sensitive or not using the Morris plot, we used the Sobol method to evaluate the contribution of the parameter. The Sobol analysis determines the percentage contribution and interaction effect of input to the overall output.

Uncertainty analysis determines the likely range of values the model output could take through differences in input values. Monte Carlo simulation is a widely used method to perform uncertainty analysis. In this method, a random sampling of input values is used to generate a range of output with a certain level of confidence [41]. To perform meaningful analysis, a very large sample might be required, increasing the computing time. Implementing the Morris method before the Monte Carlo simulation narrows the number of inputs for the uncertainty analysis by eliminating non-influential parameters identified in the sensitivity analysis.

In this study, the Regression, Uncertainty, and Sensitivity Tool (RUST) was used for sensitivity and uncertainty analysis [39]. This tool, developed using RStudio and Excel VBA, uses several global sensitivity methods, including Morris, as well as uncertainty methods, including Monte Carlo simulation and Sobol analysis.

Table 5 presents the input ranges used in this study. The lower and upper bounds of the inputs were selected based on historical data. For example, the lower and upper bounds of the crude oil price and natural gas price correspond to the lowest and highest value reported by Canada Energy Regulator for 2018-2020. $\pm 30\%$ is used where data is not available, a commonly used approach for the economic analysis of industrial processes.

Table 5: Range of parameters used in the sensitivity and uncertainty analyses

Inputs	Units	Lower bound	Base case	Upper bound
Crude oil price	\$/bbl.	37.0	56.5	85.9
HTL bio-crude oil price	\$/tonne	433.3	619.0	804.8
Capital cost	%	70.0	100.0	130.0
Natural gas price	\$/GJ	0.4	2.1	3.3
Hydrogen price	\$/kg	1.2	1.2	3.0
Electricity	\$/kWh	0.0	0.1	0.1
Make-up water	\$/m ³	0.7	1.0	1.3
Hydroprocessing catalyst	\$/kg	25.3	36.0	46.8
FCC catalyst	\$/kg	23.6	33.6	43.7
Internal rate of return	%	7.0	10.0	20.0
Operator labor wage rate	\$/h	19.2	27.5	35.7
Supervisor labor wage rate	\$/h	24.7	35.3	45.9

3.0 Results

In this section, we present the outcomes from the process simulations and the techno-economic models.

3.1 Material and product quality

3.1.1 Hydroprocessing unit

The hydroprocessing complex comprises the preprocessing unit. In the preprocessing unit, 55.1% (13.6 kg/s) of the raw HTL bio-crude meets the distillate requirement for a 10% blend with VGO. 24.7 kg/s of HTL bio-crude is required to produce the distillate. The boiling range of the distillate fraction is from IBP-521°C with its D1160 95% at 476°C. 44.9% of the raw feed is discharged as residue (D1160 5% at 465°C). In their experimental analysis, Xing et al. reported 33.5% as residue and the distillate fraction from IBP-520°C. The difference in yield is because the experimental D1160 distillation set-up used by Xing et al. collects products in a batch-wise manner. These products are close to a typical square cut, which does not fully represent a true plant cut. We developed a rigorous distillation model to produce product cuts similar to what is achievable by an actual plant. Our results from the rigorous model showed that shifting the boiling range to achieve 33.5% in residue lowers the bio-crude feed by 13.0% but increases the distillate's D1160 95% to 540°C. In this case, about 7.0% of the heavy materials are introduced into the hydroprocessing unit. As mentioned earlier, if heavy materials are present in the HTL oil, they can cause operational problems like plugging, catalyst deactivation, etc., in the hydroprocessing unit, thus increasing downtime, maintenance cost, make-up catalyst, and other operating costs. If operators are interested in taking this risk, the annual savings for reducing the bio-crude rate or residue at the expense of heavy materials in the hydroprocessing unit is \$181,741. The fuel (natural gas) rate required to produce distillate was estimated to be 0.22 kg/s. The make-up water for cooling and boiler feedwater (BFW) for steam production in the preprocessing unit are 0.2 kg/s and 4.0 kg/s, respectively. The feed to the HTL fractionation column (BC) requires two preheating heat exchangers to achieve this relatively low fuel rate.

Fig. 2 and Fig. 3 present the process flow diagram of the hydroprocessing unit for pure VGO and the coprocessing blend at 10% HTL bio-crude, respectively. Following these diagrams, the hydroprocessing unit produces 131.1 kg/s and 132.8 kg/s of hydrotreated VGO (HT-VGO) and hydrotreated 10% HTL blend (HT blend), respectively. The slight decrease in the yield of the HT-VGO is due to the high yield of fuel gases and unstabilized naphtha. The percentage increase in the fuel gases and naphtha in the HT-VGO operation is 9.9% and 53.0%, respectively. The fuel gases are released from the high and low-pressure separators and the amine unit (purge gases). It is important to mention that in the HC fractionation column, fractions below 145°C are separated as fuel gases and unstabilized naphtha. Table 6 presents the utility consumed in the hydroprocessing units. The HT blend consumes more utilities than pure VGO does, primarily because of the additional energy needed to separate distillate from bio-crude. In both cases, fuels consumed in fired heaters generate steam for reboilers and raise the feed stream to the target temperature. The amine regenerator in both cases does not require fuel energy to generate steam as there is sufficient process heat within the plant. For the unused process heats, we assumed they are supplied to other units in the refinery, a common practice to improve energy use and lower operating costs in the refinery.

Regarding product quality, we achieved a satisfactory product purity in both cases at the expense of hydrogen consumption. As mentioned earlier, the activity factors of the hydroprocessing beds were adjusted to meet the desired sulfur and nitrogen removal levels. The oxygenated compounds were also reduced to the value reported by Xing et al. by setting their conversion efficiency to 98.7%. Hydrogen consumption in the hydroprocessing units was then calculated considering hydrogen consumed in the hydroprocessing beds, solution hydrogen, and purge gases. There is a slight increase in the hydrogen consumed in the HT blend scenario, and this increase impacts the economy of the process. The HT-VGO and HT blend consume 940.5 scf/bbl. and 944.3 scf/bbl. of hydrogen, respectively.

Table 6: Utility consumed in the hydroprocessing units

Utility	HT-VGO	HT blend
Natural gas (kg/s)	0.86	1.08
Make-up water (kg/s)	31.34	33.73
Electricity (MWh)	653.73	687.35
Hydrogen consumed (scf/bbl.)	940.50	944.30

3.1.2 Fluid catalytic cracking unit

We obtained FCC experimental results, at varying process conditions, from the CanmetEnergy Devon. The experimental analyses considered coprocessing at cracking temperatures from 490°C to 530°C. The experimental results were used to develop the FCC model for both the HT-VGO and the HT blend. We calibrated the model to generate repeatable results over a range of operating conditions. The model performance was compared with the experimental yield, distillation curve, bulk properties, and other quality measures available from the experimental data. The model's forecast is satisfactory for the FCC units. The economic analysis performed for the base case in this study was based on cracking conditions at 530°C. Table 7 presents the yield results from both the experimental and process simulation analyses. At this temperature, we obtained a good agreement between the simulator prediction and experimental data with an average absolute error of 3.7% and 3.1%, respectively, for the pure VGO and HTL blend scenarios (Table 7). In the pure VGO scenarios, the maximum error is 8.3 in the dry gas stream; this may be because of the low percentage composition of methane and hydrogen sulfide in the stream. However, the dry gas composition in our model analysis is much closer to that reported in an earlier study [42]. The maximum absolute error is 8.1 in the HCO stream for the HTL blend scenarios. It is unclear what might be responsible for this error because the quality of HCO was not specified in the experimental data, so we could not verify the quality of HCO beyond the distillation curve provided, which compared favorably. If we ignore these particular errors, the average absolute error becomes 1.7% and 2.1%, respectively. These errors have little or no effect on the overall results, indicating that the results confirm the rationality of using the simulation models for analysis purposes.

Fig. 2 and Fig. 3 show the mass balance across the FCC units, while Table 8 presents the utilities consumed. The main utilities consumed in the FCC units are make-up water (for cooling), electricity, and make-up catalyst. In some FCC designs, electricity is generated using flue gas to operate all electrical devices and supplies the excess to other units in the refinery [10]. The scenario considered in this study could generate part of the electricity needed to power the air blowers using the flue gas stream that leaves the regenerator. Other electrical devices take

electricity from the refinery power system. The remaining part of the flue gas is used to generate the steam needed in the FCC unit and other units of the refinery. Because utility consumption cannot be obtained from the experimental analysis, we compared our results with literature [42]. The electricity, make-up water, and catalyst make-up rate for the HT-VGO and HT blend are 6.3 and 5.9 kWh/tonne, 0.103 and 0.104 m³/bbl, and 0.07 (5.7 tonnes/day) and 0.13 kg/bbl (9.8 tonnes/day), respectively. These results are within the values reported in an earlier study [42], 5.2 kWh/tonne of feed and 0.06 kg/bbl. (2.5 tonnes/day). Sadeghbeigi also reported that catalyst consumption rate could range from 0.045-0.45 kg/bbl. [10]. The HTL blend scenario consumes more utility than the pure VGO scenario. The difference in utility consumption is not large, suggesting that coprocessing 10% hydrotreated HTL with VGO will not require a major structural change in the FCC unit. The increase in the utility consumed in the HTL blend scenario is because of the reactions occurring in the riser resulting from the blend and the higher feed rate.

Table 7: Comparison of the fractions of yields (wt%) with the experimental and process simulation results

Product (wt%)	HT-VGO	HT-VGO *Exp	Absolute Error	HT blend	HT blend *Exp	Absolute Error
Dry gas	3.09	2.85	8.28	2.93	2.84	3.11
LPG	18.50	17.36	6.58	16.69	16.79	0.57
Gasoline	45.8	47.3	3.3	46.77	47.86	2.29
LCO	17.1	17.0	0.75	18.60	17.85	4.22
HCO	9.53	9.45	0.91	9.41	8.71	8.11
Coke	5.86	5.99	2.14	5.96	5.96	0.06

*Exp: Experimental results

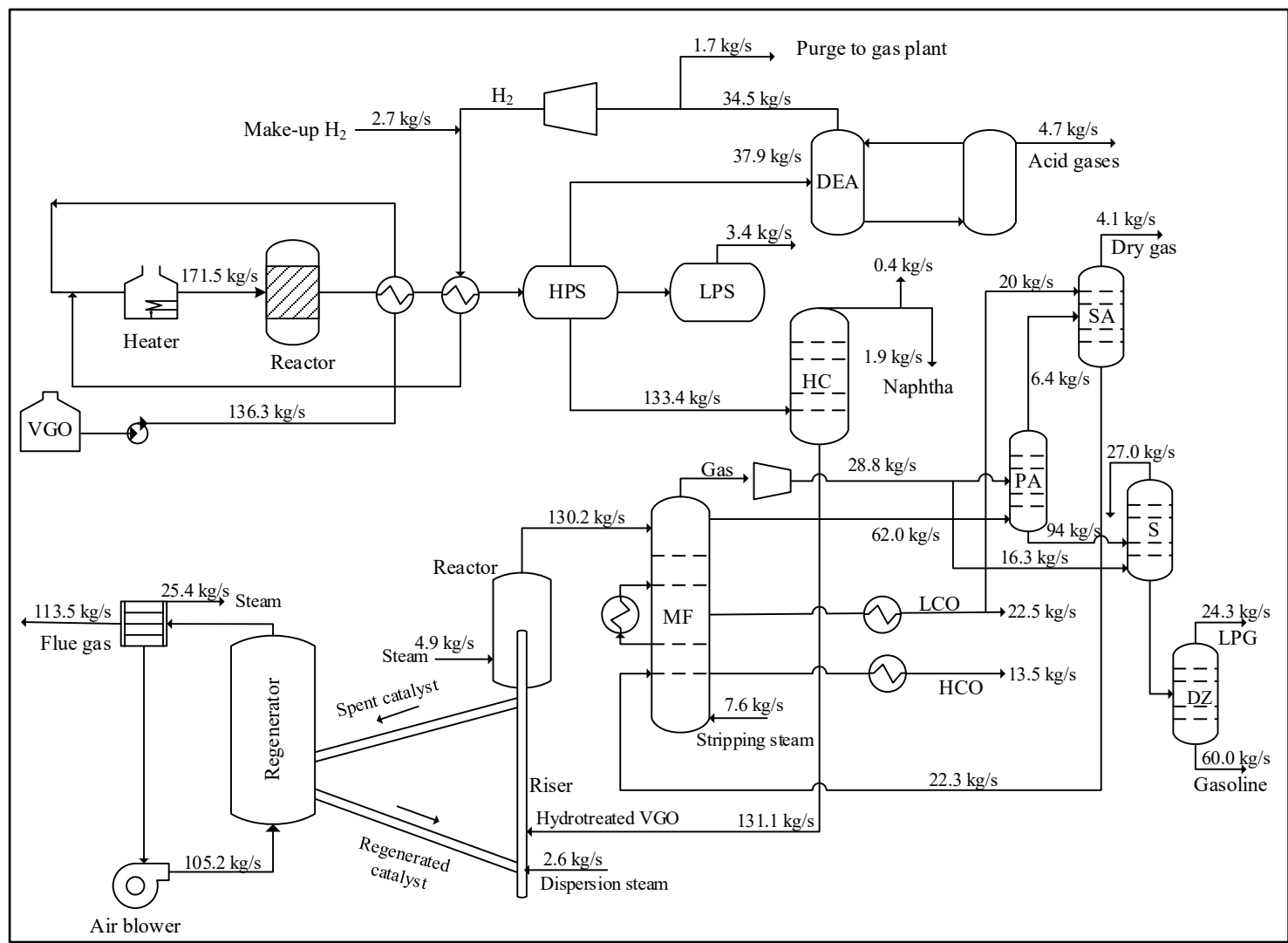


Fig. 2: Mass balance of the hydroprocessing and FCC units for the pure VGO scenario

Table 8: Utility consumed in the FCC unit

Utility	Pure VGO	HTL blend
Make-up water kg/s	93.9	94.7
Steam credit(kg/s)	12.7	13.0
Column stripping steam (kg/s)	7.63	7.63
Dispersion steam (kg/s)	2.62	2.65
Riser stripping steam (kg/s)	4.90	5.19
Electricity (MWh)	67.95	71.91
Electricity credit (MWh)	447.27	478.54
Fresh catalyst make-up rate (kg/h)	238.2	408.8

3.2 Techno-economic assessment

3.2.1 Hydroprocessing unit

The production costs of HT-VGO and HT blend for a plant capacity of 75,000 barrels per day (136.3 kg/s) of feedstock are summarized in Table 9. The cost to produce an HT blend in the hydroprocessing unit is \$95.30/bbl, which is 18.7% higher than HT-VGO. The HT blend's capital cost and COM increased by 2.7% and 19.0%, respectively. The increase in production cost is due to the increase in the cost of feedstock and the cost of integrating the preprocessing unit. The feedstock cost increases because of the high cost of bio-crude. The bio-crude price raises the feedstock cost by 20.8%, an estimated \$36,773 per day. The economic impact of the preprocessing unit is not significant; it is less than 1.0% of the HT blend production cost. Its capital and operating costs are \$8.9 M and \$10 M/year, respectively. The cost of preprocessing a tonne of HTL bio-crude is \$16.40. Using the cost allocation approach, we calculated the cost of upgrading bio-crude in the hydroprocessing unit to be \$343.50/tonne. This value is lower than upgrading bio-crude in a standalone bio-refinery but more than that reported by Tews et al. (in 2014) [29] if inflation is applied, indicating that coprocessing HTL bio-crude in a refinery hydroprocessing unit can lower production costs more than in a standalone operation. Upgrading coprocessed feedstock in a refinery unit offers benefits such as low capital and operating costs.

In the HT-VGO and HT blend scenarios, the percentage contribution of capital costs to the production cost is lower than the cost of manufacturing (COM) (Table 9). In a refinery, the COM in some of the units is usually high. Studies by Rivero et al. [43] and Oni and Waheed [44] showed that capital cost in some key refinery units is significantly low, below 5% of the production cost. In the hydroprocessing units, capital costs contribute 1.8% and 2.1% to the total production cost of HT-VGO and the HT blend, respectively. If we double the capital costs, production costs of both processes increase by ~5.0%. These results suggest that capital cost may not be sensitive to the hydroprocessing unit but can have an interaction effect with other inputs. Changes in the values of the base case capital cost factors (such as contingency, engineering fee, installation, and so on) will not impact production cost significantly. The plant's economies of scale, moreover, contribute to the relatively low capital cost per unit output. The hydroprocessing unit has considerable economies of scale, about 0.72 [45]. For a 75,000 barrel per day capacity, which is a large-scale FCC unit, economies of scale benefits help in lowering the production cost appreciably. At a lower capacity (medium or small scale), the production cost is expected to be higher.

Economic parameters like crude oil price, natural gas price, hydrogen price, internal rate of return (IRR), equipment cost has variability associated with it. It is important to understand how changes in these inputs impact the production cost of hydroprocessing the HTL blend in the refinery and how they help refiners make informed decisions. In this case, the key inputs were identified. Then, an uncertainty analysis was conducted to investigate how these inputs impact the production cost of HT-VGO and the HT blend. In Fig. 4 (a and b), the Morris plots for the production cost of both scenarios show that the crude oil price is a key input and variation in this has a significant impact. The production cost is not very sensitive to IRR and capital cost because they have a relatively low Morris mean, but they show some level of interaction effects among the other inputs. It is unclear if these interactions have a significant effect on production cost. In the HT blend scenario, the cost of production is highly sensitive to bio-crude price. Using the RUST model, we ran a Sobol simulation to estimate the contribution of each input. The results show that removing the bio-crude price, IRR, and capital costs had a considerable interaction effect on the total cost variation. These inputs were therefore included in the uncertainty analyses. Other parameters were not included in the uncertainty analyses because they have a negligible effect on the production cost. Fig. 4c presents the variability in the production cost in each hydroprocessing scenario. The product costs of HT-VGO and the HT blend range from \$57.30/bbl-\$115.60/bbl and \$72.20/bbl-\$125.20/bbl, respectively, at a 90% confidence interval. The wide variation is primarily due to the crude oil price in both scenarios. In the HT blend scenario, the crude oil price is responsible for ~98% of the total variability, while the bio-crude price accounts for less than 2%.

The previous analysis cannot provide the extent and degree to which changes in inputs will affect the differences in the production cost of the HT blend and HT-VGO. Differential analysis of the two scenarios helps understand the effects of inputs on the differences in production cost. For example, in the base case scenarios, the production cost of the HT-blend is higher, and the bio-crude price seems to be responsible for the increase. However, it is not certain if the production cost of the HT blend will remain higher than HT-VGO as the input price changes. Within the range of inputs provided in Table 5, an uncertainty analysis was performed of the differences between the production cost of the two scenarios. It is important to mention that when performing differential analysis for two similar products like the HT blend and HT-VGO, parameter dependence is an important factor to consider. For example, while capital cost, an independent variable, is common to both processing units, it would be inappropriate to use the same input data for sampling because such independent sampling generates stochastic and incomparable output. Therefore, the capital cost and bio-crude price were sampled independently. Fig. 5a shows the inputs that influence the production cost in both scenarios. These inputs (bio-crude price, crude oil price, IRR, and capital costs) are responsible for the high cost of the HT blend. The variation in the differences in the cost of both products ($\Delta_{\text{prod}} = \text{HT blend} - \text{HT-VGO}$) is shown in Fig. 5b. A positive Δ_{prod} value (i.e., subtracting HT-VGO from the HT blend equals a positive value) indicates that the production cost of the HT blend is higher. The Δ_{prod} value (per barrel of the blended feedstock) ranges from \$8.10/bbl-\$19.50/bbl with a 90% confidence interval. Fig. 5c shows that the price of bio-crude and crude oil is responsible for 88.9% of the total variability. As shown in the figure, capital costs and IRR have negligible interaction effects. The variation resulting from their interactions is determined from the difference between the 1st order and total indices (Fig. 5c). The price of bio-crude and crude oil will certainly control the price competitiveness of an HT blend because they are the largest source of uncertainty in Δ_{prod} . Furthermore, to operate the HT blend scenario at $\Delta_{\text{prod}} \leq 0$ depends on the minimum attainable bio-crude price. For example, at a crude oil price of \$56.50/bbl (base case condition), $\Delta_{\text{prod}} = 0$ (or \$81.30/bbl, the production cost of HT-VGO) when the price of HTL bio-crude is \$35.90/bbl (or \$227.70/tonne). For a competitive HT blend product, the price differential between a barrel of crude oil and a barrel of HTL bio-crude must be less than \$20.60.

Table 9: Cost breakdown of HT blend and HT-VGO products for a hydroprocessing plant capacity of 75,000 barrels per day at \$56.50/bbl crude oil price and \$97.60/bbl HTL oil price

Components	HT blend	HT-VGO
Capital cost, \$M	336.2	327.3
Cost of manufacturing (COM), \$M/y	2,288.1	1,922
Raw material, \$M/y	1,775.0	1,481.0
Utilities, \$M/y	17.9	15.8
Operating labor, \$M/y	8.3	8.3
Production cost, \$/bbl.	95.3	81.3

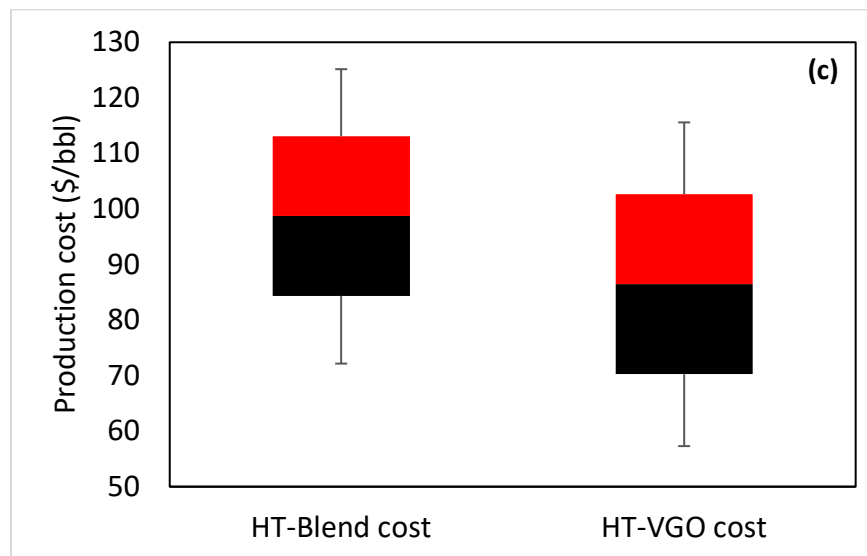
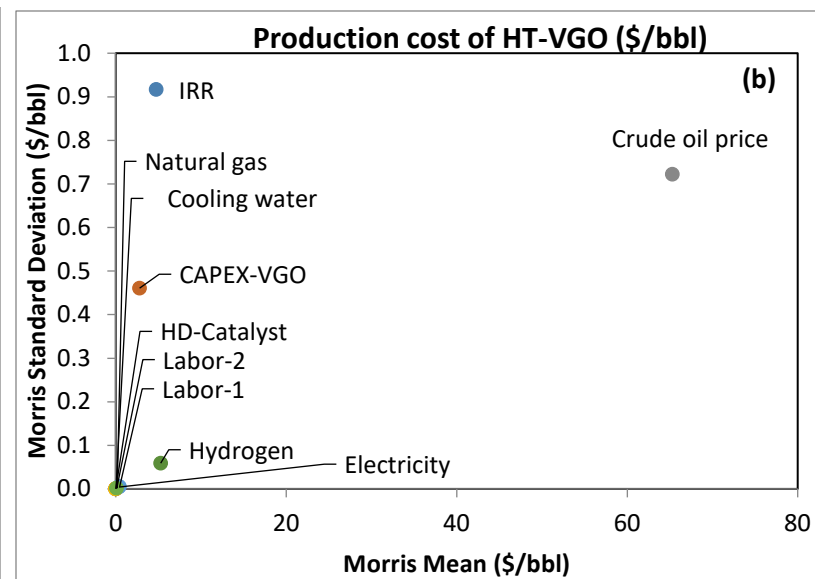
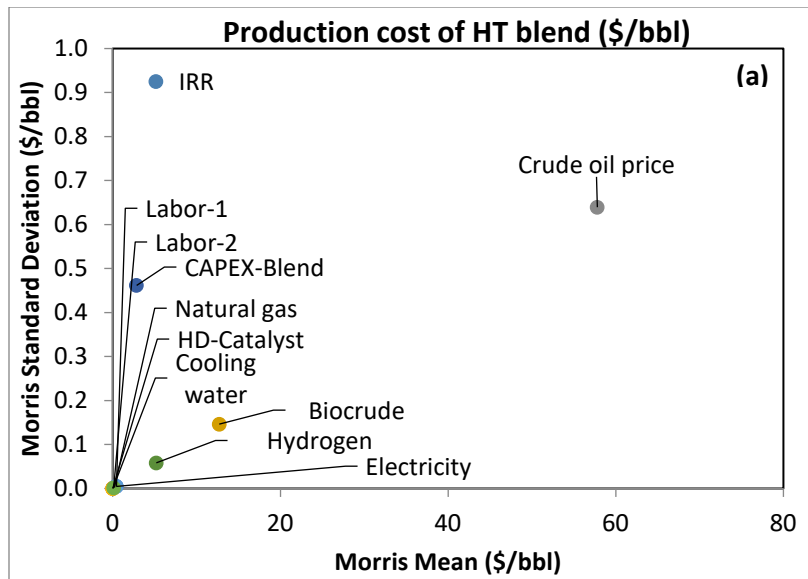


Fig. 4: Morris sensitivity plot for (a) HT blend and (b) HT-VGO production costs; and (c) Uncertainty results for HT blend and HT-VGO production costs

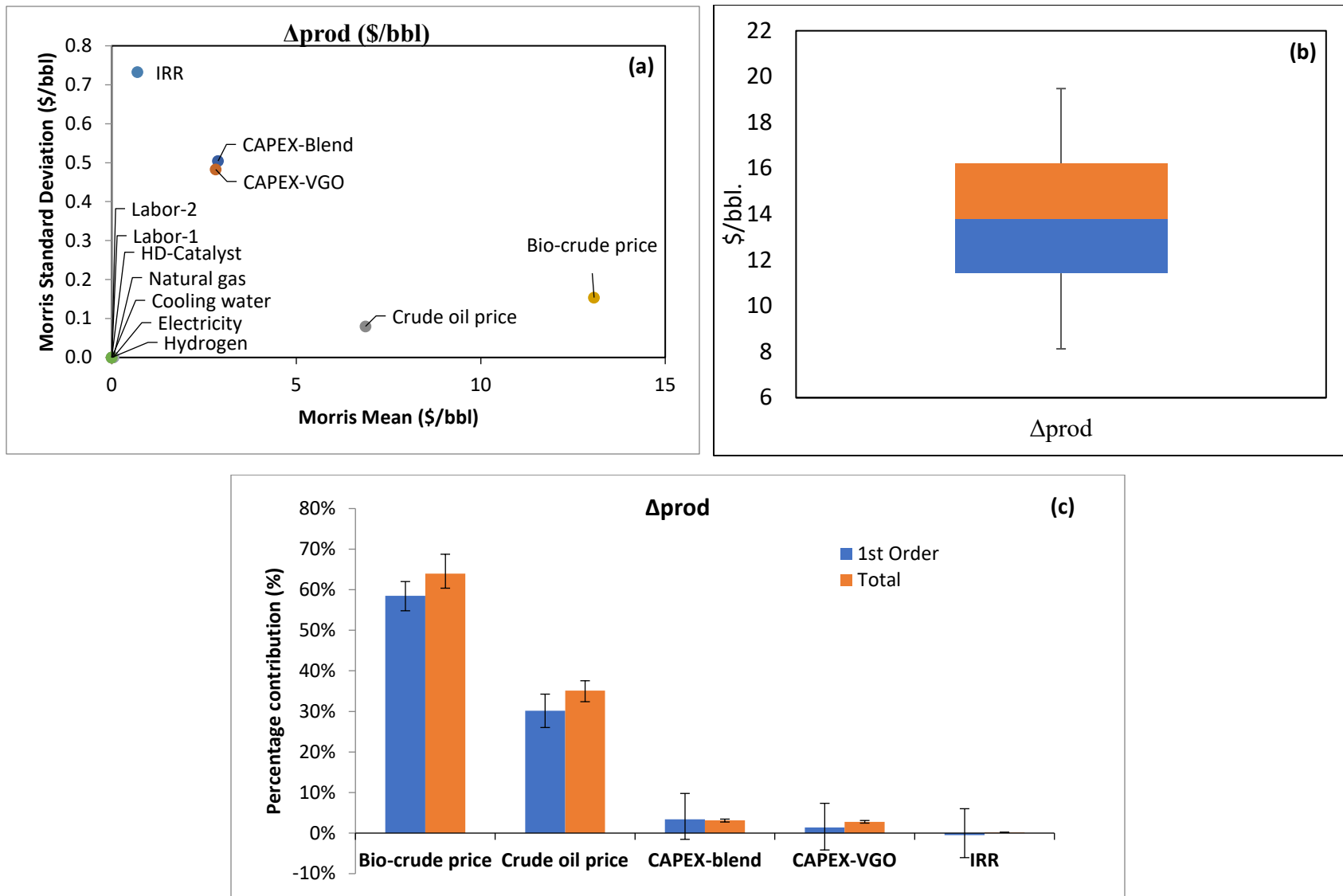


Fig. 5: (a) Morris sensitivity plot for Δ_{prod} , (b) uncertainty results for Δ_{prod} , and (c) Sobolj results for Δ_{prod}

3.2.2 Fluid catalytic cracking unit and the overall system

Aside from the cost of the feedstock, utility consumption is a critical cost component in the FCC. The utility consumed in the HTL blend scenario is 118.1% (or \$61.8 M per annum) more than the pure VGO. The higher cost is due to the expense from the make-up catalyst, which accounts for 99.6%; the rest is cooling water. The expenses from electricity consumption are lower in the HTL blend scenario by 5.5% (\$79,236 per annum). In both scenarios, more than 85% of the electricity is generated using flue gases from the regenerator's exhaust. As discussed earlier, the FCC generates heat needed for its operation in the regenerator, using the coke deposited on the catalyst as fuel instead of natural gas. For this reason, there is no natural gas consumption expense. It is worth noting that ~6.0% of the feedstock (VGO or blend) is converted to coke and used for heat production in the regenerator. These losses in the feedstock are equivalent to \$82.7 M/year and \$100.8 M/year for pure VGO and HTL blend, respectively. The FCC generates steam using flue gases from the regenerator's exhaust. The heat from the reactor's effluent is also integrated into reboilers and wherever else heat is needed. Therefore, steam credit can be generated in both FCC scenarios. However, we did not account for these credits in our analyses in order to obtain a conservative result. Steam generated within the refinery is exported to units where needed. If we account for steam credits, the pure VGO and HTL blend scenarios will generate \$32,243/year and \$32,905/year, respectively. These values have no significant impact on the cost of the products.

The capital cost for each FCC unit was estimated to be \$322 M. Because material and heat demand do not require changes in equipment sizes, the capital cost (both upstream and downstream units) of the FCC unit is practically the same for handling pure VGO and HTL blend feedstocks. The equipment can cope with changes in feedstock properties, which bring slight changes in utility demand. Besides, good process design is always overspecified to cope with changes in feedstock properties [31].

Table 10 summarizes the economic evaluation of the overall system (hydroprocessing and FCC units). The product cost in the pure VGO scenario is lower than in the HTL blend scenario. For the HT blend scenario, the cost of producing LPG, gasoline, LCO, and HCO is higher by ¢8.9/liter, ¢9.6/liter, ¢11.2/liter, and ¢11.1/liter, respectively. The HTL blend's overall production cost is 19.8% higher than the pure VGO scenario's. The inputs responsible for this increase were identified using the Morris method and the Sobol analysis to quantify their contributions. The percentage difference in the overall production cost of HTL blend and pure VGO (% Δ prod) was calculated and used as an indicator to identify these inputs. This approach avoids presenting the results for individual products in the Morris and Sobol analyses, thus making the analyses less cumbersome. Fig. 6a shows the Morris plot for the % Δ prod, while Fig. 6b shows their percentage contributions. It is important to mention that the Morris plots from each product are not different in Fig. 6 (a and b). Crude oil price is the most critical input. We ran the Sobol simulation variances, which revealed that bio-crude price has a considerable effect on the total variation, 29%. Pure VGO and HTL blend capital costs and the FCC make-up catalyst contribute 8%, 6.0%, and 4% to the total variance, respectively. The other parameters have a negligible effect on the % Δ prod. It is clear from the figure that the price of crude oil and bio-crude play a significant role in making coprocessing competitive.

In the uncertainty analyses, the sensitive inputs were used to provide the variability in the difference between the production cost of the two scenarios (Δ prod) and the % Δ prod. Fig. 7 presents a box plot representation of the uncertainty in the HT blend and HT-VGO products. P5 and P95 represent the range of product costs at a 90% confidence interval. The distribution between P5 and P95 is analogous to the values derived from the sensitivity analysis. The base

case values fall within the 90% confidence interval of the uncertainty, below their corresponding mean values. Note that Fig. 7 is suitable for comparing similar products; this is because the input distributions are completely independent. The independent inputs (bio-crude price and capital costs) were modeled independently, while the dependent input (crude oil price) was left as a dependent. Thus, the overlap between similar products can be ignored. However, a clear distinction between similar products is shown in Fig. 8a. We present the cost difference, in ¢/liter, between similar products from the two scenarios. A positive value in the plot indicates that the costs of products in the HTL blend scenario are higher than in the pure VGO scenario. The cost of producing a liter of liquefied petroleum gas, gasoline, light cycle oil, and heavy cycle oil in the HTL blend scenario increased by ¢8.4 ±4.1/L, ¢9.0 ±4.4/L, ¢10.5 ±5.2/L, and ¢10.4 ±5.1/L, respectively, at a 95% confidence interval. Fig. 8b shows the overall percentage increase in HTL blend products, %Δprod. A positive value in the plot also indicates that the costs of products in the HT blend scenario are higher than in the pure VGO scenario. In Fig. 8b, the %Δprod ranges from 7.2%-33.1% at a 90% confidence interval. This variation is primarily because of the crude oil and bio-crude price. The price of crude oil and bio-crude contributes 91.4% to the total variability, while capital costs make up less than 10%. These results indicate that the competitiveness of coprocessing an HTL blend to produce fuels in a petroleum refinery depends on the price of crude oil and HTL bio-crude. For example, under base case conditions, the HTL blend will compete with pure VGO when the crude oil price exceeds \$186.20/bbl (or US\$140/bbl) or when the bio-crude price drops below \$20.40/bbl (or US\$15.4/bbl). That said, for competitive HTL blend fuels, the price differential between a barrel of crude oil and a barrel of HTL bio-crude must be less than \$36.10. Lastly, coprocessing HTL bio-crude and VGO in hydroprocessing and FCC units will be competitive when crude oil price increases and bio-crude price decreases favorably.

Table 10: Cost breakdown of HTL blend and pure VGO products for the overall system

Components	HTL blend	Pure VGO
Total capital cost, \$M	658.30	649.40
Total manufacturing cost (COM), \$M/y	2508.97	2067.04
Utilities, \$M/y	131.98	68.14
Raw material, \$M/y	1,774.73	1,480.59
Operating labor \$M/y	16.56	16.56
LPG (\$/liters)	0.54	0.45
Gasoline (\$/liters)	0.58	0.48
LCO (\$/liters)	0.68	0.56
HCO (\$/liters)	0.67	0.56

The overall system includes hydroprocessing and FCC units.

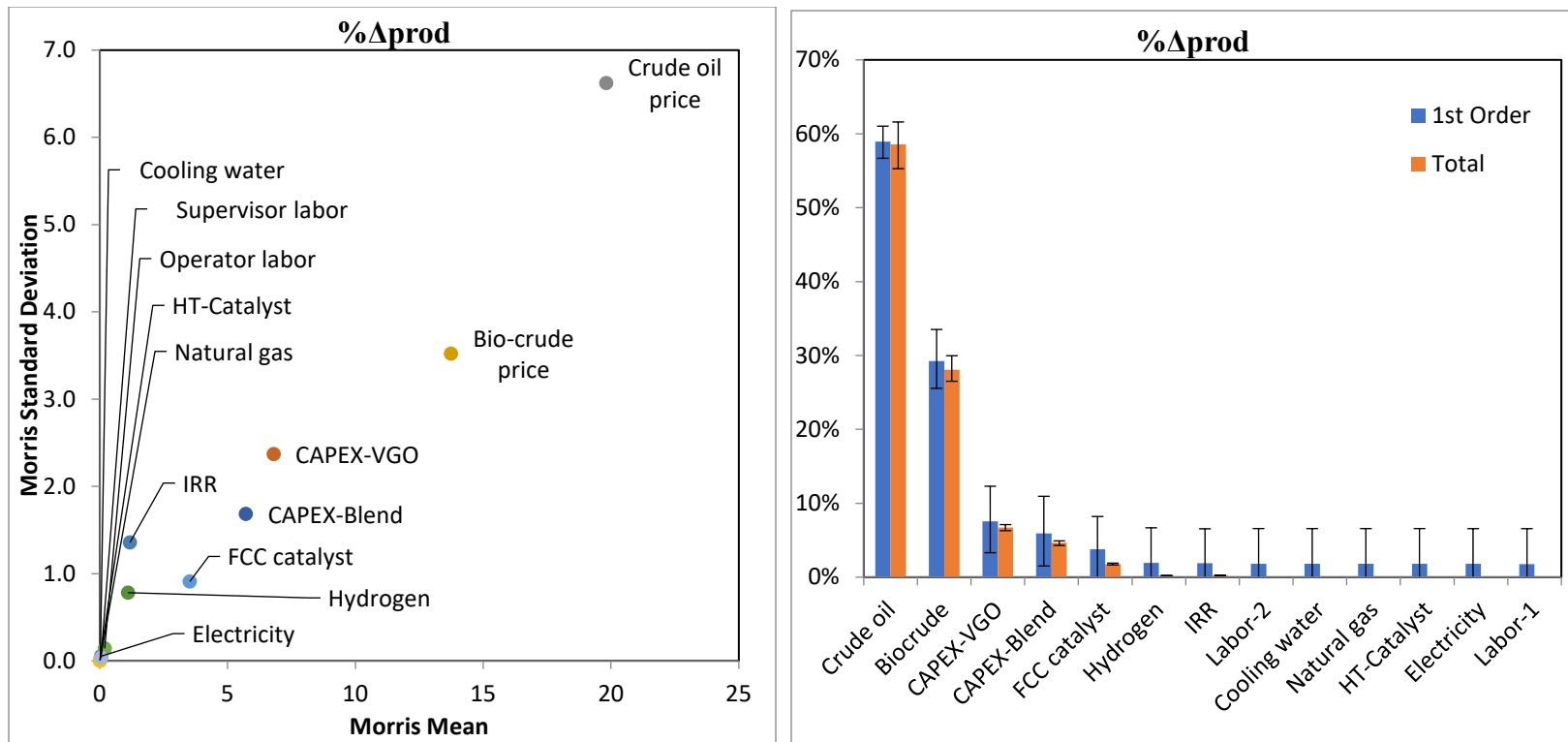


Fig. 6: (a) Morris plot for the percentage difference in the production cost (b) Sobolj results for %Δprod

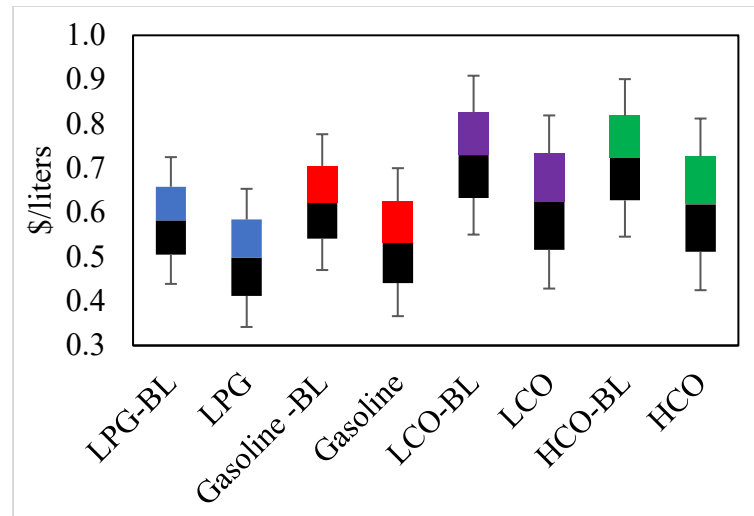


Fig. 7: The uncertainty in HTL blend and pure VGO products

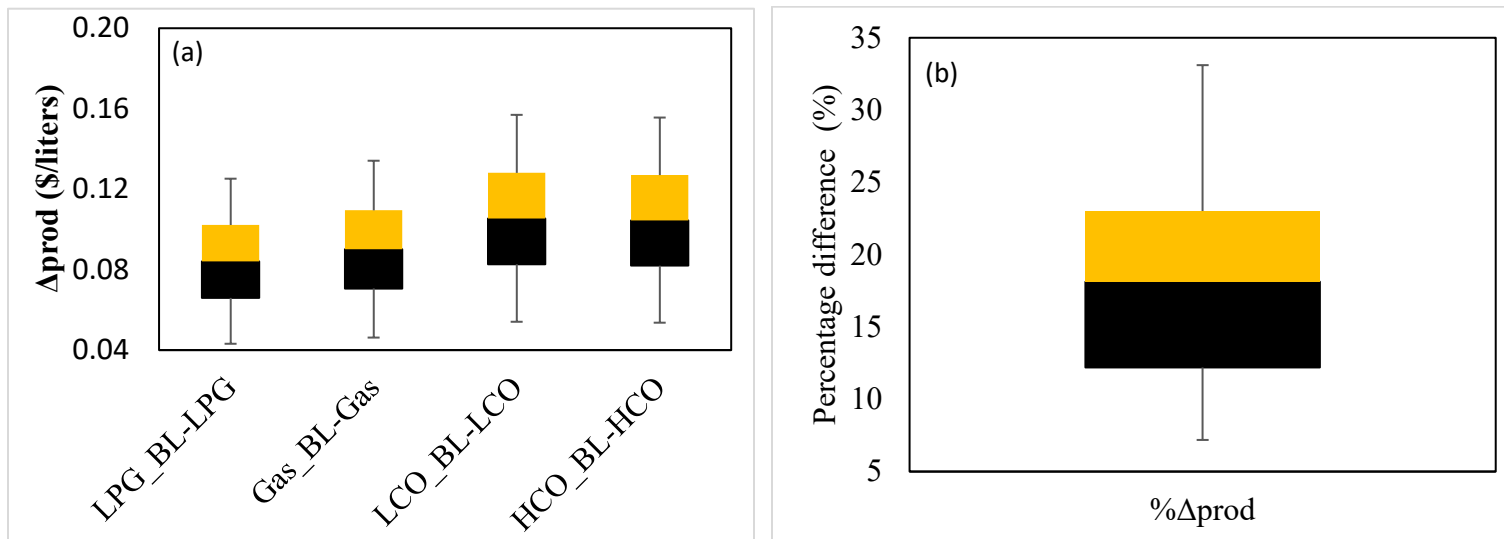


Fig. 8 (a) The uncertainty in the differences in the cost of similar product; (b) The uncertainty in percentage difference in the overall production cost of liquid products from the HTL blend and pure VGO

4.0 Discussion

Coprocessing a VGO with a 10% blend of HTL oil in refinery hydroprocessing and FCC units will incur additional cost. The demand for additional utilities and equipment size depends on the HTL bio-crude quality, the opportunity for process integration, and production location of the HTL bio-crude (e.g., at the petroleum refinery site). The additional capital investment is associated with the HTL oil production unit and the preprocessing needed in the hydroprocessing unit. While a large part of the additional cost results in a huge cost difference, the economic viability of coprocessing can be favorable depending on the crude oil price and whether the bio-crude production expense can be optimized and a carbon tax can be imposed.

A high crude oil price is economically viable for coprocessing as refiners can easily meet profit margins. This is especially true when the cost of HTL bio-crude is high. The increase in crude oil price raises the prices of intermediate products like VGO. VGO is an essential feedstock for gasoline and diesel production at a relatively low price in the FCC unit. In the global market, the price of VGO is sensitive to the crude oil price, especially when the gasoline demand is high. The increase in the price of VGO or its demand can help create a competitive market for coprocessing at a relatively low HTL bio-crude price. However, total reliance on a high crude oil price is not a sustainable solution for competitiveness. Crude oil prices rise and fall depending on seasonal demand and supply and factors that affect supply and demand unpredictably.

Exploring the economic feasibility of optimizing the production of HTL oil could be a viable option for lowering its price. For example, producing HTL bio-crude at refinery sites can help reduce energy consumption significantly, thus lowering the overall operating cost. There are opportunities for heat integration in the refinery to reduce fuel use during HTL oil production. By integrating the HTL oil production unit to the refinery FCC unit, an estimated 20% energy can be saved. In standalone HTL oil production, off-gases released during production require additional units for clean-up, thus adding to the overall cost, or can be disposed of without use. The integration of these gases into the refinery fuel gas unit can help lower operating costs and environmental impact. In addition, developing a large-scale HTL bio-crude plant could reduce production costs because of economies of scale.

Implementing a carbon levy on the huge FCC flue gases can provide economic incentives for coprocessing. The carbon levy raises the production cost for a 100% VGO FCC operation. Carbon emissions released through the flue gas can be reduced depending on the amount of bio-carbon on the catalyst leaving the FCC riser to the regenerator. For a 10% bio-crude blend, the biogenic carbon contained in the coke fraction (on the catalyst) can be up to 15.8%; this value is equivalent to a reduction of 15.8% of the carbon emissions from a fossil-based coke [46]. For a 10% HTL oil blend, biogenic carbon can be up to 10% in liquid products like gasoline and diesel [22].

Coprocessing in the hydroprocessing and FCC units represents a short- and long-term opportunity since HTL bio-crude can be produced in large quantities. HTL bio-crudes have the potential to provide a significant portion of future transportation fuels subject to availability of biomass for production of bio-crudes. However, their production cost must be comparable to other bio-based oils like pyrolysis oil and thermo-catalytic oil. A few major points can be made regarding the economic outcomes of our analysis on HTL bio-crude and other studies on pyrolysis oil. A high-level economic analysis performed in an earlier study showed that coprocessing hydrodeoxygenation oil from fast pyrolysis in the FCC units is economically attractive at crude oil prices above US\$120/bbl. In our study, we found that HTL bio-crude will be economically viable at a crude oil price of US\$140/bbl. Although the studies' used different the system boundaries, one would expect pyrolysis oil to be more expensive to produce because of its low yield and high

oxygenated content compared to HTL bio-crude. On the other hand, a 2014 study by PNNL showed that the production cost (without upgrading) of pyrolysis oil is 9.4% higher than of HTL oil. When upgrading is considered, pyrolysis oil is 35.7% higher. PNNL's results suggest that HTL could be more promising than pyrolysis bio-crude.

5.0 Key Observations

The techno-economic analysis performed in this study explores the cost of producing fuels from coprocessing hydrothermal liquefied oil (HTL) and VGO in the refinery hydroprocessing and FCC units. We developed two scenarios. The first scenario uses pure VGO as feedstock and the second uses a VGO with a 10% blend of hydrothermal liquefied oil. Process models were developed to size equipment and extract the data needed to perform techno-economic analyses. Where necessary, published data was used to fill missing economic data. Hydroprocessing and FCC unit capacities of 75,000 barrels per day were considered. An HTL bio-crude preprocessing unit was also developed to separate heavy fractions that might impede miscibility with pure VGO, cause operational problems like plugging, or even deactivate the catalyst.

In the preprocessing unit, 24.7 kg/s of HTL bio-crude is needed to produce 13.6 kg/s of distillate required for blending with VGO. The boiling range of the distillate fraction is from IBP-521°C with its D1160 95% at 476°C. 44.9% of the raw feed is discharged as residue (D1160 5% at 465°C).

Liquid product from the hydrotreated blend (HT blend) is 1.3% higher than from pure VGO. The slight decrease in the yield of the hydrotreated VGO (HT-VGO) is due to the high yield of fuel gases and unstabilized naphtha. The HT-blend consumes more utilities than the HT-VGO, primarily because of the additional energy needed to separate distillate from bio-crude. There is a slight increase in the hydrogen consumed in the HT blend scenario, and this increase impacts the economy of the process. In the FCC, the differences in the utilities consumed are not large except for the make-up catalyst, suggesting that coprocessing 10% HTL blend with VGO will not require a major structural change.

In the hydroprocessing unit, the cost of producing an HT blend is higher than producing HT-VGO. For both scenarios, production costs are affected by the cost of manufacturing. The capital cost contribution is low. The increase in the cost of the HT blend is due to operating expenses because of the HTL oil price. Although it costs more to produce an HT blend in the refinery than an HT-VGO, it will cost less to upgrade HTL bio-crude in the petroleum refinery hydroprocessing unit than in a standalone facility. In the FCC unit, there is no significant change in equipment size, thus the capital cost is the same in each scenario. However, the make-up catalyst in the HTL blend costs more than in the pure VGO scenario. Considering the overall system (hydroprocessing and FCC units), the cost of producing a liter of liquefied petroleum gas, gasoline, light cycle oil, and heavy cycle oil in the HTL blend scenario increased by $\phi 8.4 \pm 4.1/L$, $\phi 9.0 \pm 4.4/L$, $\phi 10.5 \pm 5.2/L$, and $\phi 10.4 \pm 5.1/L$, respectively, at a 90% confidence interval. The difference in the cost increase is primarily due to the crude oil and bio-crude prices, which contribute 91.4% to the total variability. That said, for competitive HTL blend fuels, the price differential between a barrel of crude oil and a barrel of HTL bio-crude must be less than \$36. These results indicate that coprocessing HTL bio-crude and VGO in hydroprocessing and FCC units will be competitive when crude oil prices increase and bio-crude prices decrease favorably.

6.0 Key Recommendations

Based on the results of this project, following are the key recommendations.

- A comprehensive economic analysis of hydrotreating HTL bio-crude before blending in the hydroprocessing unit is recommended. This information will indicate whether it is economically viable to hydrotreat HTL in a standalone hydroprocessing unit in the petroleum refinery before blending.
- Investigating the GHG emissions impact of coprocessing HTL oil using the hydroprocessing and FCC units is recommended. A life cycle GHG emissions assessment is necessary to compare the emissions from processing an HTL blend and pure VGO into transportation fuels.
- Investigating how carbon pricing will impact the attractiveness of coprocessing HTL bio-crude in a petroleum refinery is recommended. This investigation will provide information on how carbon pricing can be used to formulate policies on coprocessing the HTL bio-crude to produce transportation fuels.

Reference

1. Bridgwater T, Biomass for energy. *Journal of the Science of Food and Agriculture*, 2006. **86**(12): p. 1755-1768.
2. Sansaniwal SK, Rosen MA, and Tyagi SK, Global challenges in the sustainable development of biomass gasification: An overview. *Renewable and Sustainable Energy Reviews*, 2017. **80**: p. 23-43.
3. Demirbas A, Current technologies for the thermo-conversion of biomass into fuels and chemicals. *Energy Sources*, 2004. **26**(8): p. 715-730.
4. Almario, M.P., L.H. Reyes, and K.C. Kao, Evolutionary engineering of *Saccharomyces cerevisiae* for enhanced tolerance to hydrolysates of lignocellulosic biomass. *Biotechnology and Bioengineering*, 2013. **110**(10): p. 2616-2623.
5. Asmaa AMA, Mustafa AM, and Kamal EY, A techno-economic evaluation of bio-oil co-processing within a petroleum refinery. *Biofuels*, 2018. **12**(6): p. 645-653.
6. Fogassy G, et al., Biomass derived feedstock co-processing with vacuum gas oil for second-generation fuel production in FCC units. *Applied Catalysis B: Environmental*, 2010. **96**(3-4): p. 476-485.
7. Stefanidis SD, Kalogiannis KG, and Lappas AA, Co-processing bio-oil in the refinery for drop-in biofuels via fluid catalytic cracking. *Wiley Interdisciplinary Reviews: Energy and Environment*, 2018. **7**(3): p. e281.
8. Dyk S.van, et al. DROP-IN BIOFUELS: The key role that co-processing will play in production. 2019 [cited 2012 November, 12]; Available from: <https://task39.sites.olt.ubc.ca/files/2019/02/IEA-Bioenergy-Task-39-Drop-in-Update-Executive-Summary-February-2019.pdf>.
9. Freeman CJ, et al. Initial Assessment of U.S. Refineries for Purposes of Potential Bio-Based Oil Insertions. 2013 [cited 2021 November, 12]; Available from: https://www.pnnl.gov/main/publications/external/technical_reports/pnnl-22432.pdf.
10. Sadeghbeigi, R., Fluid catalytic cracking handbook: An expert guide to the practical operation, design, and optimization of FCC units. 2020: Butterworth-Heinemann.
11. Shorey SW, Lomas DA, and Keesom WH, Use FCC feed pretreating methods to remove sulfur. *Hydrocarbon Processing*, 1999. **78**(11): p. 43-43.
12. French RJ, Stunkel J, and Baldwin RM, Mild hydrotreating of bio-oil: effect of reaction severity and fate of oxygenated species. *Energy & Fuels*, 2011. **25**(7): p. 3266-3274.
13. Lindfors C, et al., Co-processing of dry bio-oil, catalytic pyrolysis oil, and hydrotreated bio-oil in a micro activity test unit. *Energy & Fuels*, 2015. **29**(6): p. 3707-3714.
14. Bryden K, Weatherbee G, and Habib ET, Flexible pilot plant technology for evaluation of unconventional feedstocks and processes. *Catalagram*, 2013. **113**: p. 3-21.
15. Brady MP, et al., Corrosion of stainless steels in the riser during co-processing of bio-oils in a fluid catalytic cracking pilot plant. *Fuel Processing Technology*, 2017. **159**: p. 187-199.
16. Wang C, Venderbosch R, and Fang Y, Co-processing of crude and hydrotreated pyrolysis liquids and VGO in a pilot scale FCC riser setup. *Fuel Processing Technology*, 2018. **181**: p. 157-165.
17. Badoga S, et al., Co-processing of Hydrothermal Liquefaction Biocrude with Vacuum Gas Oil through Hydrotreating and Hydrocracking to Produce Low-Carbon Fuels. *Energy & Fuels*, 2020. **34**(6): p. 7160-7169.
18. Huber GW, Iborra S, and Corma A, Synthesis of transportation fuels from biomass: chemistry, catalysts, and engineering. *Chemical Reviews*, 2006. **106**(9): p. 4044-4098.
19. Wu L, et al., Techno-economic analysis of bio-oil co-processing with vacuum gas oil to transportation fuels in an existing fluid catalytic cracker. *Energy Conversion and Management*, 2019. **197**: p. 111901.

20. Marker TL, et al., Opportunities for biorenewables in oil refineries. Final technical report. 2005, UOP LLC, Des Plaines, IL, United States: United States.
21. Talmadge FB, et al. Analysis for co-processing fast pyrolysis oil with VGO in FCC units for second generation fuel production-TCS—Symposium on Thermal and Catalytic Sciences for Biofuels and Biobased Products Chapel Hill, NC. 2016 [cited 2021 November 12]; Available from: https://www.researchgate.net/publication/311146745_Analysis_for_co-processing_fast_pyrolysis_oil_with_VGO_in_FCC_units_for_second_generation_fuel_production.
22. Zhang Y and Alvarez-Majmutov A, Production of Renewable Liquid Fuels by Coprocessing HTL Biocrude Using Hydrotreating and Fluid Catalytic Cracking. Energy & Fuels, 2021.
23. Wu L, et al., Techno-economic analysis of co-processing of vacuum gas oil and algae hydrothermal liquefaction oil in an existing refinery. Energy Conversion and Management, 2020. **224**: p. 113376.
24. Xing T, et al., Co-hydroprocessing HTL biocrude from waste biomass with bitumen-derived vacuum gas oil. Energy & Fuels, 2019. **33**(11): p. 11135-11144.
25. Netzer D. Alberta bitumen processing integration study. 2006 [cited 2021 January 18]; Available from: <https://open.alberta.ca/dataset/7d728b7f-e97c-4c01-ba2a-b527399b40fa/resource/127b6abd-47d0-496f-9cc8-338bf9e9f032/download/albertabitumenprocessintegrationreport06.pdf>.
26. Liu YA, Chang AF, and Pashikanti K, Petroleum Refinery Process Modeling: Integrated Optimization Tools and Applications. 2018.
27. AspenTech. Aspen Technology, Inc. Massachusetts USA. 2021 [cited 2021 November 14]; Available from: <https://www.aspentech.com/en>.
28. AspenTech, Aspen HYSYS Petroleum Refining Unit Operations & Reactor Models. Reference Guide. Vol. 9. 2016, Bedford, MA, USA: Aspen Technology, Inc.
29. Tews IJ, et al., Biomass direct liquefaction options. techno-economic and life cycle assessment. 2014, Pacific Northwest National Lab.(PNNL), Richland, WA (United States).
30. Peters MS, Timmerhaus KD, and West RE, Plant design and economics for chemical engineers. Vol. 4. 2003: McGraw-Hill New York.
31. Turton R, et al., Analysis, synthesis and design of chemical processes. 2008: Pearson Education.
32. Al-Mayyahi MA, et al., Investigating the trade-off between operating revenue and CO2 emissions from crude oil distillation using a blend of two crudes. Fuel, 2011. **90**(12): p. 3577-3585.
33. Canada Energy Regulator. Commodity Prices and Trade Updates. [cited 2021 November 21]; Available from: <https://www.cer-rec.gc.ca/en/data-analysis/energy-commodities/commodity-prices-trade-updates/>.
34. EPCOR. Water rates: Multi-Residential and Commercial Rates. [cited 2021 November 21]; Available from: <https://www.epcor.com/products-services/water/rates-terms-conditions/Pages/commercial-multi-residential-rates.aspx>.
35. KVA-International. FCC Equilibrium Catalyst Pricing. [cited 2019 May 2]; Available from: <https://kva-international.com/services/fcc-equilibrium-catalyst>.
36. GLJ. Price forecast-price charts. [cited 2020 September 1]; Available from: <https://www.bloomberg.com/energy>.
37. Calculator, C.S. [cited 2020 May 2]; Available from: <http://www.canadavisa.com/canada-salary-wizard.html>.
38. Natural Resources Canada. Monthly Average Wholesale (Rack) Prices for Regular Gasoline in 2019. [cited 2021 November 15]; Available from:

https://www2.nrcan.gc.ca/eneene/sources/pripri/wholesale_bycity_e.cfm?priceYear=2019&productID=9&locationID=66,8,10,39,17&frequency=M#priceGraph.

39. Di Lullo G, et al., Extending sensitivity analysis using regression to effectively disseminate life cycle assessment results. *The International Journal of Life Cycle Assessment*, 2020. **25**(2): p. 222-239.
40. Morris MD, Factorial sampling plans for preliminary computational experiments. *Technometrics*, 1991. **33**(2): p. 161-174.
41. Ren J, Zhang W, and Yang J, Morris sensitivity analysis for hydrothermal coupling parameters of embankment dam: A case study. *Mathematical Problems in Engineering*, 2019. **2019**.
42. Parkash, S., *Refining processes handbook*. 2003: Elsevier.
43. Rivero R, Rendón C, and Gallegos S, Exergy and exergoeconomic analysis of a crude oil combined distillation unit. *Energy*, 2004. **29**(12-15): p. 1909-1927.
44. Oni AO and Waheed MA, Methodology for the thermoeconomic and environmental assessment of crude oil distillation units. *International Journal of Exergy*, 2015. **16**(4): p. 504-532.
45. Mohajerani S, Kumar A, and Oni AO, A techno-economic assessment of gas-to-liquid and coal-to-liquid plants through the development of scale factors. *Energy*, 2018. **150**: p. 681-693.
46. Fogassy G, et al., The fate of bio-carbon in FCC co-processing products. *Green Chemistry*, 2012. **14**(5): p. 1367-1371.